NAVAL SHIP RESEARCH AND DEVELOPMENT CENTER
Bethesda, Md. 20034

SOME ENVIRONMENTAL EFFECTS ON HEADFORM CAVITATION INCEPTION

by

Terry Brockett

SHIP PERFORMANCE DEPARTMENT
RESEARCH AND DEVELOPMENT REPORT

October 1972

Report 3974

SOME ENVIRONMENTAL EFFECTS ON HEADFORM CAVITATION INCEPTION

TABLE OF CONTENTS

LIST OF FIGURES

LIST OF TABLES

NOTATION

P	Local Pressure
P_o	Static pressure in test section
P_v	Vapor pressure corresponding to measured test-section temperature
R	Maximum radius of headform
$\mathrm{Re} = \frac{2VR}{\nu}$	Reynolds number
t	Time
V	Free-stream speed measured with venturi
X	Distance from nose along headform centerline
$Y(X)$	Ordinate measured from axis of symmetry
ν	Kinematic viscosity
ρ	Mass density
$\sigma_i = \frac{P_o - P_v}{\frac{1}{2}\rho V^2}$	Cavitation number for inception

ABSTRACT

Cavitation-inception tests were performed on two headforms for which changes were made in the environment. Quantities which were varied, included type and amount of dissolved gas, chemical additives, time rate of change to cause inception, and temperature changes. Experimental procedure and relative air content had an appreciable effect on cavitation inception while the other environmental changes had little effect. Both headforms had the same designed minimum pressure coefficient; however, for one it was located 0.03 diam from the nose, and for the other, 0.73 diam. Although inception was characterized by traveling bubbles on both headforms, significant differences occurred in the bubble dynamics. Inception was determined both visually and by counting the number of cavitation occurrences.

ADMINISTRATIVE INFORMATION

The work reported here was supported by the General Hydrodynamics Research Program of the Carderock Laboratory of the Naval Ship Research and Development Center under Subproject S-R009-0101, Problem 526-815 from 1967 to 1969.

ACKNOWLEDGMENTS

A special word of thanks is given to the Instrumentation Department for its support during the development and selection of electronic components. Portions of the described work have been reported in the 1969 American Society of Mechanical Engineers Cavitation Forum Papers: Terry Brockett, "Cavitation Occurrence Counting – Comparison of Photographic and Recorded Data," and Frank B. Peterson, "Cavitation on a Headform Using Occurrence Counting."

INTRODUCTION

Provided that it can be anchored in an appropriate test facility, it is usually a simple matter to observe cavitation inception on a given body. Repeated tests often give different conditions at inception, and different observers often detect inception at different conditions but, in general, these differences are small. Unfortunately the results of such tests are usually not of direct interest in themselves. Instead the test bodies are usually models for which information is gathered relating to a prototype operating in its medium. The problem is then to extrapolate the information from the test facility to give predictions of the prototype performance. Rules and formulas governing the extrapolation are called scaling laws.

In spite of the extensive research on cavitation inception during the past few decades, our knowledge of the proper scaling laws is still not complete. The only generally accepted scaling law is that based on the cavitation number

$$\sigma_i = \frac{P_o - P_v}{\frac{1}{2}\rho V^2} \tag{1}$$

where P_o is the undisturbed static pressure,

P_v is the vapor pressure of the test liquid,

ρ is the mass density of the test liquid, and

V is the reference liquid speed.

It has been known for many years that the scaling law derived from Equation (1) has been inadequate as pointed out in one of the first[1] survey papers on cavitation as well as in the latest.[2–5] Several different possibilities for the missing links in the scale-effect problem are mentioned in these reports. These hypotheses are related to the models for cavity nuclei (or fluid weak spot), the most popular of which are dependent upon interfacial phenomena. The models are either trapped free gas or the interfacial bond between liquid and solid. The free gas is considered to be in the form of either bubbles in the free stream, free gas trapped on the surface of solid particles entrained in the free stream (defined as Harvey nuclei in Reference 3), or free gas trapped on the surface of the test body. The liquid-solid interface model could be either the surface of the test body or of a solid particle moving with the liquid.

The possibility of the rupture site originating as a gas bubble in the free stream is currently receiving much attention in cavitation research. The most promising investigation in this area was the calculation of nuclei trajectories first proposed and carried out by Johnson and Hsieh.[6] In their analysis, spherical gas bubbles which enclose a constant mass of gas are entrained in the liquid and are acted upon by the pressure field of the test body as

---

[1]Eisenberg, P., "On the Mechanism and Prevention of Cavitation," David Taylor Model Basin Report 712 (Jul 1950). A complete listing of references is given on page(s) 80–82.

[2]Peterson, F. B., "Cavitation Inception, (Part of Report on Cavitation)," 15th American Towing Tank Conference, Ottawa, Canada (1968).

[3]Holl, J. W., "Limited Cavitation," Proceedings of American Society of Mechanical Engineers Symposium on Cavitation State of Knowledge, Evanston, Ill. (Jun 1969).

[4]Johnson, V. E., Jr. and P. Eisenberg, "Environmental and Body Conditions Governing the Inception and Development of Natural and Ventilated Cavities," Appendix 1, Report of the Cavitation Committee, 11th International Towing Tank Conference, Toyko, Japan (1966).

[5]Eisenberg, P., "Environmental and Body Conditions Governing the Inception and Development of Natural and Ventilated Cavities (an updating of the survey prepared for the 11th ITTC)," Appendix 1, Report of the Cavitation Committee, 12th International Towing Tank Conference, Rome, Italy (1969).

[6]Johnson, V. E. and T. Hsieh, "The Influence of the Trajectories of Gas Nuclei on Cavitation Inception," Proceedings of the Sixth Naval Hydromechanics Symposium, AGR-136, Office of Naval Research, Washington, D. C. (1966).

the liquid flows past it. The effect of the pressure field on the bubble trajectory and subsequent cavitation potential is defined as screening. Hsieh[7,8] extended the calculations to include different flow-field geometry and a more refined analysis of the bubble growth. By including dynamic effects in the bubble-growth calculations, no instability was found, and the definition of inception had to be changed from bubble instability to pseudocavitation for which the bubble would grow to an arbitrary visible size simply in response to the pressure field (the gas mass is constant). At present the growth analysis is rather crude for body-bubble interactions, and the various postulates[3] for the nature of the bubble interface, e.g., organic skin and particulate skin,[9] have not been investigated—nor have Harvey nuclei, gas diffusion, gravity effects, etc.

Experimental verification of the trajectory calculations requires that the bubble spectrum in the free stream be measured. Instrumentation systems for measuring the spectrum of gas bubbles acoustically have been described,[10,11] and work is in progress[5] for optical detection of bubbles. An attempt[10] to correlate the measured free-stream bubbles with cavitation on a headform was promising but not entirely successful.

The other models for the cavitation-inception process concern conditions at the body-liquid surface. The specific models of the rupture site are trapped by gas on the surface and the bond between solid and liquid. Investigations of surface conditions are typified by the work of Van der Walle,[12] Peterson,[13] and Reed.[14] The experiments of Acosta and Hamaguchi[15] with a body coating provided further evidence of the importance of the surface conditions.

A slight modification of both of the previously described models is concerned with bubble growth in the boundary layer. Emphasis in these calculations has been on bubble growth rather than initial formation. Holl[3] has summarized investigations of this type.

Other possible contributing factors to the scale-effect problem mentioned in the literature are surface roughness, accuracy of model construction, turbulence, and separation.

---

[7]Hsieh, T., "The Influence of the Trajectories and Radial Dynamics of Entrained Gas Bubbles on Cavitation Inception," Hydronautics, Inc., Report 707-1 (Oct 1967).

[8]Hsieh, T., "Cavitation Inception for a Two-Dimensional Half Body in a Uniform Stream with a Free-Stream and a Solid Bottom," Hydronautics, Inc., Report 707-2 (Mar 1968).

[9]Turner, W. R., "Model for the Persistent Microbubble," Abstract Journal of the Acoustical Society of America, Vol. 36 (1964); Vitro Laboratory, Technical Note 01654.01-2 (1963).

[10]Schiebe, F. R. and J. M. Killen, "New Instrumentation for the Investigation of Transient Cavitation in Water Tunnels," 15th American Towing Tank Conference, Ottawa, Canada (1968).

[11]Brockett, T., "Computational Method for Determination of Bubble Distributions in Liquids," NSRDC Report 2798 (Apr 1969).

[12]Van der Walle, F., "On the Growth of Nuclei and the Related Scaling Factors in Cavitation Inception," Proceedings of the Fourth Naval Hydromechanics Symposium, AGR-92, Office of Naval Research, Washington, D. C. (1962).

[13]Peterson, F. B., "Cavitation Originating at Liquid-Solid Interfaces," NSRDC Report 2799 (Sep 1968).

[14]Reed, R. L., "The Influence of Surface Characteristics and Pressure History on the Inception of Cavitation," Master of Science Thesis, Department of Aerospace Engineering, Pennsylvania State University (Mar 1969).

[15]Acosta, A. J. and H. Hamaguchi, "Cavitation Inception on the ITTC Standard Headform, Final Report," California Institute of Technology, Hydro Laboratory Report E-149.1 (Mar 1967).

These suggestions are not models for cavitation since they are assumed to effect only the pressure distribution as computed for the analytical body shape, although roughness might also contribute to surface nuclei. With these specific models proposed for scale effects, the possibility exists that with additional calculations and test data, e.g., bubble spectrum, surface conditions, model accuracy, and turbulence level, some estimates could be made for scale effects. The drawback of such calculations is that current experimental evidence does not clearly indicate which model is dominant. Such a situation arises because cavitation dynamics initiate at the microscopic level and for the most part their effects are observed on the macroscopic level. Hence direct confirmation of the previously described ideas has not been possible. To date, specific models have been justified by how well they agree with the trends of certain gross-cavitation measurements.

Two of the series of gross-cavitation measurements of particular relevance to the present report are the International Towing Tank Conference (ITTC) studies[16] of headform cavitation inception and the studies of additive effects on acoustic cavitation by Bernd.[17] The ITTC studies were tests of geometrically similar bodies in various test facilities. This ITTC body was a modified ellipsoid headform from the family tested by Rouse and McNown[18] with a minimum pressure coefficient of -0.6 at an axial location of 0.3 diam from the nose. Cavitation inception occurred over the range of cavitation numbers from 0.4 to 1.1. The reasons for this wide range of data are still being investigated.[19]

The investigation by Bernd rated the effects of various substances as they influenced the cavitation inception caused by a sonar transducer in the liquid. He interpreted the results as the relative ability of the substance to form a film at the bubble surface which prevented dissolving of the bubble contents. One of the materials which had a pronounced effect on his experimental results was lauric acid.

The investigation undertaken and reported herein was to evaluate some of the previously described ideas and to gather other information regarding environmental effects on headform cavitation inception. Environmental changes were made which were expected to influence the behavior of gas nuclei. In addition, these changes were intended to reflect changes possible in day-to-day testing and hence would allow some conclusion to be drawn about the care necessary in selecting water conditions for a test series. Headforms were chosen for the study since they were the simplest body shape compatible with the 12-inch variable pressure water tunnel at the Center. Two headforms were used in the testing; although the designed minimum

---

[16]Lindgren, H. and C. A. Johnsson, "Cavitation Inception on Headforms, ITTC Comparative Experiments," Appendix V, Report of the Cavitation Committee, 11th International Towing Tank Conference, Toyko, Japan (1966).

[17]Bernd, L. H., "Cavitation, Tensile Strength, and the Surface Films of Gas Nuclei," Proceedings of the Sixth Naval Hydrodynamics Symposium, ARC-136, Office of Naval Research, Washington, D. C. (1966).

[18]Rouse, H. and J. S. McNown, "Cavitation and Pressure Distribution Headforms at Zero Angle of Yaw," State University of Iowa Studies in Engineering, Bulletin 32 (1948).

[19]Johnsson, C. A., "Cavitation Inception on Headforms, Further Tests," Appendix V, Report of the Cavitation Committee, 12th International Towing Tank Conference, Rome, Italy (1969).

pressure coefficient was the same for both, the axial locations were different. The locations were different so that the effect of bubble screening could be evaluated, since calculations indicated a different cavitation potential for different locations of the minimum pressure. Headforms will be discussed in the next chapter.

No direct attempt was made to evaluate surface effects. An independent study of surface effects using the same headform shape as one of the test bodies in this report has been conducted by Peterson.[19, 20] To minimize surface effects, both headforms were made of brass to represent the surface characteristics of usual metal test bodies. The same cleaning procedure was used throughout the test series whenever the body was exposed to the air and then immersed again. In this way, the surface conditions would be uniform. Details of the cleaning procedure are given later in the report.

The subjective nature of the traditional visual or acoustic "call" of cavitation inception has been recognized for some time. Recently Schiebe[10, 21] has proposed a more objective technique based on counting cavitation occurrences. The suitability of this technique was confirmed in preliminary tests,[22, 23] and the method has been used throughout the test series. This further experience has not entirely upheld the initial promise of the technique but it has been adequate for the present investigation. The technique and some of its limitations are discussed in the appendix.

Use of the instrumentation explicitly defines cavitation *inception* as a certain rate and magnitude of cavity *collapse* signals. The initial experiments[22] established that the collapse amplitude was roughly related to maximum bubble dimensions and that the amplitude distribution peaked above the noise level. Thus, the instrumentation could be set to compare with visual calls. These visual calls were made with the use of strobe lighting, and they also implied a certain (qualitative) rate of occurrence for the traveling bubbles.

Study of the experimental results presented here suggests that these two distributions (the traveling bubbles observed and the collapse pulse amplitude) respond differently to type of dissolved gas, reference static pressure, etc. The differences do not seem important for small changes, leading to the conclusion that for a limited range of environmental variations a more objective and consistent definition of the inception point can be determined using the counting technique.

These differences lead to a more fundamental question: Is the traditional visual call the proper definition of cavitation inception? The point of view taken in this report is that

---

[20]Peterson, F. B., "Water Tunnel-High Speed Basin Cavitation Inception Studies," Contribution to the Cavitation Session, 12th International Towing Tank Conference, Rome, Italy (1969).

[21]Schiebe, F. R., "Cavitation Occurrence Counting—A New Technique in Inception Research," Cavitation Forum Paper, American Society of Mechanical Engineers Annual Meeting (1966).

[22]Brockett, T., "Cavitation Occurrence Counting—Comparison of Photographic and Recorded Data," Cavitation Forum Paper, American Society of Mechanical Engineers Conference, Evanston, Ill. (1969).

[23]Peterson, F. B., "Cavitation on a Headform Using Occurrence Counting," Cavitation Forum Paper, American Society of Mechanical Engineers Conference, Evanston, Ill. (1969).

it is and that the instrumentation is intended to determine this point more objectively. Once correspondence in the two calls was found, no changes were made in the settings unless the two calls were clearly different. However, the appearance of bubbles on the body is not in itself significant. If it were not for the detrimental effects of cavitation, the scaling procedures would be little more than a curiosity. The four principal effects of cavitation are: noise, vibration, damage, and force divergence. Force divergence is usually not apparent at inception for streamlined bodies, and the other three effects are more clearly connected with collapse than with initial growth of nuclei. If one takes the point of view that these effects are more important than the appearance of voids in the fluid, then it is reasonable to define inception based on some measure of these effects. At the present time, such a criteria cannot be postulated. Damage cannot yet be measured conveniently on a macroscopic scale, and the results reported here show that a considerable variation occurs for the cavitation noise of bubbles of the same maximum size. Additional complications would occur if the type of cavitation pattern were unknown. Hence, the visual call is still considered the better standard since no new scaling parameters are introduced. Thus, the occurrence-counting technique is of restricted usefulness in general; however, once it is calibrated with visual calls, it does improve the consistency of a given set of experiments performed at nominally the same conditions.

HEADFORM SHAPES

Headforms were selected which had extremes in the axial location of minimum pressure and which were smooth curves. The test series to be discussed here was performed in the NSRDC 12-inch water tunnel.* Examination of the operating range of the 12-inch water tunnel indicated that a minimum pressure coefficient of -0.8 was reasonable since data could be taken from 15 to 25 ft/sec. From the headforms tested by Rouse and McNown[18] one of the modified ellipsoid headforms was selected which had a minimum pressure coefficient of -0.8 at 0.03 diam from the leading edge. For this headform $a/b = 3$ and $d/a = 2$. The pressure distribution (computed using the Douglas program[24]) and headform shape are shown in Figure 1. To minimize machining errors, as large a model as possible was desired. Rouse and McNown[18] indicated that no tunnel blockage corrections would be needed for a diameter of 2 in. Thus, a 2-in.-diam headform was manufactured in brass from a template. No check was made of its contour. The surface was polished to a 4-μin.-rms finish.

*This tunnel is capable of speeds to above 25 ft/sec with the open-jet test section. Recent tunnel additions include an improved vacuum pump and an external flow deaerator.

[24]Smith, A. M. O. and J. Pierce, "Exact Solution of the Neumann Problem. Calculation of Non-Circulatory Plane and Axially Symmetric Flows about or within Arbitrary Boundaries," Douglas Aircraft Company, Inc., Report ES26988 (Apr 1958).

A second headform was designed by analytical trial and error so that it had a minimum pressure coefficient of -0.8 at a distance of 0.73 diam from the leading edge. The equation for this shape is

$$\frac{Y}{R} = 2\sqrt{\frac{X}{7}}\,[0.6 - 1.340571X + 3.694036X^2 - 2.516708X^3 + 0.524687X^4] \tag{2}$$

for $X/R \leq 1.750$ and a cylinder of radius R beyond this point. Headform shape and pressure distribution are shown in Figure 2. The small pressure peak at $X/R = 0.1$ was retained to provide a markedly changed pressure distribution so that bubbles flowing by the body would be in a significantly different pressure field compared to the first headform.

Figure 3 shows model construction details for the second headform. The modified ellipse headform is similar internally, except that the interior void is 1/8 in. from the nose.

The second headform was fabricated in brass on a numerical control lathe. It was anticipated that its shape would be quite accurate. However, measurement of the profile did not bear out the expected accuracy. The analytical and measured ordinates are shown in Table 1. (Insufficient points were taken to calculate the potential pressure distribution with available computer programs.) As can be seen, the nose region is considerably off, so that an increase in the first pressure peak can be expected. Surface finish on this model was 10 μin. rms.

PRELIMINARY EXPERIMENTS WITH THE MODIFIED ELLIPSOID HEADFORM

The modified ellipsoid headform was the first to be manufactured, and a substantial initial testing program was accomplished with it.

An investigation of the laminar separation properties of the headform* showed that laminar separation occurred at less but not greater than a Reynolds number ($\mathrm{Re} = 2VR/\nu$) of 1.6×10^5. This corresponded to 9.3 ft/sec at 77 F and to 13.7 ft/sec at 50 F. Thus, separation did not occur on this headform during the tests, since the minimum velocity was 15 ft/sec, and the minimum temperature was about 65 F. The procedure used for the separation tests was to paint the headform with a mixture of lemon yellow fluorescent pigment, vinegar, and 20-weight motor oil. The tunnel was filled with water, and a steady-state speed was established at atmospheric pressure. Two 15-W ultraviolet fluorescent bulbs were used for illumination, although white light was usually satisfactory. The tunnel water speed was established, and the oil pattern was allowed sufficient time to develop on the surface of the model. If separation still occurred, the speed was increased in discrete steps until the separation bubble was washed off the surface. The tunnel was drained, and the headform

*The headform used in these tests was another model of the one used for the rest of the program.

was repainted. The test procedure was repeated, starting with the water speed just under the value at which the separation bubble disappeared in the previous test. Separation disappeared at 13.7 ft/sec and 50 F at an X/R value of approximately 1.0. Time effects were not studied. Separation studies on the ITTC headform have been reported in References 25 and 26.

Tests[20] were performed in the high-speed towing basin with the same headform as that used in the present tests as well as others of the same shape. The incipient cavitation number of all tests ranged from 0.6 to 0.8. The average σ_i for the three tests with the same headform as used in the present study is 0.61.

Another series of tunnel tests[23] was performed with the same headform used in the tests reported here. In these tests, the oxygen-to-nitrogen ratio of the air in the test water was varied over a range typical of tunnel operation. In addition, tests were performed at an air content of 1 percent, relative to atmospheric pressure saturation. The average cavitation-inception number was 0.79 to 0.80, indicating no effect of air content or of the ratio of the two gases. The criterion used for inception was that there be one occurrence every 10 sec. As will be explained later, this was not the criterion used here of 1 event per second. From Figure 1 of Reference 23 the criterion used here would result in an inception call 16 sec later than the value shown, giving a value of $\sigma_i = 0.69$. This is in excellent agreement with the results of the present tests discussed in the following sections. For the previously described tests, inception was initiated by increasing the speed and holding the pressure constant. Inception and desinence were not significantly different.

EXPERIMENTAL PROCEDURE

The headform mount was rigidly fastened on the shaft support spider in the downstream nozzle. Relative to the downstream nozzle, the headform was out of alignment 0.3 deg, nose down. Construction of the headform mount is discussed in Reference 22 and Appendix A.

Because of the internal sting mount for the hydrophone, care was needed to prevent air being trapped in the interior void—such air might reradiate the collapse pulse. To prevent this possibility the headform surface was cleaned with reagent-grade acetone and was air dried. The water level was raised above the mount, and all air bubbles were removed from the sting mount area. The headform was immersed, and all bubbles were removed from the interior void. Care was taken not to touch the nose region of the headform as it was screwed onto the mount, and the vent was sealed.

---

[25]Etter, R. J., "Flow Visualization Studies on the ITTC Body of Revolution," Hydronautics, Inc., Report ITTC-2 (Jan 1968).

[26]Johnsson, C. A., "Pressure Distribution, Streamlines, and Cavitation Inception Tests on a Modified Ellipsoid Headform," SSPA, PM BK 24-1 (27 Dec 1967).

The modified ellipsoid headform was used to determine significant effects in the test program. Testing the pointed headform could then be less extensive.

In the majority of tests, the procedure was to wait a fixed time, approximately 4 min, at a pressure several centimeters, usually 3 cm, of mercury greater than the inception value or about 2 ft/sec lower than the inception value. This period is called the resting state. The pressure or speed was then varied to produce cavitation.

In general, air content changes consisted of deaerating the water with the external flow deaerator. For one set of data points, the air content was raised by admitting atmospheric air to the tunnel water. In general the air content drifted toward high values during a particular test series, if the air content were less than saturation based on test section pressure, and drifted toward lower values, if the air content were greater than saturation based on test section pressure. Gas content was measured with the Van Slyke apparatus, except for tests using carbon dioxide as the dissolved gas. For these tests, the gas content was determined with a gas chromatograph. The tunnel water was deaerated to approximately 1 1/2 percent saturation relative to atmospheric pressure. Carbon dioxide gas was allowed to enter the desorber-absorber unit to bring the absolute pressure to approximately 25 cm Hg. Water was then circulated through the unit in the normal manner, except that atmospheric pressure was maintained in the tunnel. Occasionally more gas was admitted to the desorber-absorber tank to maintain the 25-cm pressure. Periodic checks of the tunnel water saturation level were made, and, when the desired level of 16-percent saturation relative to atmospheric pressure was reached, the absorption was stopped.

The discriminator setting for the occurrence counting was maintained at 0.2 V for the modified ellipsoid and at 0.08 V for the pointed headform. Blanking time was uniformly at 1 msec. The discriminator level was set to have visual and acoustic data agree for inception calls. Blanking time was sufficient to prevent counting multiple collapses. For more details see Reference 22 and Appendix A.

Accuracy of the measurements is estimated to be ± 1 percent in dynamic head and ± 0.1 cm Hg in pressure. For the constant speed tests: at 24 ft/sec, σ_i can be in error by approximately ± 1 1/2 percent; at 20 ft/sec, σ_i can be in error by approximately ± 2 percent; at 15 ft/sec, σ_i can be in error by approximately 2 1/2 percent. For the constant pressure tests, the maximum error in σ_i is about 1 1/2 percent.

EXPERIMENTAL RESULTS

During the experimentation, a criteria of one cavitation occurrence every 5 sec was arbitrarily used to define inception. A more careful analysis later indicated that one-event-per-second data were in better agreement with visual calls and produced more consistent data than the one-event-every-5-sec criterion. This is shown in Figure 4, where time stability is being checked over approximately a 2-hr period for the modified ellipsoid headform. For these

tests, the speed was held constant, and the pressure was varied. During runs the pressure was held constant for at least 3 min at 19 to 21 cm Hg pressure. Inception was generally in the range from 16 to 18 cm Hg pressure. Occasional visual calls were made. The data, for which inception is defined as one occurrence every 5 sec, indicate a slight rise in the cavitation number with time, and the values are slightly higher than the visual calls. The results for the one event per second as the criterion for inception are in better agreement with the visual calls and have less deviation from the average than do the values for the one event every 5-sec criterion. Cavitation desinence is also shown for the 2-per-second criterion. These data are in good agreement with the inception calls and have the same average value. Peterson's tests[23] show that good agreement between inception and desinence is also found for speed changes. Rate-meter overload characteristics are such that desinence data for only low rates of change are good.* Thus, the only useful desinence data are those for pressure changes which are slow enough to permit the rate-meter capacitors to discharge less than full-scale prior to reaching the criteria for desinence.

In Figure 5 the inception values from Figure 4 are plotted against the rate of change of pressure. The number beside some of the data indicates the number of points with that value. These data also indicate that the one-per-second criterion is more consistent than the one event per 5-sec. The desinence data are also shown on the plot for the one-event-per-second criterion. The scatter is slightly greater than for the inception points but small in any event. The data for one occurrence per second also indicate that the incipient cavitation number is approximately constant for various rates of change of the pressure up to 0.1 cm Hg per sec. The increase above this rate is slight, and there are not enough data available to draw conclusions.

From these tests, it is concluded that over a short time period, the cavitation inception call as determined by the occurrence counting technique is stable. Tests to be discussed next will show it is also stable over several weeks. The present tests also show that for this type of cavitation, inception and desinence (from occurrence counting) occur at the same value; hence, only inception will be considered in discussing the remaining data. No visual calls for desinence were made.

The first series in the test program was to provide reference conditions for the other tests and to provide data for the effect of air content. Figure 6 shows the effect of air content fixed at 24 ft/sec. Inception was determined by lowering the pressure at fixed speeds. The circles represent averaged values, and the vertical lines indicate the range of values. These data are all based on inception, defined as one cavitation event per second. Although the results of other tests, i.e., lauric acid as an additive and a wetting agent additive, are also shown, they will be discussed later. The line drawn through the average data points

*Once the count rate exceeds full scale, the meter remains at that point, even when the input is disconnected. A finite discharge time, depending on the magnitude of the overload, is needed before the meter again responds to individual pulses.

connects values obtained in the same water over a 20-day period. Saturation based on test section pressure at the headform centerline occurs at 21 percent air content relative to atmospheric pressure. The data show a transistion around this air content from a relatively constant or slightly rising σ_i above the air content to a relatively constant value below it. Slightly higher σ_i were obtained (8 on Figure 6) when new water was put into the tunnel. (Only the test section was drained and allowed to remain dry overnight as it was the first time the headform was out of the water since testing had started 20 days before.) This was not considered significant since the difference bordered on experimental accuracy. However, other tests with new water also showed the slight increase in σ_i; see Figure 6. The data obtained with the additives fit consistently with other new water results (8 through 12 on the curve). One set of data was obtained with water about 15 F colder than the rest of the tests. This range was thought to be representative of the range of temperatures encountered in day-to-day tunnel tests. Here, too, the conclusion was that there was at most a minor effect.

The "possible bad amplifier" notation beside callout 5 in Figures 6 through 8 has been made because the amplifier had to be changed before testing on the next workday. At the time of change, the amplifier was producing noise of sufficient amplitude to trigger the Single Channel Analyzer (SCA). It is not known whether this influenced callout 5 or not; however, since the data do not fit the trend of the other data it is strongly suspected that it did.

Figures 7 and 8 show data for 20 and 15 ft/sec, respectively. The numbers on the curves are the same as in Figure 6. Although few data were taken for new water with these speeds, they appear to have a greater effect than at the higher speed.

Figure 9 compares the results for the three speeds for the same water. In general, these curves indicate a decrease in σ_i with speed and also with air content. Again air content decrease appears to be roughly at the local saturation level. The decrease with speed needs further confirmation with visual calls as will be discussed later.

In Figure 10, the results for the reduced surface tension are shown. The wetting agent used in these tests was Tergitol, Penetrant 4, manufactured by Union Carbide. Figure 10 shows data for visual calls as obtained using the occurrence counting technique, both for the one-event-every-5-sec criterion and for the one-event-per-second criterion. The measured value of surface tension was the same before and after the test. Measurements, made with a commercial instrument available from Central Scientific Company, consisted of manometer readings of the pressure required to form bubbles of identical radius.

In Figure 11 the results of the tests with lauric acid are given in detail. The lauric acid ($CH_3(CH_2)_{10}COOH$) was obtained from Fisher Scientific Company. Based on the work of Bernd,[17] this was expected to have an effect on the inception values. It was estimated that about 50 g of the material would dissolve in the water of the 12-in. water tunnel. Approximately 300 g were poured around the high-pressure side of the filter elements used for the tunnel, and the water circulated through it for 2 hr. The tests were then performed.

The visual tests and the data for cavitation at one event per second indicate a slight decrease in σ_i with time. This is not shown in the data for inception at one event every 5 sec. Measurements at the end of the testing showed that the surface tension was the same as for untreated water. In any event, the decrease in σ_i is small enough to make further investigation questionable.

The final series of tests performed at constant speed with this headform is shown in Figure 12. In these tests, carbon dioxide was used as the dissolved gas. The gas content was 16 percent, relative to atmospheric saturation. During the inception tests, rate meter output did not occur until after the visual call had been made. It is hypothesized that the cavitation bubble contained a considerable quantity of carbon dioxide gas which cushioned the collapse, thereby producing little noise. Accordingly, the discriminator level was lowered to 0.08 V, and the value of σ_i was then considerably higher; see Figure 12. However, the majority of data are for a discriminator level of 0.2 V. Inception values were determined as one event every 5 sec. For this test, the data from the occurrence counting technique were not believed to be compatible with the other data taken; therefore, they were not shown in Figure 6.

Concurrent with the tests at constant speed, other tests were performed with the pressure held constant and the speed varied. Such tests are typical of full-scale cavitation inception. Because the flow regulator was manually controlled, no visual inception calls were made for this portion of the experiments. Figure 13 shows the data obtained for constant pressure. These data were taken with the same water and at the same time as the results shown in Figure 9 and appropriate data in Figures 6 through 8, i.e., possible bad amplifier. In general, there are fewer points than for the constant speed results. However, the data showed quite different trends from the trend shown in Figure 9 for constant speed. The results in Figure 13 indicate a minimum σ_i as a function of air content for a given pressure. Although not enough air contents were checked to allow firm conclusions, the minimum σ_i appeared to be near the saturation value, based on the test-section pressure. In general, higher σ_i values at a fixed air content correspond to slow (0.06 to 0.4 ft/sec^2) changes in speed, and lower values of σ_i correspond to higher rates of change in speed (0.6 to 1.6 ft/sec^2).

For the pointed headform, only a limited number of tests were undertaken. Visual cavitation on this headform differed from that on the other. For the modified ellipsoid headform, an extensive series of tests (discussed in Appendix A) were performed correlating high-speed movies with recorded noise pulses. Cavitation originated near the minimum pressure line in the form of discrete bubbles nearly hemispherical in shape. The bubbles traveled along the body, collapsed, and rebounded. Although similar tests were not undertaken for the pointed headform, visual observation of cavitation on this headform using strobe lighting showed that near inception, cavitation also occurred as traveling bubbles, elongated in the flow direction. At sufficiently low σ values, $0.51 < \sigma < 0.56$, a ring of cavitation formed around part or all of

the headform. Figure 14 shows the cavitation pattern at $\sigma = 0.5$. This is a single flash photograph with an exposure time of about 0.05 sec. Cavity collapse near inception did not produce signal amplitudes as large as those for the ellipsoidal headform. The discriminator level was lowered to 0.08 V to bring the cavitation-inception determination in agreement with the visual calls. Figure 15 shows the test results using two contents of air. In this series, the speed was held constant, and the pressure was lowered until cavitation occurred.

The visual inception data indicate a relatively constant σ_i value with changes in speed at 20 percent air content and a lower σ_i at 20 and 15 ft/sec than at 24 ft/sec for the low air content. The occurrence counting technique with the one-event-per-5-sec criterion indicates that σ_i decreases with speed for both kinds of air content. In agreement with the visual calls, the occurrence technique for one event per second indicates a relatively constant σ_i for the high air content results and a drop in σ_i for the two lower speeds at low air content. The one-event-per-second criterion for inception produces more consistent results and agrees with the trends of the visual calls as it did with the modified ellipsoid headform.

DISCUSSION

In this section, some trends in the data will be noted, and some comments will be made about their relation to other data both reported here and taken in other facilities. Finally, the trend of the data will be discussed in relation to the various nuclei models discussed in the introduction.

The technique used to establish cavitation on the body, i.e., speed or pressure changes, had a pronounced effect on the trend of inception values as a function of air content. The different techniques have different effects on the pressure history of a free-stream bubble and possibly different effects on boundary-layer growth, explained in the following text.

The tests made with varying speed produce different pressure changes in the tunnel than do tests for which the pressure is varied. For the tests reported here, a change in pressure of approximately 3 cm Hg from the resting state was used to cause inception. This change occurred uniformly over the entire body of tunnel water. For the speed variation tests, the waiting was done about 2 ft/sec less than the inception value. Thus, from 22 to 24 ft/sec, the dynamic head in the test section changed by approximately 3 cm Hg but in the water upstream of the model, before the 3 : 1 contraction, the pressure changed only 0.3 cm Hg. Thus, the overall effect is smaller than with pressure changes.

In addition, it is reasonable to suppose that speed changes would have an effect on boundary-layer growth and, thus, on the pressure distribution on the body. During the oil-film studies for laminar separation it was noted that it took some time after the flow was steady to establish steady-state conditions on the body, especially if the ring of oil indicating separation were being washed away at the selected speed. (However, see Reference 25 for a

different interpretation of these "time effects.") Whether this is the result of having oil on the surface is not known but it does indicate a time effect for speed changes, which could be important for low speeds.

These differences are the most obvious between the two techniques; however, it is not known if they actually contribute to the different data trends or not. They are mentioned only to point out some overall differences which have not been mentioned in the literature.

The previously described change of σ_i with air content was not noticed in previous Center tests[23] with speed changes. The same headform was used and gradients ranging from 0.01 to 1.0 ft/sec^2 showed no effect on σ_i for various air contents. However, those tests were for only one test-section pressure, $P_o \simeq 0.25$ atmosphere. The data reported here (Figure 13) for $P_o = 0.22$ atmosphere do not show as large a change as do the other two lower pressures. In addition, for the results given in Reference 23 a different criterion for inception was used than was used in this investigation.

For both headforms, a decrease in σ_i with a decrease in speed was noted in the occurrence-counting data. At the highest speed, the results of the occurrence counting were made to agree with the visual call. However, data for visual calls at the lower speeds were taken for only the pointed headform, and they did not give as pronounced an effect as did the occurrence results. In Figure 15, the average difference between visual and occurrence calls is at 24 ft/sec, $\Delta\sigma_i = 0.01$; at 20 ft/sec $\Delta\sigma_i = 0.018$; and at 15 ft/sec, $\Delta\sigma_i = 0.03$. In all cases the visual call was higher than was the occurrence call. This difference might have been caused by the bubble dynamics. That is, at low test-section static pressure, the bubble collapse might not produce peak pressures as large as those at high test-section pressure. This possibility should be further investigated since in some situations it could be as serious a drawback to the use of the occurrence-counting technique as is the adjustment of discriminator level with change in test-body shape and the expected variations with type of cavitation.

At several points in the testing program, the discriminator level had to be lowered to bring the acoustic data more in line with the visual calls. For tests with carbon dioxide as the dissolved gas, a comparison with the other data was not made. As noted in the introduction, the visual call is accepted as the standard; hence, the comparison is properly made with the other visual calls for this headform. The test series made with lauric acid (Figure 11) had an average visual call of $\sigma_i = 0.68$. Air content for these tests was 17 percent relative to atmospheric pressure. The reduced surface tension series (Figure 10) had an average visual call of $\sigma_i = 0.69$. Here the air content was 12 percent relative to atmospheric pressure. With the short term-time stability checks (Figure 4) at an air content of 27 percent, the average visual $\sigma_i = 0.70$. For the test series with CO_2, the gas content was 16 percent, and the average of the visual inception calls was $\sigma_i = 0.69$. Thus, using carbon dioxide as the dissolved gas in the tunnel water does not have a significant effect on the inception process, although it does reduce radiated noise and, by implication, perhaps reduces damage as well.

These tests together with those in Reference 23 (where the oxygen-nitrogen ratio was changed with no difference in σ_i) indicate that the important gas characteristic is the relative saturation value rather than the absolute value.

For the tests made at constant speed, the rate of pressure change had little effect on σ_i; see Figure 5. This is in agreement with the recent results[19] of the ITTC study, although the ITTC study had larger[6] variations than has been reported here. However, in the ITTC study the pressure was lowered from atmospheric until cavitation occurred rather than from the waiting pressure as adopted in this study. Ripkin and Killen[27] indicated that a waiting time at a pressure near inception helped to stabilize the free-stream bubbles.

Deviation of the data from the mean is about the same for inception as for desinence. This is also in agreement with the 12th ITTC results for large smooth test bodies (diameter > 1.75 in.) but in disagreement with data for small bodies (diameter < 1/2-in.) as well as with other experience.[3] It is expected that model size has a strong effect on this finding, the 2-in.-diam models used in this study being sufficiently large to be unaffected.

That there are differences in results for speed versus pressure changes to initiate cavitation are also supported by the 12th ITTC tests. However, no investigations in the literature showed the increase in σ_i at low air contents that was given in Figure 13. This point is mentioned later in discussing the various nuclei models.

The discussion[16] of the headform data presented to the 11th ITTC included a description of the appearance of the cavitation. Inception was found to occur at different axial locations and to be of different patterns. The photographs presented showed cavitation to be attached, and some of the descriptions noted clouds of bubbles at inception. However, one description was of traveling bubbles as were found throughout the test program reported here.

Although cavitation at inception was the form of traveling bubbles on both bodies tested in the present study, the most striking difference between the bodies was the shape of the traveling bubbles. Since both had traveling bubbles, it is hypothesized that the microscopic inception process was the same for both but that different forces acted during the growth and collapse cycles. For instance, the small calculated pressure peak on the pointed headform (Figure 2) might have triggered transition to turbulent flow, while the flow might have remained laminar on the modified-ellipsoid headform.

However, an even more complex form of cavitation was noted on the same modified-ellipsoid headform when tested in the towing basin.[20] In those tests, cavitation was observed which remained attached to a point and also traveling bubbles of both distorted and smooth shape, as were observed in the water tunnel. From these observed cavitation patterns, it was concluded[20] that the solid surface of the model was the most probable source of the nuclei. The shape difference in the traveling bubbles was attributed to different locations of the origin site relative to the minimum pressure line. No explanation is given as to why similar

[27]Ripkin, J. F. and J. M. Killen, "Gas Bubbles: Their Occurrence Measurement and Influence in Cavitation Testing," International Association for Hydraulic Research Symposium on Cavitation and Hydraulic Machinery, Edited by F. Numachi, Sendai, Japan (1962).

differences did not occur in the water tunnel or why the attached cavitation did not occur there; however, it has been concluded that the origin of tunnel cavitation might also be the model surface. The principal argument in reaching this conclusion was that the inception conditions did not depend on air content for the available water tunnel tests.[23] For the tests reported here, having a greater number of air contents, the incipient cavitation number is a function of air content. Ripkin and Killen[27] argued that the total dissolved air content (usually several orders of magnitude greater than the free-air content) supported the free-air content. As the total air content decreases, the number of free bubbles should be reduced, and it should be more difficult to initiate cavitation. Thus, the data should show a decreasing cavitation number with decreasing air content. In general, this is the trend of experiments, both those in this study and those reported elsewhere.

However, the addition of surface active materials (lauric acid) and of wetting agents should produce changes in the results. Such changes were not found. Bernd[17] argued that in his experiments the source of nuclei was gas bubbles in the liquid, and he showed that materials like lauric acid changed the cavitation properties of the liquid. He postulated that the mechanism was the formation of an organic skin at the bubble wall. Since neither of the above two additives had an effect on the cavitation number, the bubble interface did not appear significant in the present tests. In addition, for cavitation inception caused by speed changes, σ_i increased with decreasing air content at low saturation values (Figure 13). This is inconsistent with the hypothesis of free-stream gas bubble nuclei.

By default then, this would leave the solid-liquid interface as the logical weak spot. However, it is not clear how speed and air content would influence this bond. Hence, firm conclusions about cavity origin are not possible from the present experiments.

The screening calculation[6, 8] indicates a variation of σ_i which increases with speed as shown by most of the data. In addition, the location of minimum pressure on the two bodies was expected to influence the cavitation potential of the free-stream nuclei. The air-content range used for the pointed headform showed approximately the same trends as did the tests for the modified-ellipsoid headform, which would indicate screening was not important for the two shapes. Calculations for each body would be necessary to draw firm conclusions from the tests.

The data presented by Holl[3] for temperature changes in a water tunnel show that experimentally the incipient cavitation number rises with increasing temperature while the calculations for bubbles in the free-stream and in the boundary layer indicate a constant σ_i value in the normal temperature range (less than 100 F). For high increasing temperatures, either a constant or a decreasing value of σ_i is found depending on effects included in the calculations. The experimental values reported here (9 in Figures 6 through 8) show a slight decrease with increasing temperature; however, the change is not considered significant. Hence, these results agree with the calculations based on bubble growth.

The previous discussion shows that the experiments with environmental changes support in some aspects one nuclei model and in other aspects another nuclei model. All trends of the data are not explained by any single model. Holl[3] points out that different types of cavitation may occur between different facilities and even during the tests at one facility. This appears to be borne out by the present series of tests. As a consequence of this behavior, it is concluded that to date none of the postulated cavitation-inception models combines the necessary gross properties to be used in cavitation predictions.

The simplest of all scaling laws is that cavitation occurs when the lowest pressure on the body reaches vapor pressure. This assumption results in a scaling law that the negative of the minimum hydrodynamic pressure coefficient equals the cavitation number, Equation (1), when cavitation first occurs. The underlying assumption has been proven correct for static liquids used in practical situations, e.g., the boiling temperature of tap water is a unique function of pressure. Most of the studies of cavitation scale effects have considered perturbations of Equation (1). In the present study, it has been shown that cavitation events occur when the analytical minimum pressure is near the vapor pressure but that these are not in sufficient number to define an inception call, either visually or acoustically. A knowledge of the actual pressure distribution is needed before any significance can be attached to this finding.

SUMMARY

An extensive experimental program has been performed with headforms to establish environmental effects on cavitation inception. Inception calls have been made both visually and with instrumentation which have detected the rate of cavitation occurrences.

Tests were performed over a range of air contents and water speeds. Inception was established by varying either the pressure or speed while one of the two remained constant. Operations performed on the test water included temperature changes, type of dissolved gas (CO_2 was used), and additives (lauric acid and a commercial wetting agent).

The following results were obtained.

1. For tests at *constant speed*, σ_i as a function of air content was higher for air contents greater than approximate saturation relative to test section pressure than for air contents that were lower. This effect would give about a 15 percent change in σ_i, based on the extreme values.

2. For tests at *constant pressure*, a minimum in σ_i was reached at approximately test-section saturation air content. This effect was more pronounced for low pressures (and thus low speeds) than for high pressures. This effect could be as much as 25 percent from low to high σ_i at a given pressure.

3. In general, σ_i decreased with a decrease in either speed or pressure. However, it is unclear how much of this might have been caused by the physics of the bubble collapse, i.e., dynamic effects on radiated noise. Typically this effect was about 5 percent for the tests at constant speed, i.e., 15 to 24 ft/sec; and a maximum of 45 percent increase for tests at constant pressure.

4. There was a slight increase in σ_i when new water was used. This effect appeared more pronounced under local saturation than over. This conclusion is clouded by other changes to the test water. At most, the magnitude of the change would be about 5 percent at the high speed.

5. The rate of change in water speed appeared to have an effect on σ_i. In general, low gradients produced high σ_i's.

6. The rate of pressure change in the range from 0.02 to 0.5 cm Hg/sec did not have an appreciable effect on σ_i.

7. A change in the type of dissolved gas, surface tension, and temperature did not have an effect on the cavitation inception. Nor, contrary to the investigation of Bernd,[17] did the use of lauric acid as an additive have a significant effect on σ_i.

8. The two headforms exhibited differences in the cavitation bubble shape; however at high speed (24 ft/sec) and the same air content, σ_i was 0.69 for both bodies. Although both headform shapes had the same designed minimum pressure of 0.8, the agreement in σ_i values was not considered significant because of the measured machining errors on the pointed headform. (There is no reason to expect the modified ellipsoidal headform to be any more accurately constructed; however, no measurements were made.)

9. No significant difference was found between inception and desinence.

In this series of tests, the significant variables were relative air content and procedure to initiate cavitation (speed versus pressure changes). Hence, these would be the most important items to be noted in the day to day testing. In addition, the data indicate that careful consideration should be given to experimental techniques for collecting acoustical data on a model scale.

The experimental results do not overwhelmingly support the calculations based on any single model of the cavitation nuclei discussed in the introduction. The trend of the data is in general agreement with that of previous headform studies, except as noted in the discussion.

Additional testing is recommended, especially for the pointed headform.

RECOMMENDATIONS

Several additional studies using these headforms are desirable. High-speed movies with correlation of the sound pulse on a plastic model of the pointed headform are needed to

investigate the inception process and to help in explaining the need for a lower discriminator level. In addition, this investigation might contribute to the results found by Schiebe[21] in which the headform tested had two peaks in the amplitude distribution of the first collapse pulses. For the modified ellipsoid headform, the amplitude distribution had only one peak. It is anticipated that the amplitude distribution for the pointed headform has a peak centered at a lower level than for the modified ellipsoid. Perhaps the ITTC headform tested by Schiebe, with its minimum pressure located between the two extremes used in this study, might have both of the types of bubble collapses. Such a study might show that certain relative locations of cavitation would produce different amounts of noise and perhaps respond differently to the environment. The proposed experiments should help explain the differences in the shape of the acoustic-amplitude curves.

A study of the boundary layer characteristics of the pointed headform should also be undertaken. The adverse pressure gradient near the nose shown in Figure 2 might easily lead to laminar separation or change the boundary layer to a turbulent one. Time effects should also be noted in such a study.

Discussions with machine shop personnel have led to the belief that use of the numerical control lathe now at the Center will result in a close tolerance headform. Thus, the existing pointed headform should first be flycut to bring it to the correct shape and then retested.

Coordinate measurements of both headforms should be taken at sufficient points to use as input to the Douglas program.[24] The actual potential minimum pressure would then be known for comparison with the measured σ_i. (The minimum pressure for the actual shape is expected to be slightly lower than for the analytical shape.) At 24 ft/sec and 20-percent air content, σ_i for both headforms is 0.69 with fresh water. The minimum pressure for the analytical ordinates is 0.8 for both headforms.

Finally, it is recommended that the pointed headform be tested in the towing basin. When the ellipsoid headform was tested[20] in the towing basin, the type of cavitation was substantially changed. Cavitation occurred mostly at fixed locations and was distorted in shape compared to the smooth traveling hemispheres noted in the water tunnel. The pointed headform might show similar striking changes.

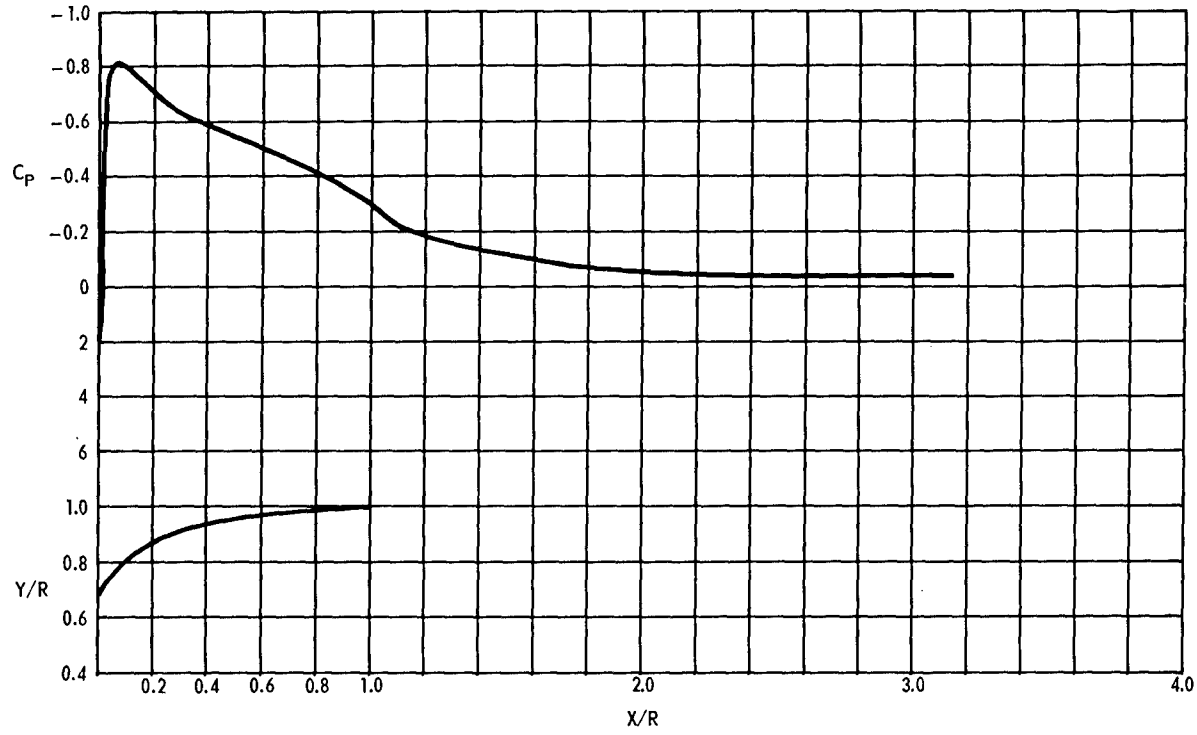

Figure 1 – Modified Ellipsoid Headform, Pressure Distribution and Shape

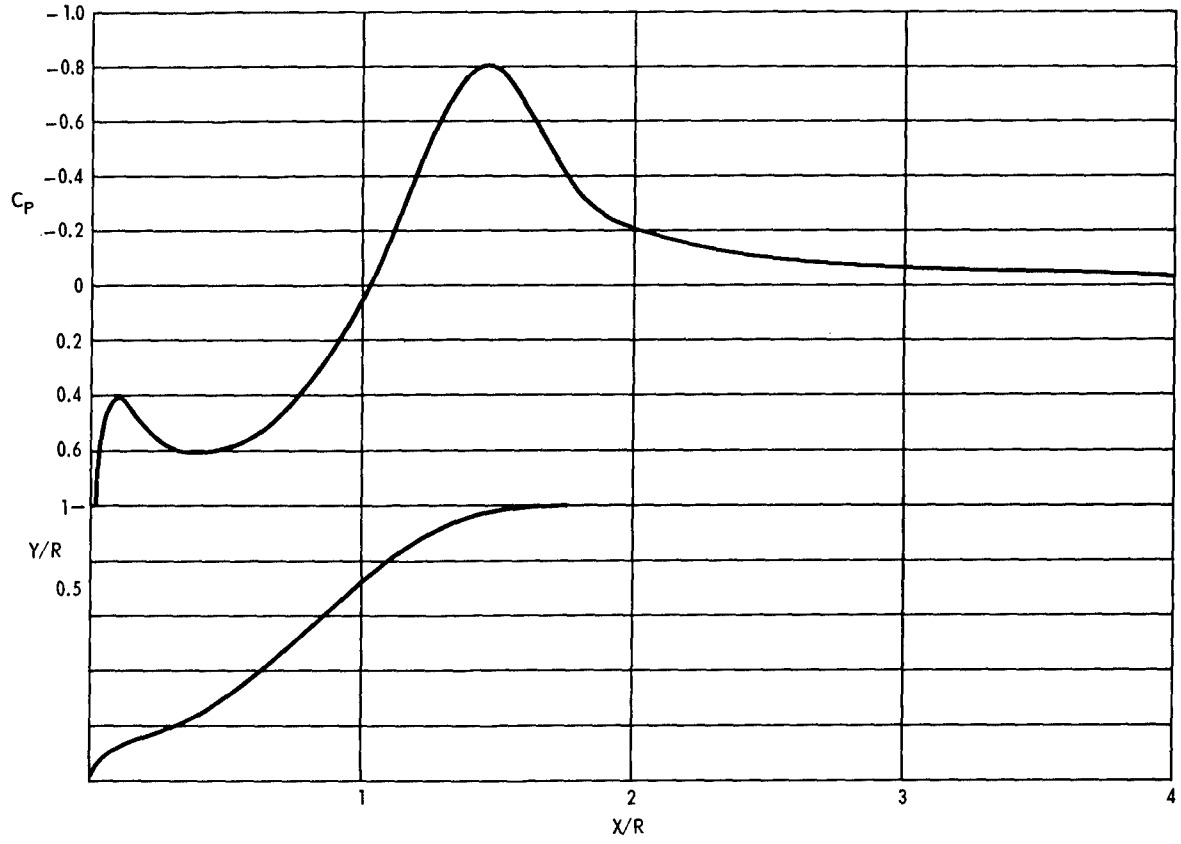

Figure 2 – Pointed Headform, Pressure Distribution and Shape

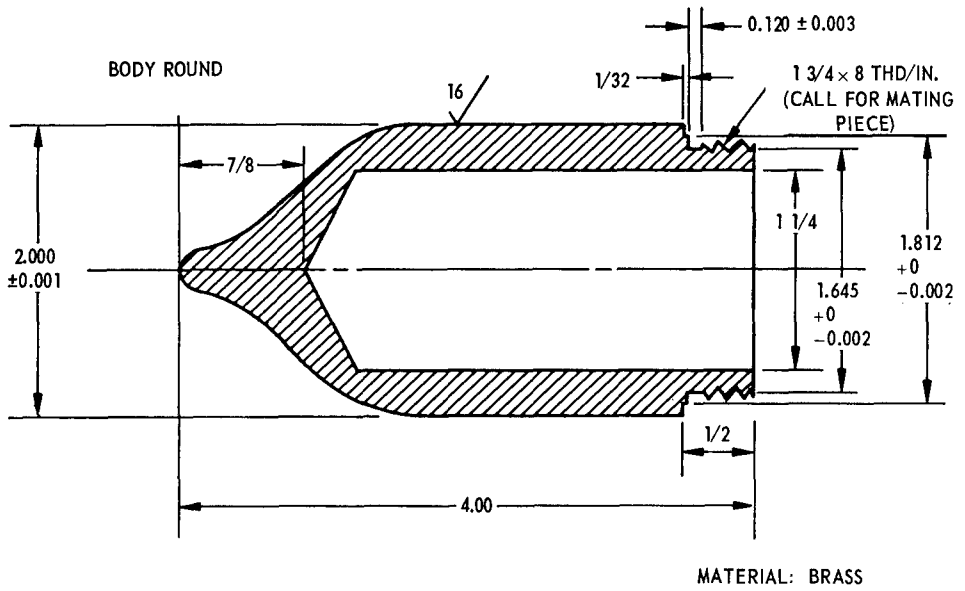

Figure 3 – Construction Details for Pointed Headform

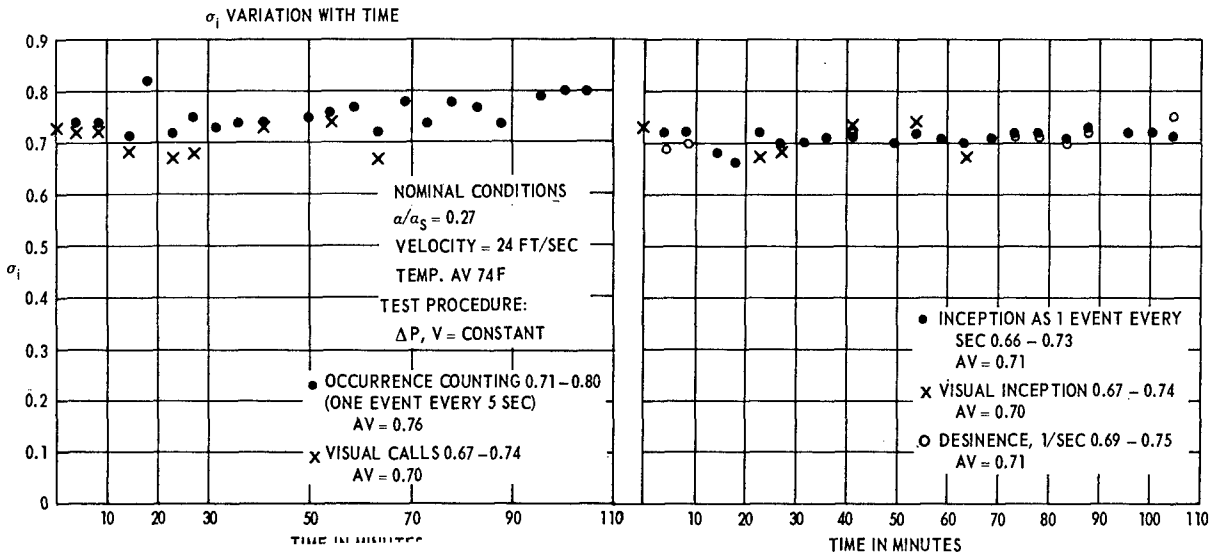

Figure 4b – One Event Every Second

Figure 4 – Short-Term Time Stability Checks with Modified Ellipsoid Headform

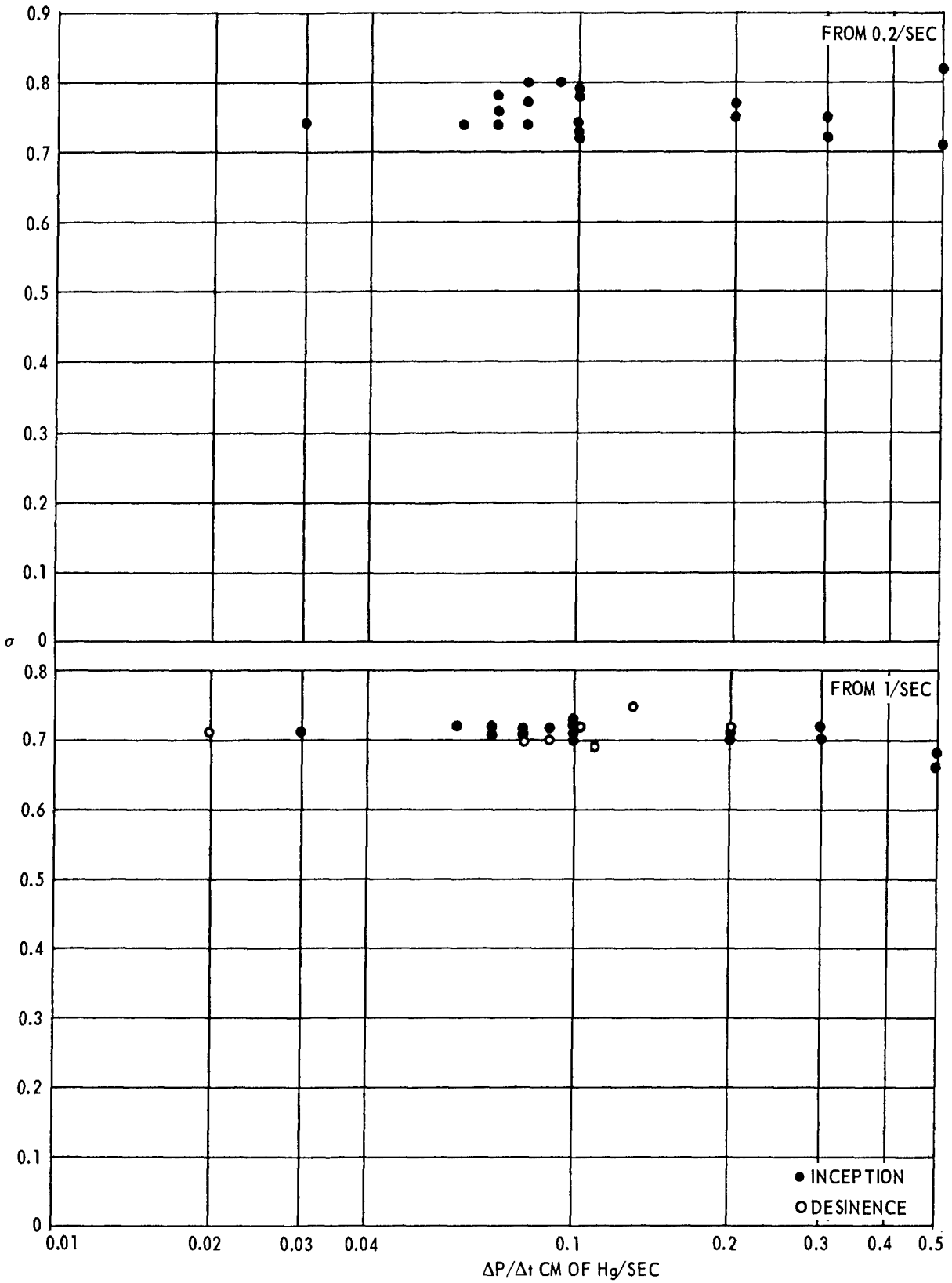

Figure 5 – Short-Term Time Stability Checks, Rate of Change of Pressure

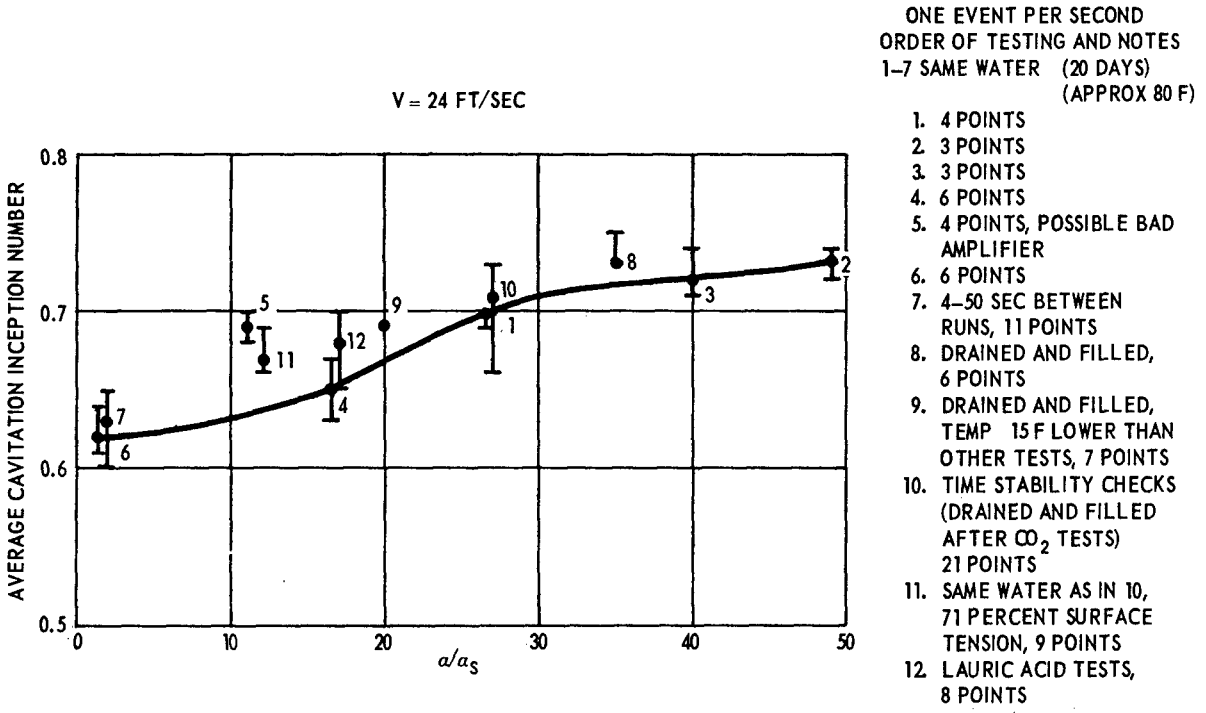

Figure 6 – Cavitation Inception for the Modified Ellipsoid Headform at 24 Feet per Second

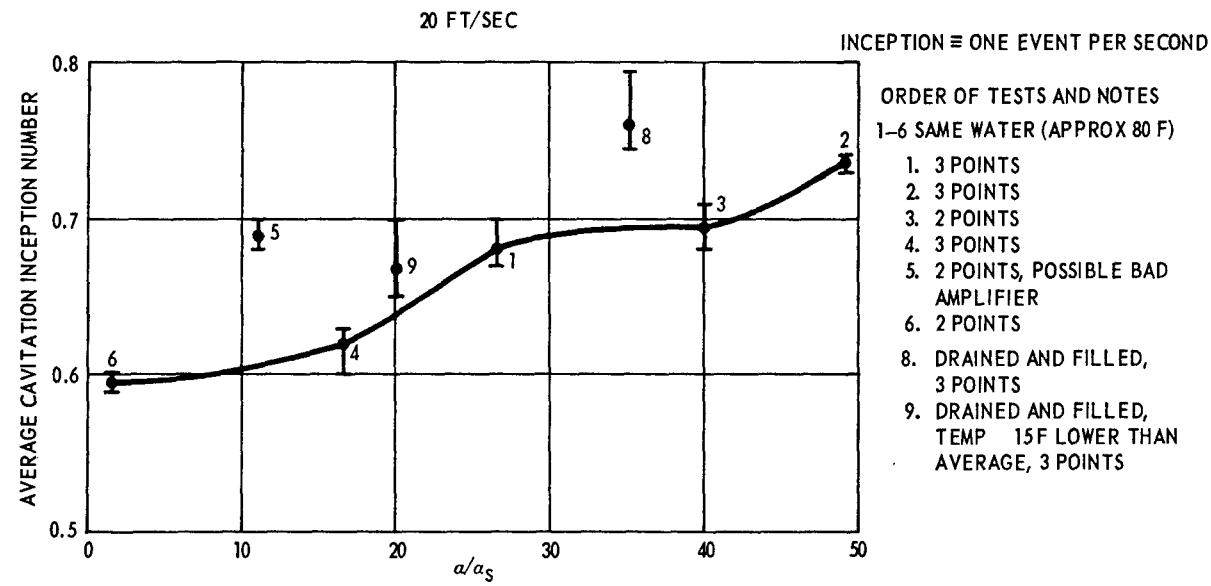

Figure 7 – Cavitation Inception for the Modified Ellipsoid Headform at 20 Feet per Second

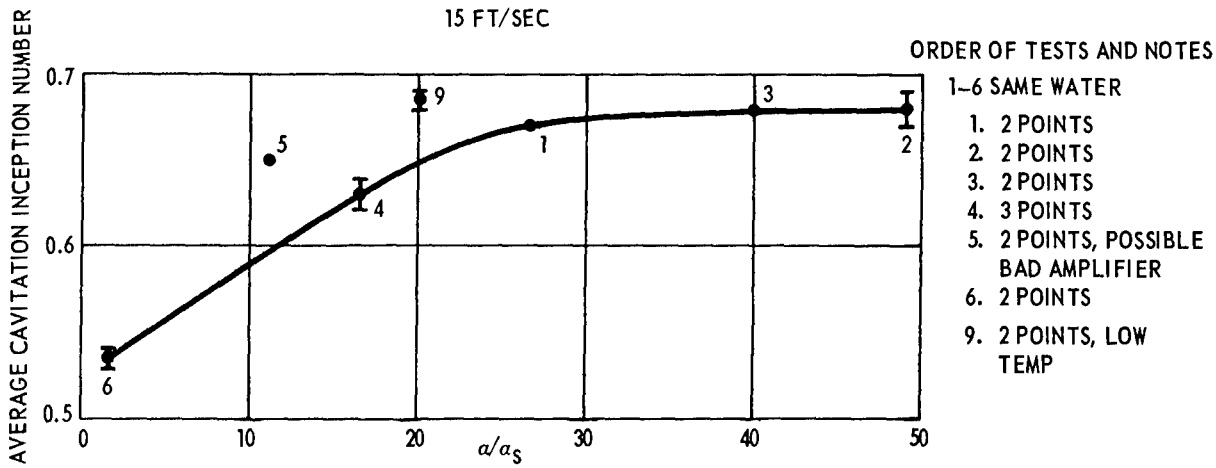

Figure 8 – Cavitation Inception for the Modified Ellipsoid Headform at 15 Feet per Second

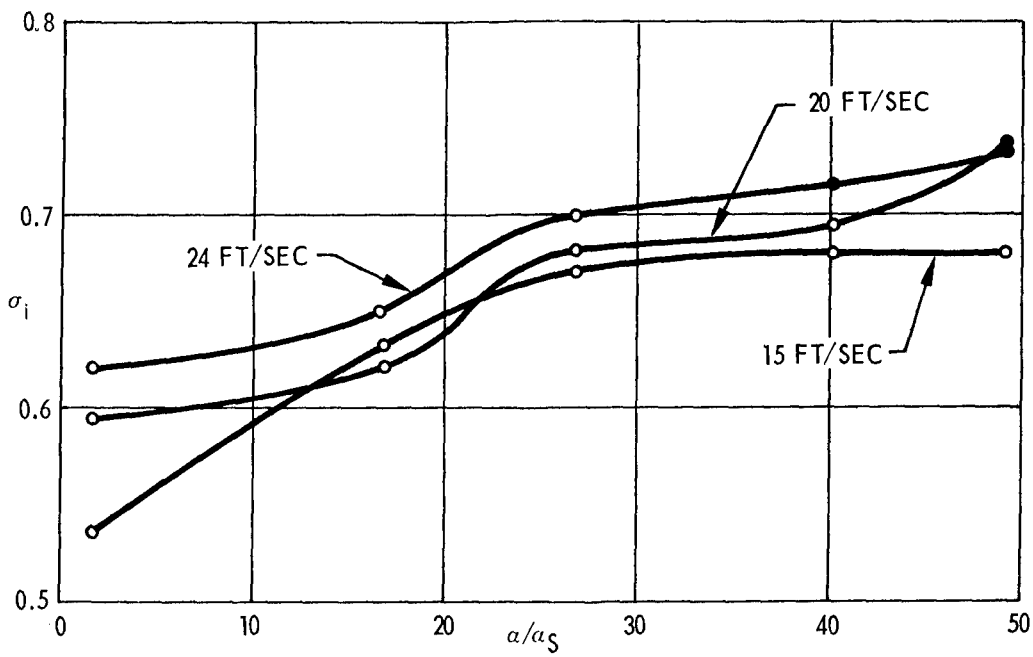

Figure 9 – Cavitation Inception for the Modified Ellipsoid Headform at the Three Speeds, Average Values

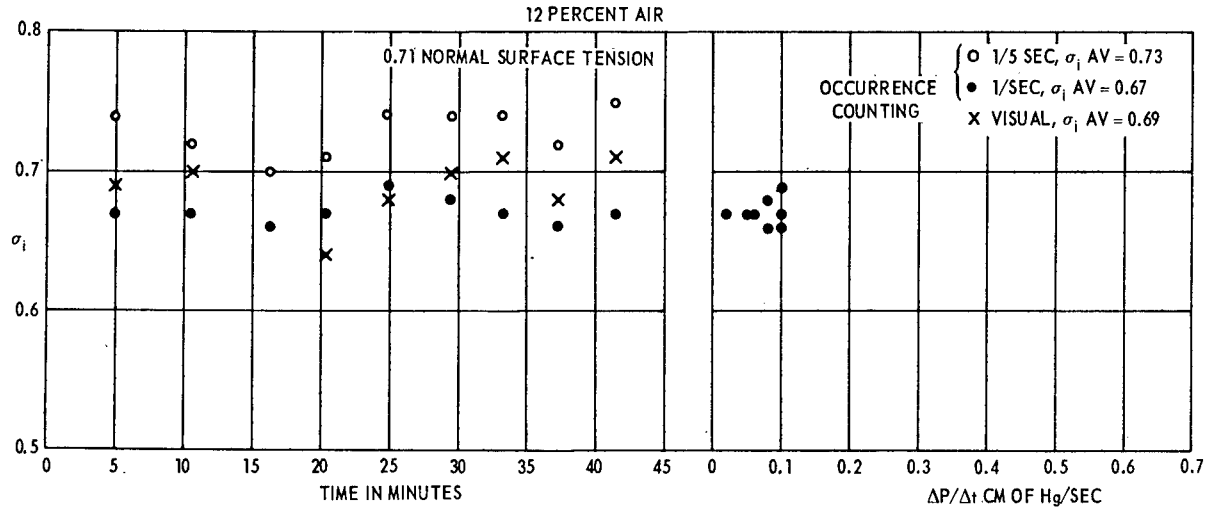

Figure 10 – Cavitation Inception for the Modified Ellipsoid Headform at Reduced Surface Tension

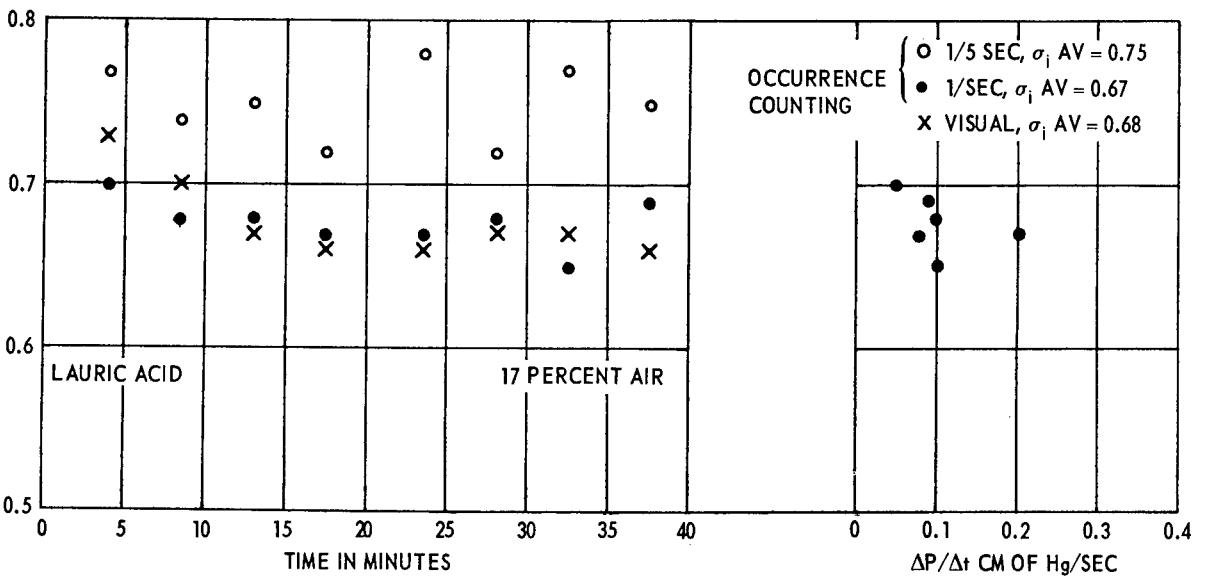

Figure 11 – Cavitation Inception for the Modified Ellipsoid Headform with Lauric Acid

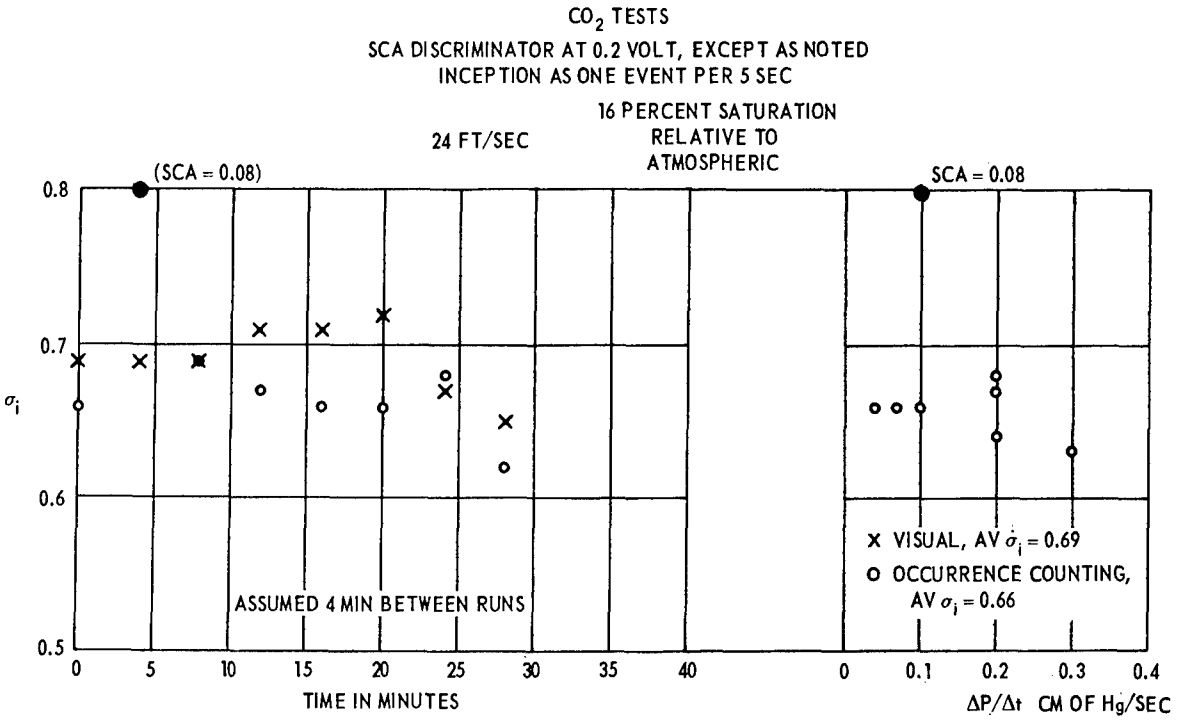

Figure 12 – Cavitation Inception for the Modified Ellipsoid Headform with Carbon Dioxide as the Dissolved Gas

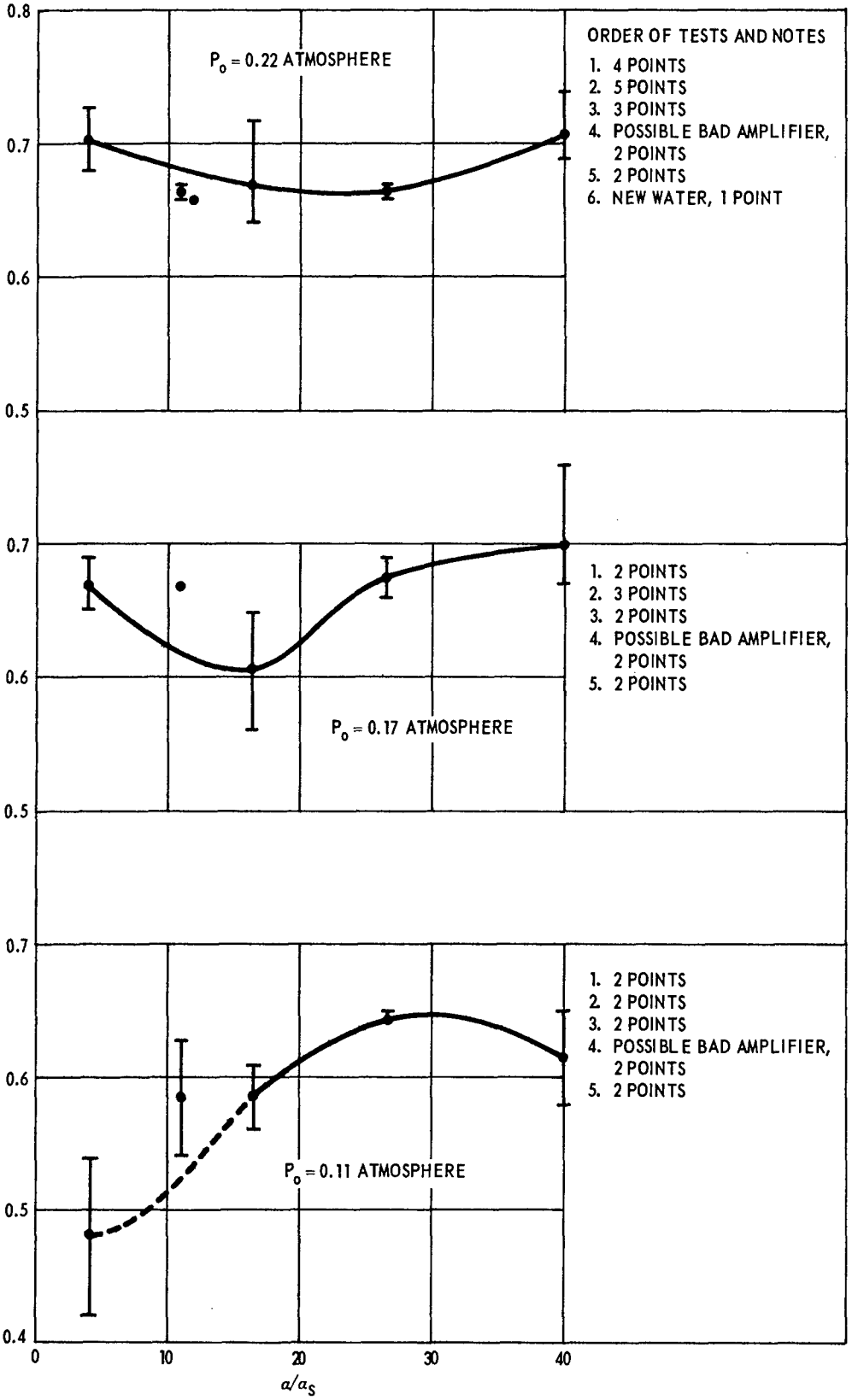

Figure 13 – Cavitation Inception for the Modified Ellipsoid Headform for Constant Pressure

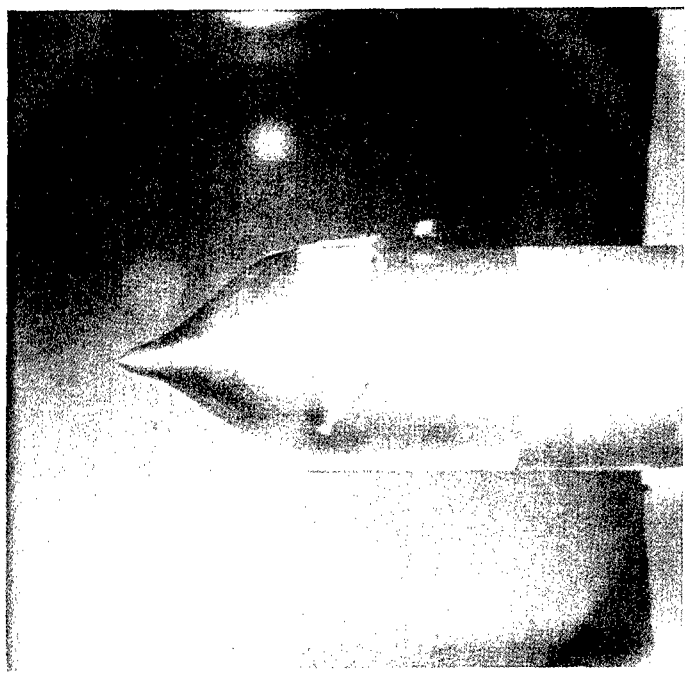

Figure 14 – Ring Cavitation on the Pointed Headform

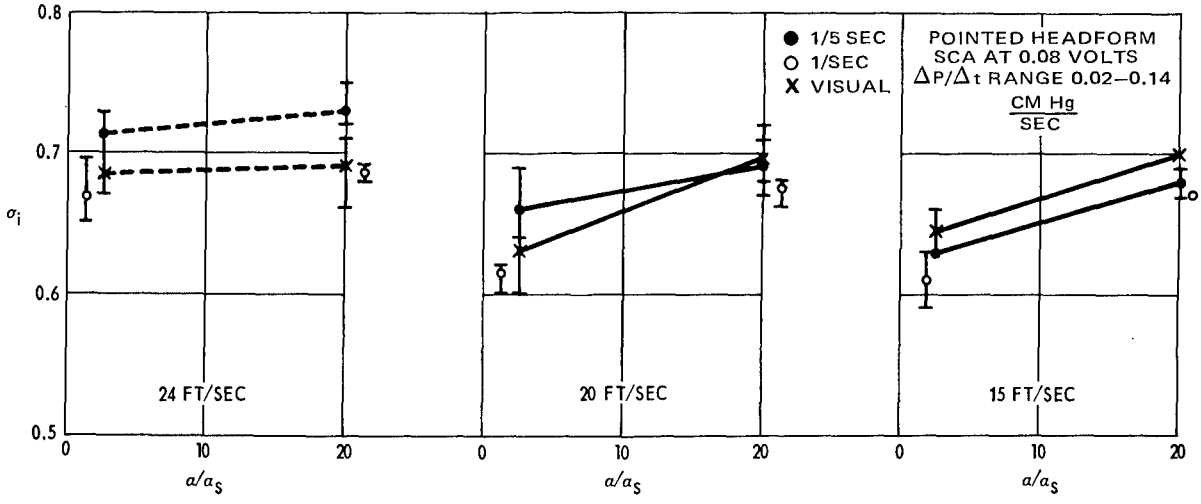

Figure 15 – Cavitation Inception for the Pointed Headform at Three Speeds and Two Air Contents

TABLE 1 – MEASURED AND ANALYTICAL ORDINATES FOR THE POINTED HEADFORM

	Measured	Analytical
X	Y	Y
00.0000	00.0000	0.0000
00.0013	00.0200	0.0163
00.0057	00.0376	0.0338
00.0096	00.0457	0.0435
00.0140	00.0558	0.0521
00.0219	00.0653	0.0640
00.0245	00.0692	0.0736
00.0316	00.0760	0.0754
00.0367	00.0808	0.0805
00.0403	00.0836	0.0837
00.0490	00.0904	0.0908
00.0586	00.0967	0.0976
00.0700	00.1036	0.1047
00.0875	00.1126	0.1139
00.1093	00.1222	0.1236
00.1320	00.1309	0.1323
00.1532	00.1387	0.1398
00.1750	00.1466	0.1472
00.1925	00.1525	0.1531
00.2187	00.1617	0.1620
00.2537	00.1727	0.1747
00.3061	00.1936	0.1958
00.3500	00.2135	0.2161
00.3937	00.2369	0.2390
00.4375	00.2623	0.2645
00.4811	00.2901	0.2925
00.5250	00.3209	0.3232
00.5688	00.3532	0.3560
00.6125	00.3886	0.3906
00.6562	00.4254	0.4269
00.7000	00.4634	0.4645
00.7437	00.5017	0.5029
00.7875	00.5412	0.5419
00.8313	00.5807	0.5811
00.8750	00.6195	0.6200
00.9187	00.6582	0.6583
00.9625	00.6957	0.6957
01.0062	00.7348	0.7318
01.0501	00.7675	0.7665
01.0938	00.8007	0.7991
01.1375	00.8312	0.8297
01.1812	00.8586	0.8580
01.2251	00.8835	0.8838
01.2687	00.9060	0.9069
01.3125	00.9265	0.9274
01.3562	00.9443	0.9450
01.4000	00.9591	0.9600
01.5312	00.9883	0.9892
01.5750	00.9933	0.9943
01.6188	00.9964	0.9975
01.6625	00.9980	0.9992
01.7062	00.9990	0.9999
01.7500	00.9992	1.0000
02.0495	00.9996	1.0000

APPENDIX A

CAVITATION OCCURRENCE-COUNTING: TECHNIQUE AND INSTRUMENTATION

APPENDIX A – TABLE OF CONTENTS

INTRODUCTION

Several years ago Schiebe[21] proposed that monitoring the rate of cavitation collapse would provide a more objective determination of inception than did existing acoustic methods or visual calls. A technique based on counting the number of collapses would provide straightforward interpretation as opposed to previous acoustic methods with which either overall noise or band levels were used to detect inception. Some of these alternate methods for acoustic detection have been discussed by Bindel,[28] Lehman,[29] Iyengar,[30] and Kendrick.[31] These alternatives are highly subjective in interpretation of both the inception condition and meaning of the level. In the occurrence counting technique a fixed rate of events could be used to identify the inception condition without ambiguity of interpretation as long as a one-to-one correspondence between a collapse pulse and a cavitation event can be established.

In the paper by Schiebe,[21] some of the instrumentation used at St. Anthony Falls Hydraulic Laboratory was discussed and experimental results for the ITTC headform were presented. In a subsequent memorandum, he related further experiences with the instrumentation.

At Carderock, a series of tests involving headforms was planned for the 12-in. water tunnel for which the counting technique appeared well suited. The results of these tests have been discussed in the main body of this report. In addition, tests[20] were planned for the towing basin for which visibility might not always be sufficient to permit inception calls. These two test series provided the motivation for the instrument development described here. Further motivation was provided by peculiar results obtained by Schiebe; in Reference 21 and his memorandum, he stated that a collapse-signal amplitude distribution was obtained which had two peaks that were attributed to different kinds of cavitation. Also it was found necessary to change the tunnel water daily to obtain consistent results.

In the following sections of the Appendix, the instrumentation is described, and results comparing photographs of cavitation bubbles with the corresponding acoustic pulse are presented for a headform in a water tunnel. These results are compared with experiments from other activities. In addition, aspects of the technique which need further investigation are described.

---

[28]Bindel, S., "Comparison between Model and Ship Cavitation, an Assessment of Available Data," 11th International Towing Tank Conference, Tokyo, Japan (1966).

[29]Lehman, A. F., "Some Cavitation Observation Techniques for Water Tunnels and a Description of the Oceanics Tunnel," American Society of Mechanical Engineers Symposium on Cavitation Research Facilities and Techniques, Philadelphia, Pa. (1964).

[30]Iyengar, K. S., "Radio Measurement of Cavitation Noise," American Society of Mechanical Engineers Symposium on Cavitation Research Facilities and Techniques, Philadelphia, Pa. (1964).

[31]Kendrick, A. L., "Techniques of Cavitation Noise Research," American Society of Mechanical Engineers Symposium on Cavitation Research Facilities and Techniques, Philadelphia, Pa. (1964).

INSTRUMENTATION

HYDROPHONE MOUNTING

The most critical portion of the instrumentation is that which changes the pressure signal generated by the cavity collapse into an electrical signal for further processing. The requirement for faithful reproduction of the sound demands consideration of the hydrophone and its placement as well as of the material between the cavity collapse and the sensing element.

A satisfactory mount is one for which the shape of the acoustic pulse monitored inside the headform is similar to that monitored outside the headform when a nearly acoustically transparent material is used for the headform. A trial and error procedure was used to find a satisfactory mount. Figure 16 shows the end product of the investigation, and Figure 17 shows it assembled and disassembled. In Figure 17 can be seen a short stub shaft which is used to hold the mount in position. The stub is mounted on the propeller shaft-support spider in the downstream nozzle of the 12-in. tunnel and is locked in place with the dished, round nut shown. An Atlantic Research LC6 piezoelectric hydrophone is pushed through the tube sting and is glued in position with Dow-Corning Silastic at the end of the tube. Since the exposed metal on the hydrophone is part of the circuit, it is covered with Silastic to prevent ground-loop noise. The tube sting is then screwed into the mount, positioning the hydrophone at the axial position where the cavitation bubbles collapse—approximately 1 in. from the nose for the headform shape shown. This position was selected to minimize transmission distortion. The shaped headform is screwed onto the mount underwater; care must be taken to insure no air bubbles are trapped inside. When the unit is assembled, the vent screw is tightened, sealing the water inside the headform. The headform is 2 in. in diameter and 3 1/2 in. in length from the nose to where it joins the mount. The headform wall thickness is 3/8-in., and the interior void extends to within an eighth inch of the nose. Both a brass and a Delrin headform of the modified ellipsoidal shape were constructed since the Delrin gives good acoustic match with water. (The calculated impedance ratio for Delrin is about 1.3 as compared with more than 10 for metals; brass is 23, and aluminum, 11.)

Figure 18 shows the headform mounted in the tunnel. Signals received with this setup and the plastic headform will be described in the section giving results of the evaluation experiments.

SIGNAL-PROCESSING INSTRUMENTATION

The experimental results to be described later show that the pulse shape is essentially a single negative peak. For the tests with the brass headform, where ringing is caused by the poor impedance matching, the significant portion of the wave is the first (negative) half cycle.

Instrumentation was assembled, having the capability to discriminate between the input acoustic pulses based on the amplitude of the first half-cycle of the cavitation collapse pulse and give the rate-of-occurrence as output. As much as possible, commercial instrumentation was used in the processing package.

A schematic of the instrumentation finally selected is shown in Figure 19. This instrumentation consists of the Atlantic Research LC-6 hydrophone to generate the electrical signal and the processing electronics. Hydrophone sensitivity is about 0.02 V/psi at the end of the cable. Frequency response is to 600 kHz. First a high-quality voltage amplifier, with a gain of 100 (40 dB), amplifies the signal. Then an electronic filter is used to remove low-frequency tunnel noise. (This filter has not been necessary in all tests but is used for consistency because of its attenuation; gain = 0.6.) Next the signal is inverted by a custom made amplifier (circuit diagram in Figure 19) which also matches the low-input impedance of the next piece of instrumentation: an Ortec Model 406 A single channel analyzer (SCA), which generates a 10 V spike for each input signal exceeding a preset positive voltage level.* These spikes are routed into another custom made unit which is essentially a one-shot multivibrator with an adjustable pulse duration, followed by a differentiator to make one positive spike for each pulse. This adjustable pulse duration, or blanking time, permits all but the first half cycle of the signal to be rejected. The differentiated output spike is fed into a Canberra Industries Model 1480 linear ratemeter, where the pulse rate is detected and displayed.

Figure 20 shows the frequency response of the electronic filter at high pass of 10 kHz. Also shown is the frequency response of the buffer amplifier and the combined frequency response seen by the SCA.

EVALUATION EXPERIMENTS

The instrumentation was assembled, and preliminary testing was performed. Although the units worked properly, two questions remained. What is a proper discriminator level? What is a proper blanking time? To answer these questions and also to gain more insight into the cavitation process, high-speed movies of the cavitation were taken while the hydrophone output was being recorded on a high-speed recorder. A straightforward evaluation of the instrumentation would have been to check that every spike occurring at the hydrophone corresponded to a cavitation collapse. This was not attempted because of the difficulty of photographing the entire headform surface. Instead, the film showing one side of the body was analyzed, and each bubble on the surface was noted. At each film position for which a bubble was seen, the corresponding location on the tape was examined for sound. The amplitude

*This unit will accept input pulses having a wide range of rise times. Another manufacturer's unit with rise-time adjustment could not be set satisfactorily.

distribution for these sound pulses gives a guide for the discriminator setting, and the time between the first and subsequent collapses for each bubble determines the blanking time.

Color movies were taken of the headform with cavitation bubbles present. The 16 mm film was rated ASA 125. It was found necessary to force develop the film by one stop to ASA 250 for the black Delrin headforms but not for the brass headforms. For three of the four tests reported, film speed was 5000 frames per second, and it was 11,000 frames per second for the other tests. The overall *f* number was 2.8 for the black plastic and 4 for the brass. Exposure time was one-tenth of the time between frames.

The camera used in these studies was a Redlake Hycam with a slotted-disk shutter. When the slot in the disk rotated past a photoelectric pickup opposite the shutter, a pulse was produced as each frame was exposed. This frame pulse was also recorded on the tape to correlate the film with the tape. In addition, the output from a timing-mark generator was recorded on both the tape and film to provide another check of the correlation and to establish film speed. The timing mark generator put out a 300-V spike every msec, two spikes every 10 msec, and 3 spikes every 100 msec. These spikes are put on the film four frames before it is exposed; however, they are put on the tape as they are being generated. Thus, the marks on the film are delayed four frames.

Illumination was provided by 2 high-intensity theatrical arc lights and 11, 1000-W focusing, sealed-beam lights. One arc light and four sealed-beam lights were shown through a clear plastic hatch cover. Three sealed-beam lights were aimed through the far viewing port and were reflected to the headform with a mirror placed on the bottom of the open-jet test section. The other arc light and four sealed-beam lights were used at the front observation port. In addition, two 750-W flood lights were used to illuminate a white cardboard sheet at the far observation port for background. Figure 21 shows the lighting arrangement and instrument rack.

The signal from the hydrophone was amplified and filtered with a 10 kHz high-pass active filter. The output of the filter was recorded on high-quality magnetic tape with an Ampex FR 1300 tape recorder operating at 60 in./sec. At this speed, frequency response to 300 kHz is expected. Noise of approximately 0.08 V was played back on the recordings. It is not known if this noise is from the flow and tunnel operation or from the instruments, but it is suspected to be flow and tunnel noise.

Figure 22 shows the instrumentation wiring. No special care was needed for grounding with this setup.

The headform used in these tests was the modified ellipsoid described in the main text that was taken from the work of Rouse and McNown.[18] Both black Delrin and brass headforms were used. Most of the data were taken on the plastic headform. They will be discussed in the following section.

The film was examined with a projector having a frame counter. The film could be run forward and backward at speeds up to 24 frames per second. The frame location of bubble

appearance, collapse, and eventual disappearance was noted. For each location on the film where a bubble was found, the corresponding location on the tape recording was analyzed for the acoustic signal. Figure 23 shows the tape analysis. The frame counter on the film projector gave the location of bubble collapse. This number was set on a Hewlett Packard preset counter, and the tape was played back from a position well ahead of the start of the frame pulses.

From the film record, bubbles as small as about 0.01 in. in diameter could be measured. It is expected that bubbles about half this size could be seen if they were coming from the free stream and were cavitating on the body since the free-stream location would be known. The majority of bubbles were measured with the black headform as background. The maximum dimension would be the distance across the highlight. Thus, the possibility exists that the bubbles are slightly larger than measured since the edge definition might be poor. This error is estimated to be less than 15 percent and would not apply to bubbles in silhouette on the outline of the headform.

Noise in the system was a function of pressure and speed. When the tunnel was still, the single channel analyzer would not trigger even with nominally zero volts for the discriminator setting. For the experimental results to be discussed, the playback tape noise was 0.08 V. This limited the amplitude resolution from the recordings to about 0.1 V.

The tape and film record were synchronized by use of a timing-mark generator as mentioned previously. The groups of three spikes occurred at sufficiently large intervals that they could be considered event marks, i.e., unique positions. At several points on the film, a collapse occurred near one of these three spikes. These were displayed on the oscilloscope and were photographed with the hydrophone signal and frame pulses. For all cases that this was done the acoustic pulse was found to occur at bubble collapse as determined from the film.

RESULTS OF EVALUATION EXPERIMENTS

Use of the Delrin headform provided acoustic signals that were considered good reproductions of the sound generated at the bubble collapse, determined by comparison with signals measured in the flow field. Thus, the following discussion will be concerned mostly with these results. Cavitation bubbles on the brass headform were similar but the acoustic signal was different and will be discussed later.

A summary of test conditions and results for the plastic headform is given in Table 2.

Because of a gain of 1.7 between the point of recording and the point determining the occurrence rate, the recorded signals greater than 0.3 V equivalent to a SCA discriminator level of 0.5 V. Table 2 shows that only one-third of the average occurrence rate was found from the analysis of the recordings.

TABLE 2 – SUMMARY OF EXPERIMENTAL RESULTS WITH PLASTIC HEADFORM

Water Speed	24 ft/sec
Static Pressure at Headform Axis	6.6 in Hg
Cavitation Number	0.67
Temperature, deg F	83
Air Content:	
Relative to Atmospheric	10.5 percent
Relative to Static Pressure	48 percent
Overall Average Occurrence Rate During Run in Events per Second	25
Discriminator Setting	0.5 V
Blanking Time	1 msec
Total Visible Occurrences in Film	124
Corresponding Collapse-Pressure Amplitudes greater than 0.3 V	78
Approximate Elapsed Time for Film Recording	10 sec

Table 3 is an analysis of the film. The frame location of first bubble appearance on the film is given; maximum bubble size is given; location of collapse and last appearance on the film are given. Film speed is also tabulated, with a maximum of 5500 frames per second. Results of the tape analysis are also listed in Table 3. The maximum amplitude of the signals is given together with the time elapsing to the second collapse, if one has occurred.

The cavitation bubbles were always translating along or near the surface. Most bubbles appeared to originate on the body near the minimum pressure line and to grow and collapse as they moved along the body. The bubble wall was smooth and approximately a hemisphere. Some bubbles appeared to be flatter than a hemisphere. Although no bubble wall distortion was seen in the growth and initial collapse, distortion did occur in the rebound and second collapse for some of the bubbles. In a few cases it appeared that the bubble had broken up at initial collapse.

A typical sequence of bubble growth and collapse is shown in Figure 24. Total time for this sequence is about 3 msec. The noise signature is shown in Figure 25 where the frame pulses are also given. The initial positive voltage spike in this picture was typical of signals received. The polarity of this spike corresponds to a tensile wave which is in disagreement with the expected compression at bubble collapse. The negative voltages, corresponding to the compression portion of the cycle, are considered the significant portion of the signal, and all data in Table 3 are based on the maximum amplitude of that portion of the wave. The signal shown in Figure 25 would result from an amplitude of the compression wave

of approximately 0.8 psi at the hydrophone. Numbers on the frame pulses correspond to numbers on the frames in Figure 24. This is the bubble starting at frame number 15581 in Table 3. The distortion appearing in some of the early frames has been caused by highlights from the many lights used. (Only bubbles in this location on the headform had the individual highlights. The same effect was noted in the tests with the brass headform.) In the rebound, it appears that the bubble breaks up but coalesces in the last frame.

Figure 26 shows another bubble sequence on the plastic headform with the bubble originating in the free stream. This is the bubble which starts at Frame 13297 in Table 3. No acoustic signal was found for this bubble. As can be seen from Table 3, this is typical. That is, cavitation bubbles,* which apparently have originated in the free stream, generally do not produce noise, while bubbles that appear to originate on the body do produce noise. However, size resolution was limited to about 0.01 in. Thus the possibility exists that all cavitation bubbles have originated in the free-stream nuclei which are too small to be seen in the film. The large quantity of air believed to be in the free-stream nuclei might account for the absence of the acoustic signal. The original film record indicated most of these free-stream bubbles cast a shadow on the body, indicating they were a short distance from the surface. This increased distance would also contribute to a decreased acoustic signal.

Figure 27 shows typical oscilloscope traces from the tape analysis. Variations in maximum amplitude and time to second collapse can be seen. As can also be seen, the pulse shape for the headform cavitation is complicated. The wave forms show an initial voltage rise, corresponding to tension, followed by a large negative spike, corresponding to compression. As already explained the compression is considered the significant portion of the wave. In these pictures, it can be clearly seen that the decay is not smooth but has many satellite peaks superimposed. Although the mechanism is not known for the leading positive voltage pulse, it has been ignored because so little energy is involved with it. Comparisons have been made with the pulse shape from other investigations made later, and it has been found that such shapes have been described previously.

The amplitude distribution for the initial compression pulse is shown in Figure 28.** As can be seen, there is considerable randomness in the graph; however, only one peak is obtained as opposed to the two peaks reported by Schiebe,[21] who argues that his two peaks correspond to different types of cavitation.

Bubbles occurring on the brass headform were visually similar in shape to those on the plastic. However, noise signals were considerably different. The difference was probably caused by the impedance mismatch between water and brass. Assuming that the collapse is on the surface so that the sound travels directly through the brass to the water-filled interior,

---

*The point of view taken in this report is that the visual appearance of cavitation is the standard. This requires that bubbles which grow to sizes comparable with the other data with no apparent detrimental effect are also included in the analysis.

**A scale error was found in the distribution reported at the 1969 American Society of Mechanical Engineers Cavitation Forum.[22]

one would expect that most of the sound should be transmitted into the interior water, and little should pass back into the brass. Thus, the pressure waves are being reflected with little attenuation in the interior, and the signal is much different from that of the plastic model. Signals with the brass headform are shown in Figure 29.* These are from large cavitation bubbles. As can be seen, the received signal is quite different from the plastic. These figures also show that the first negative spike is not always the largest, although the results of the plastic headform show that the first negative pulse is most significant.

Table 3 shows that only 16 (13 percent) of the cavitation bubbles occurred on the lower portion of the body while 77 (62 percent) of the bubbles occurred on the upper portion. This progressive decrease of the number of bubbles with depth might be caused by the hydrostatic pressure gradient; see Figure 14. No alignment check was made at the time of these tests. The headform was later reinstated and was found to be out of alignment with respect to the downstream nozzle by 0.3 deg, nose down. This alignment error is insignificant (besides not being in the right direction to explain the results) and cannot be used to explain the differences in preference for the upper surface. Visual observation had not indicated a preferential location; however, observation was generally done above the centerline, so the lack of bubbles on the lower surface would not be noticed. No other preference was noted. No correlation was found for maximum bubble size versus collapse amplitude. For the bubbles in Table 3, Figure 30 shows the collapse pressure amplitude versus maximum dimensions. As can be seen, only in general does the amplitude increase with size. As already mentioned, the most accurate size measurements were made for bubbles in silhouette. A separate plot was made for only these bubbles but no improvement in the scatter of Figure 30 was found.

The information sought with the experiment just described was a reasonable discriminator setting and a reasonable blanking time. Obviously the discriminator setting will depend on the material and size of the headform as well as the bubble dynamic while the blanking time should not change unless the pressure and velocity field change. The amplitude distribution plot (Figure 28) shows that the interval containing the largest number of pulses is that from 0.3 to 0.4 V, and only 14 percent of the pulse amplitudes appear below 0.3 V. Thus, the value of 0.3 V is a satisfactory discriminator level. It is more than twice the noise level and most of the pulses (86 percent) are higher than this value. This corresponds to a value of 0.5 V at the SCA, since the buffer amplifier has a gain of 1.7.

From Table 3, the maximum time to the second collapse was found to be 0.85 msec. A value of 1 msec was chosen as the blanking time. This blanking time has a negligible effect on the true count rate of the inception conditions.

In actual practice the discriminator level was determined for the brass headform by comparing with visual calls: a value of 0.2 V at the SCA was generally used. The 1 msec blanking time as determined for the plastic headform was used for tests with the brass model.

*The film footage corresponding to these traces is part of an unclassified 16 mm color movie produced by the Center, "Cavitation Inception on a Headform in a Water Tunnel and High Speed Basin," TMB-M2205 (Mar 1969).

DISCUSSION OF ACOUSTIC PULSE

Cavitation patterns in the form of traveling bubbles are not unusual near inception.[16, 19, 20] However, the shape of the acoustic collapse pulse has been examined in few investigations of the cavitation phenomena in hydrodynamic situations. Hence, the discussion will be concerned mostly with the collapse pulse.

In tests[20] performed in the towing basin, using the same shape headform, a bubble lifetime, i.e., from first appearance to *initial* collapse, of the order of 1 msec was reported for hemispherical bubbles. From Figure 25, a bubble life in the tunnel is about 2.5 msec. The calculated time of collapse[32] for a spherical cavity in unbounded inviscid flow is proportional to the inverse of the square root of the static pressure. Although the conditions of the headform data are not identical with the spherical bubble, the overall effect should be approximately correct. The pressure ratio between the two facilities is such that a factor slightly greater than two should relate the bubble lifetimes; hence, the lifetimes are considered consistent.

The two points to be discussed about the acoustic data are (1) the shape of the pulse and (2) the peak-amplitude correlation with the bubble-size data. Several investigations have been made for the pulse shape at cavity collapse. Most of these are given in the reference lists of Iyengar[30] and Jones and Edwards.[33] Unfortunately these investigations have usually been of cavitation bubbles produced by a spark discharge or exploding wire or of bubbles produced in an oscillating pressure field. However, Harrison[34] has investigated noise-pulse shapes for cavitation in a venturi and with spark bubbles. He reported similar pulse shapes, except that the venturi experiments gave shorter pulses. He did not show photographs of the pulse shape but reported that, after correction for transmission distortion, the venturi pulses were described by $\exp(-|t|/\alpha)$, where α was between 10 and 30 μsec. The signals shown in Figure 27 took less than 10 μ sec to reach e^{-1} of the negative peak value. The pulse shapes in Figure 27 are more complicated than a simple exponential decay; the wave forms show an initial rise followed an almost instantaneous large negative spike. The decay is not smooth but has many satellite peaks superimposed.

Jones and Edwards[33] have given a schematic of the pulse shape which is quite smooth both in its rise and decay. Their pulse must travel through both a Duralumin bar and a glass rod before it is recorded. Hence, these data are not suitable for comparison.

---

[32] Lamb, H., "Hydrodynamics," Dover Publications, Inc., New York (1945).

[33] Jones, I. R. and D. H. Edwards, "An Experimental Study of the Forces Generated by the Collapse of Transient Cavities in Water," Journal of Fluid Mechanics, Vol. 7, Part 4 (Apr 1960).

[34] Harrison, M., "An Experimental Study of Single Bubble Cavitation Noise," David Taylor Model Basin Report 815 Revised Edition (Nov 1952); Journal of the Acoustical Society of America, Vol. 24 (1952).

Millen[35] measured pulse shapes for spark-gap bubbles and has shown the pulse shape, which is quite similar to those shown in Figure 27, except for the initial peak indicating tension. The frequency response of his system was roughly the same as that used in the present study.

Using a focused array of magnetostrictive devices, Bohn[36] obtained photographs of cavitation pulses. The response of his hydrophone system was fairly uniform to 1000 kHz. The majority of the photographs presented show shapes without the initial tension. For a very short pulse duration (~3 μ sec) obtained in undersaturated water (air content 70 to 80 percent) he presented two examples having a leading peak indicating tension.

Hence, the pulse shapes found in this study are similar to some of the results found in the literature for cavitation bubbles in water produced by spark gaps and by oscillating pressure devices.

The other point needing discussion is the relationship between the bubble size and collapse amplitude. For most investigations [33–35] for which such correlation has been attempted, a single curve relating maximum size (or lifetime) of the bubble to collapse amplitude was found. For the artifically generated bubbles, e.g., spark-gap generation, uniformity in the results is expected. Even Harrison[14] argued that his venturi cavitation nuclei were air bubbles in the flowing liquid and were uniform. No such claim can be made for the nuclei in this investigation. One previous investigation did find a variation in collapse amplitude with initial air content. Osborne[37] measured the collapse pressure for bubbles of different air content. Although no observation of maximum size was made, collapse time was measured and no single curve relating the various quantities was found. In these tests the hydrophone-amplifier frequency response peaked at 30 kHz and fell off rapidly at more than that frequency. In addition, the volume of water was quite small and considerable reflections could be expected. Although these results are somewhat inconclusive, another investigation by Millen[35] also indicates the variability in the acoustic pulse amplitude in certain situations. He reported that with fresh water, his results were erratic until the water had stood several days, during which time the gas content reached equilibrium. Ripkin and Killen[27] indicated that a continual supply of free gas in circulating water would occur. Such free gas would cause the water to be always like the fresh water in the Millen tests. This would indicate that the free-stream gas bubbles would be the dominant form of cavitation nuclei. However, a test series with the brass model of this headform, discussed in the main text of the report, had cavitation patterns similar to those on the plastic headform, and the data did not entirely

---

[35]Millen, R. H., "An Experimental Study of the Collapse of a Spherical Cavity in Water," Journal of the Acoustical Society of America, Vol. 28 (1956).

[36]Bohn, L., "Acoustic Pressure Variation and the Spectrum in Oscillatory Cavitation," (In German) Acustia, Vol. 7 (1957).

[37]Osborne, M. F. M., "The Shock Produced by a Collapsing Cavity in Water," Transactions American Society of Marine Engineers, Vol. 69 (1947).

support conclusions based on this model. It may be that part of the cavitation nuclei originate in the free-stream and that the air content of the bubbles varies sufficiently to produce the marked variations in collapse amplitude shown in Figure 30.

One motivation for the present study was the result found by Schiebe[21] for the time instability of his date and the amplitude distribution curve with two peaks. The test series for environmental effects found no time instability. The more interesting result obtained by Schiebe was the amplitude curve, since he interpreted the two peaks as two different types of cavitation. The plot in Figure 28 is interpreted as having only one peak. The randomness in the data (Figure 30) and the previous discussion of the possible explanation indicate that conclusions based on the amplitude curve would be questionable.

The main purpose of this discussion section has been to show that the pulse shape and correlation of size versus noise peak are not anomalous but are consistent with results from other experiments. Conclusions about the utility of the counting technique are given later.

INSTRUMENTATION FOR CAVITATION-INCEPTION STUDY

The brass headform used in the evaluation experiments was tested for cavitation inception in the 12-in. water tunnel at the Center. The inception condition was determined with the instrumentation just described. The results of this study have been given in the main body of the report.

To provide for data consistency as well as possible reevaluation, the data were recorded on a Sandborn chart recorder. The ratemeter output was displayed on one channel; dynamic head, i.e., speed, on a second; and pressure, on a third. The time between runs and rate of change of the variables could be determined from this record. The Sanborn recording for a typical run is shown in Figure 31. The various traces are marked in the figure.

The first series of tests was performed to investigate the effect of the discriminator setting. Inception was defined as one event per second for these tests. As can be seen in Figure 32, as the discriminator level is raised the incipient cavitation number decreases. Both speed and pressure changes were used in these studies as shown in the figure. For consistency, these data were all run at relatively high rates of change. No data were taken at less than 0.2 V for pressure changes. The ratemeter time constant (time to discharge to $1/e$ of the pulse amplitude) used for all tests was 0.5 sec.

The instrumentation was also used to detect cavitation on a second body. What is significant in relation to the counting technique is that at the discriminator level used for the modified ellipsoidal headform, inception with the counting technique occurred systematically after the visual call for the new headform. At the time the visual call was made, no signals had exceeded the 0.2-V discriminator level. The discriminator level was lowered to 0.08 V to agree with the visual call.

This was done at the high-speed condition. At the two lower speeds, there were differences between the visual and counting inception values. These differences were systematic; the lowest speed, and therefore lowest inception pressure, had the greatest difference. Visual calls were not made at the lower speed for the modified ellipsoidal headform, thus it is not known if similar discrepancies would have occurred. Although the discriminator level changed, the one-event-per-second criteria were satisfactory when the new headform was used.

For a series of headform tests[20] in the towing basin, the inception calls were made with the counting technique also. With the plastic headform and a discriminator setting of 0.5 V, no acoustic signals triggered the SCA--even when cavitation was visible on the body. Spot cavitation[20] was observed on this body. When the discriminator was lowered to 0.2 V, acoustic and visual cavitation occurred about the same time. High-speed movies and tape recordings of the acoustic signals for other runs were later analyzed. Typical photographs were shown in Reference 20. The sound records showed only a few signals with amplitude typical of those found in the water tunnel. Apparently the cavitation patterns in the towing basin were such that the noise was less intense than for the traveling bubbles in the water tunnel.

The implications of the previously described findings are discussed in the next section.

COMMENTS ON THE COUNTING TECHNIQUE

The results of the counting technique to date have been encouraging. By recording the ratemeter output, future reinterpretation of the results is possible as has been shown in this study. In addition, a quantitative result is obtained as opposed to the qualitative result obtained from visual calls or previous acoustic methods. Sufficient adjustments are available to permit an arbitrary definition of inception or to change the definition when necessary.

As with any new instrument, several areas need further investigation. Two of these are the effects of model size and type of cavitation. It is expected that changes in model size would affect the count rate relative to visual calls. For instance, Schiebe,[21] using a 5/8-in.-diameter headform, found that 10 events per second was equivalent to visual inception, while the results reported here correlate for about one event per second. Based on the experience reported here, some of this difference might have been caused from using a different facility and a different headform shape. However, one does expect that a difference will occur from using different model sizes. Sufficient experience might lead to a universal curve, giving model size versus rate of occurrence for inception. Note that for the experiments reported here both of the headforms were of the same diameter, and the same rate of occurrence was used for inception.

The type of cavitation, i.e., spot or sheet as opposed to traveling bubbles, occurring on the headform is expected to be a critical factor. The discriminator setting had to be

adjusted for differences in body shape and for operation in a different facility. Hence, visual calls are needed in order to calibrate the instrument. In some situations this would be a serious drawback to use of the counting technique. Further work is needed for this aspect.

Another problem with the type of cavitation involves the dynamic scale effects on the radiated noise. Results from the tests of the new headform discussed in the last section indicated a systematic though small difference between visual and occurrence inception values as the speed was decreased. It is hypothesized that the amplitude of the collapse pulse depends on the static test-section pressure and thus, produces low amplitude signals at low pressures with a consequently lower inception value. If this hypothesis is correct, it is a serious drawback to the use of the counting technique since σ_i determined with it would be a function of static pressure.

For test bodies which are not axisymmetric in shape, the optimum hydrophone mounting configuration will not be straightforward. In turn this would not permit straightforward interpolation of the results.

The lowest background noise level found to date for the plastic headform is about 0.8 mV at the end of the hydrophone cable. For a signal amplitude of twice this value, the pressure amplitude must be 5.10^3 dyn/cm^2 (0.08 psi) at the hydrophone. The transmission path should be carefully examined to insure that the hydrophone is receiving the maximum signal possible. It is suggested that in future tests the overall sensitivity be established by listening to a sound source outside the headform. By repeating this test with and without the headform, the attenuation across the headform could be determined thus, permitting an estimate of the collapse pressure peak.

SUMMARY

An instrumentation system for detecting headform-cavitation inception, based on the number of cavitation occurrences, has been evaluated and has been found useful for the given situation. Once adjustment of the instrumentation to agree with visual calls is made, the data are more consistent than simultaneous visual calls, and the results are quantitative and can be recorded for later reference.

The instrumentation consists of a hydrophone to detect the collapse pulse and suitable electronics to give the rate of cavitation occurrences. Provisions are included to set the level of collapse pressure which must be exceeded to be counted and to prevent counting multiple cavity collapses.

Photographs taken of the cavitation showed traveling bubbles nearly hemispherical in shape with the initial collapse usually followed by a rebound and second collapse. The associated noise pulse was found to occur at bubble collapse with a smaller pulse from the second collapse. An amplitude distribution for the initial collapse pulse showed a single peak. The amplitude distribution provided a guide in setting the discriminator level. Similarly, the time between collapses gave information for the blanking time.

A series of tests with a 2-in.-diameter headform was performed, using the instrumentation. It has been found that an occurrence rate of one event per second correlates well with visual calls and provides consistent data. At present, a visual check of the inception condition is needed, since the correct discriminator level is a function of headform shape, possibly the static pressure of the test water, and probably the test facility.

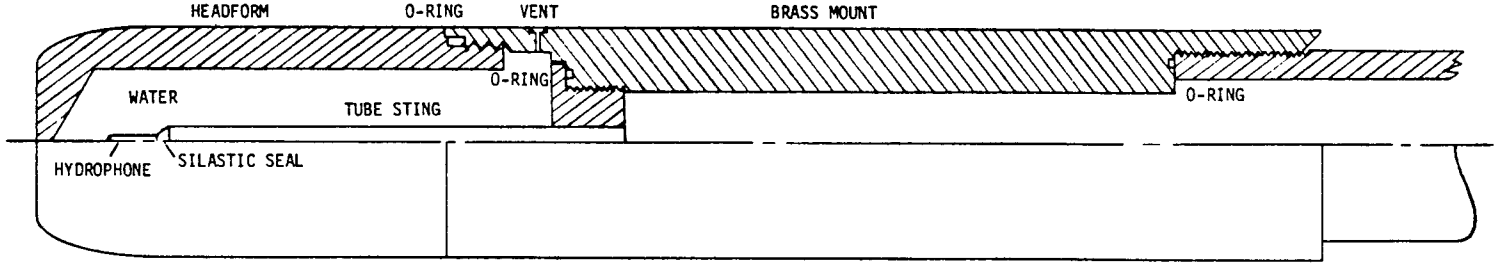

Figure 16 – Headform and Hydrophone Mount

Figure 17a – Disassembled

Figure 17b – Assembled

Figure 17 – Headform Mount

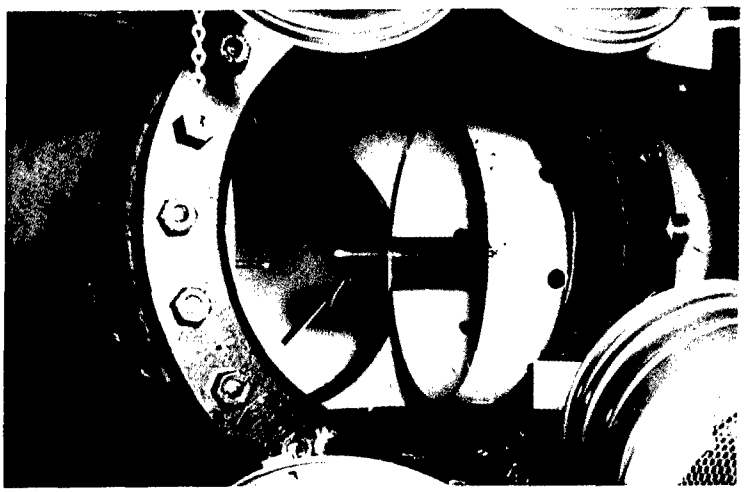

Figure 18 – Headform Mounted in 12-Inch Water Tunnel at Center

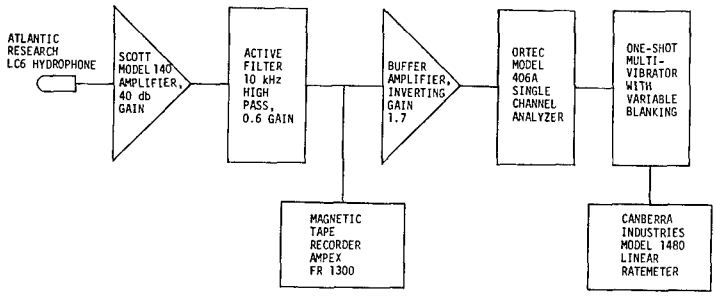

Figure 19a – Instrumentation

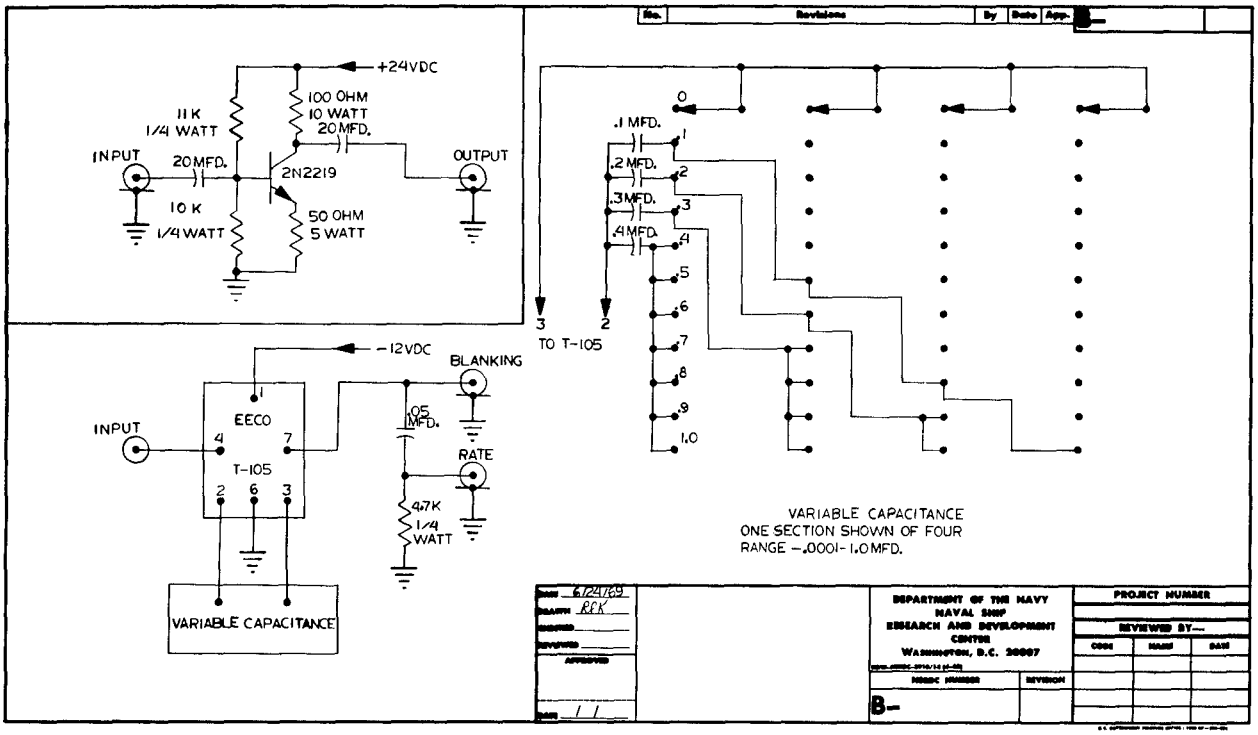

Figure 19b – Circuit

Figure 19 – Blanking Unit Diagrams

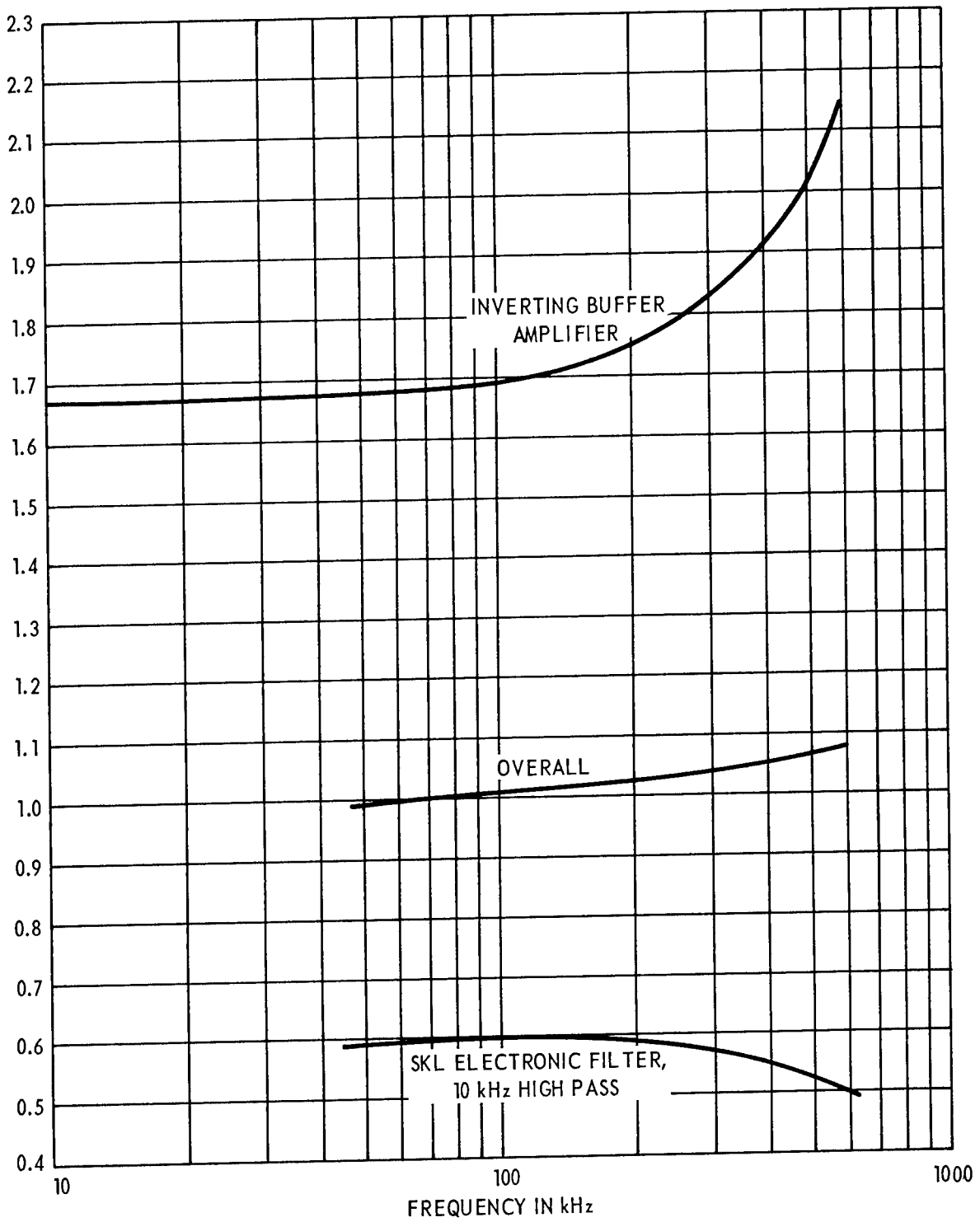

Figure 20 – Frequency Response of Buffer Amplifier and Electronic Filter

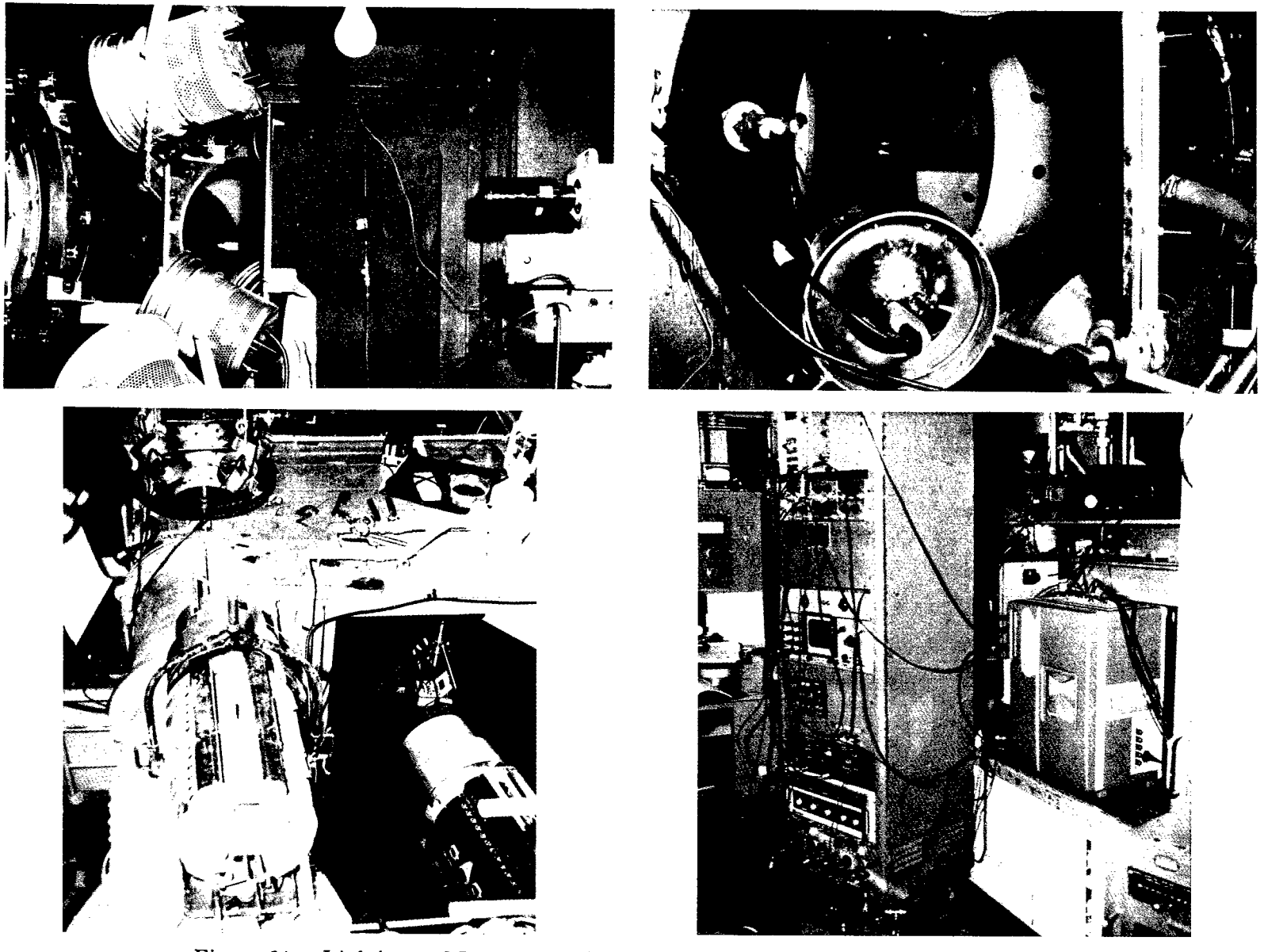

Figure 21 – Lighting and Instrumentation Arrangements for Evaluation Experiments

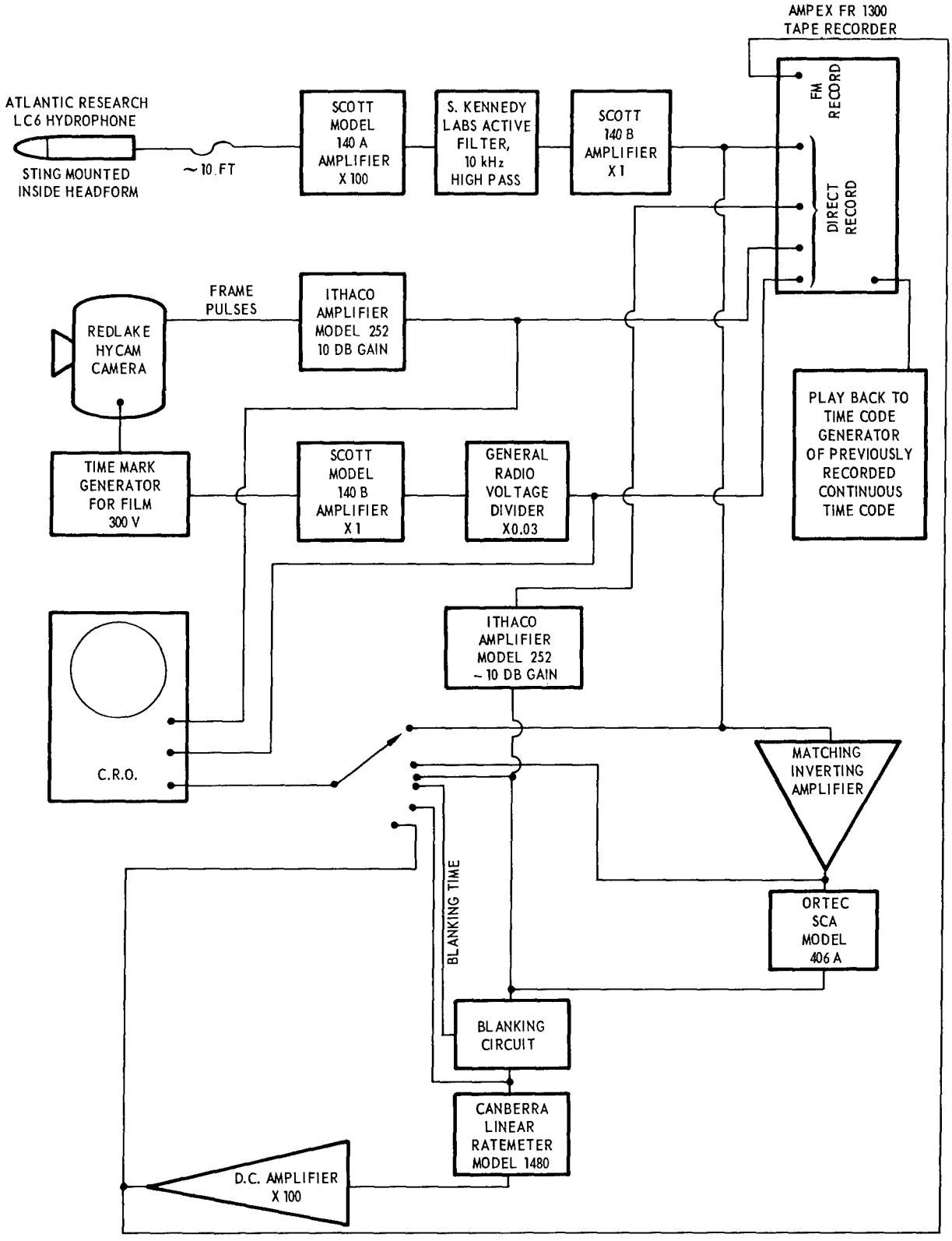

Figure 22 – Wiring Diagram for Instrumentation Used in Evaluation Experiments

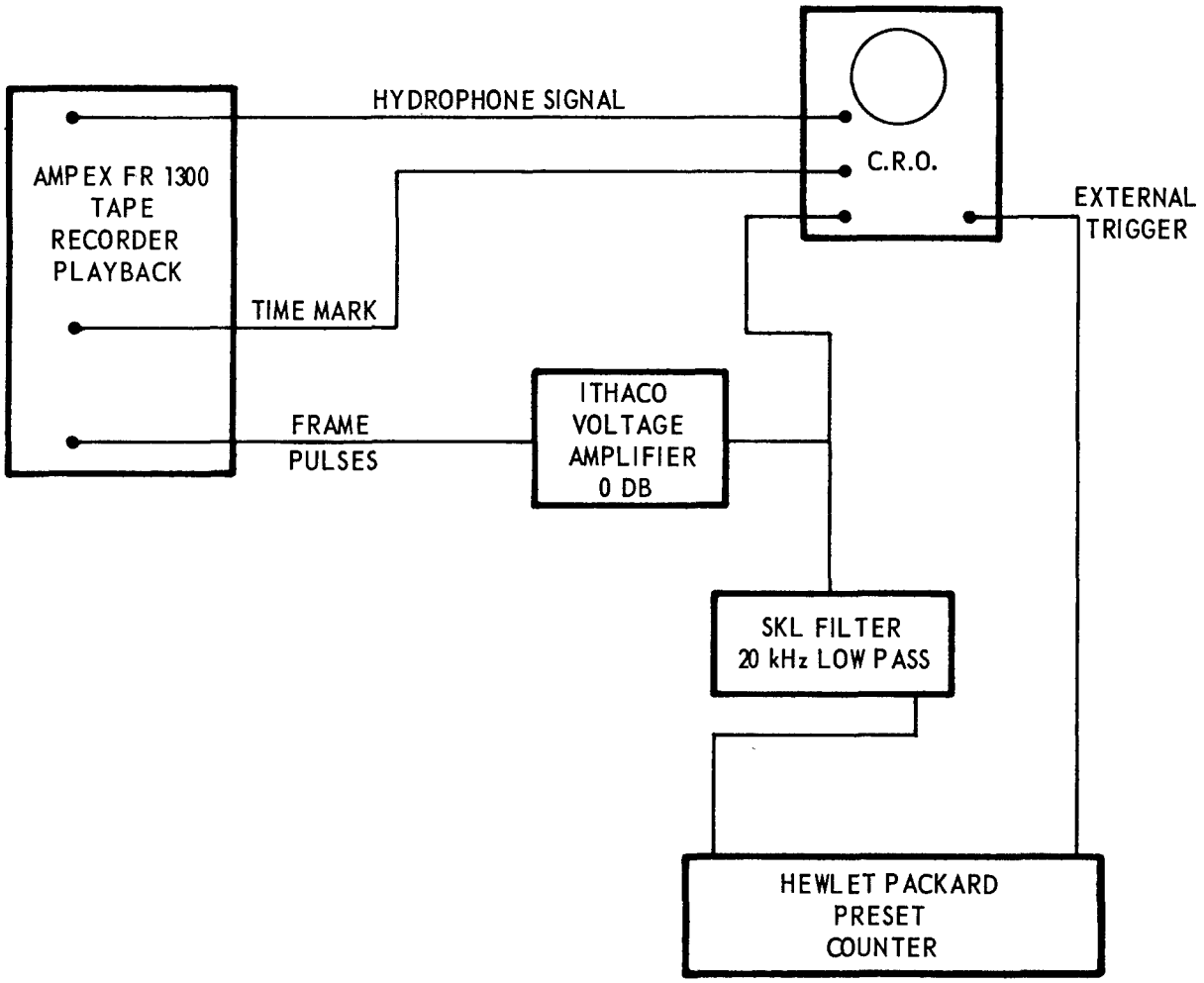

Figure 23 – Wiring Diagram Used in Tape Analysis

Figure 24 – Cavitation Bubble on the Headform

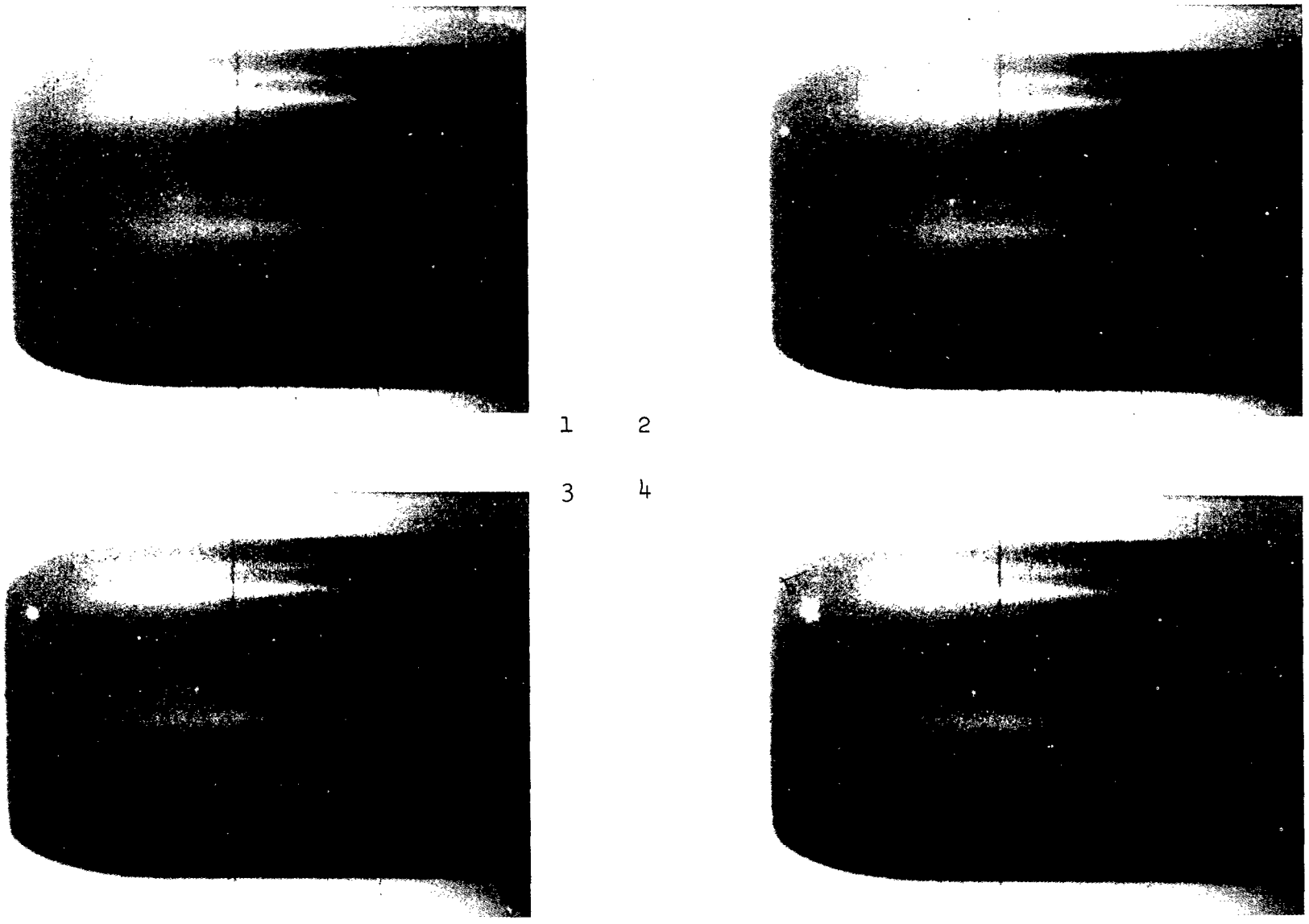

Figure 24 (Continued)

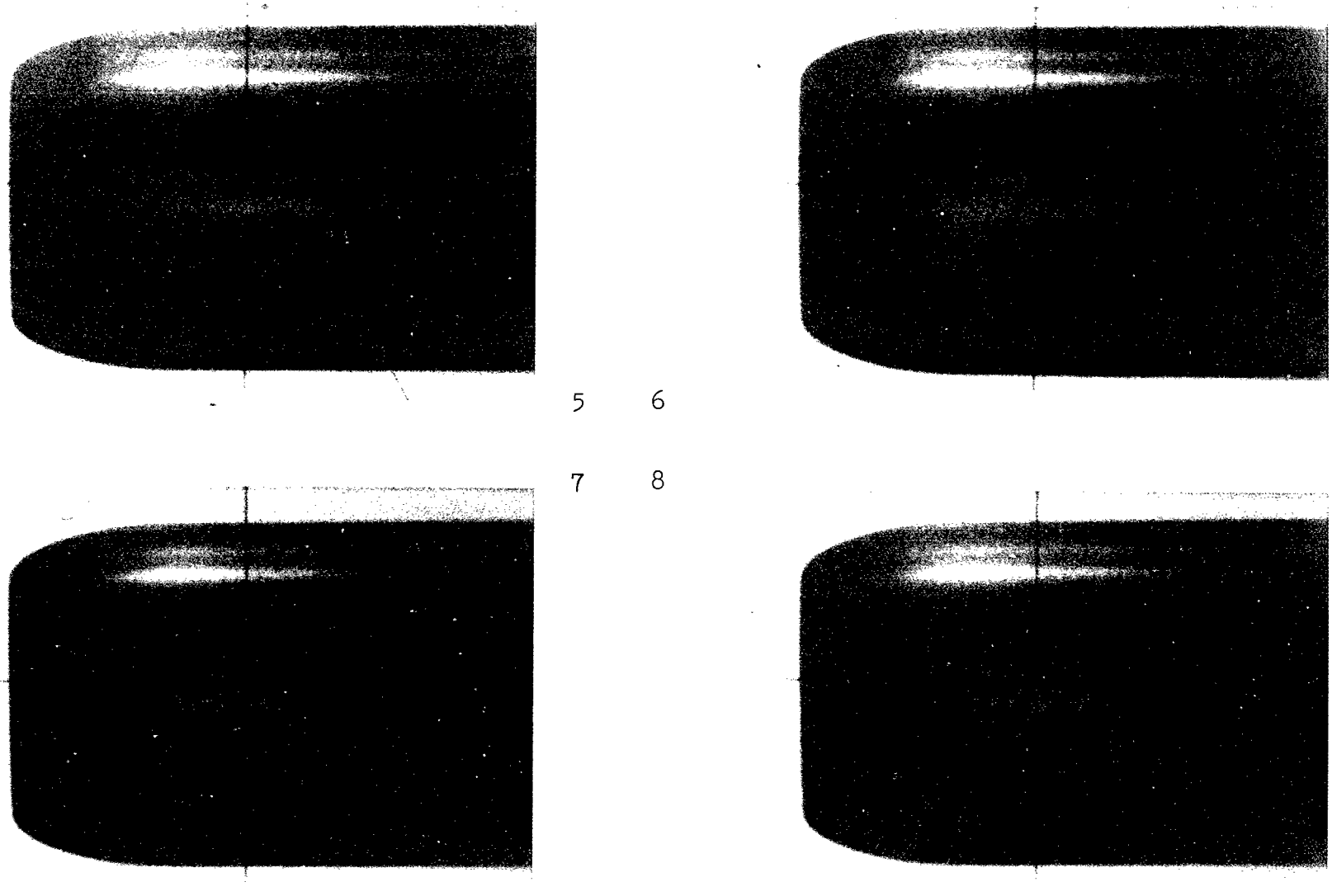

Figure 24 (Continued)

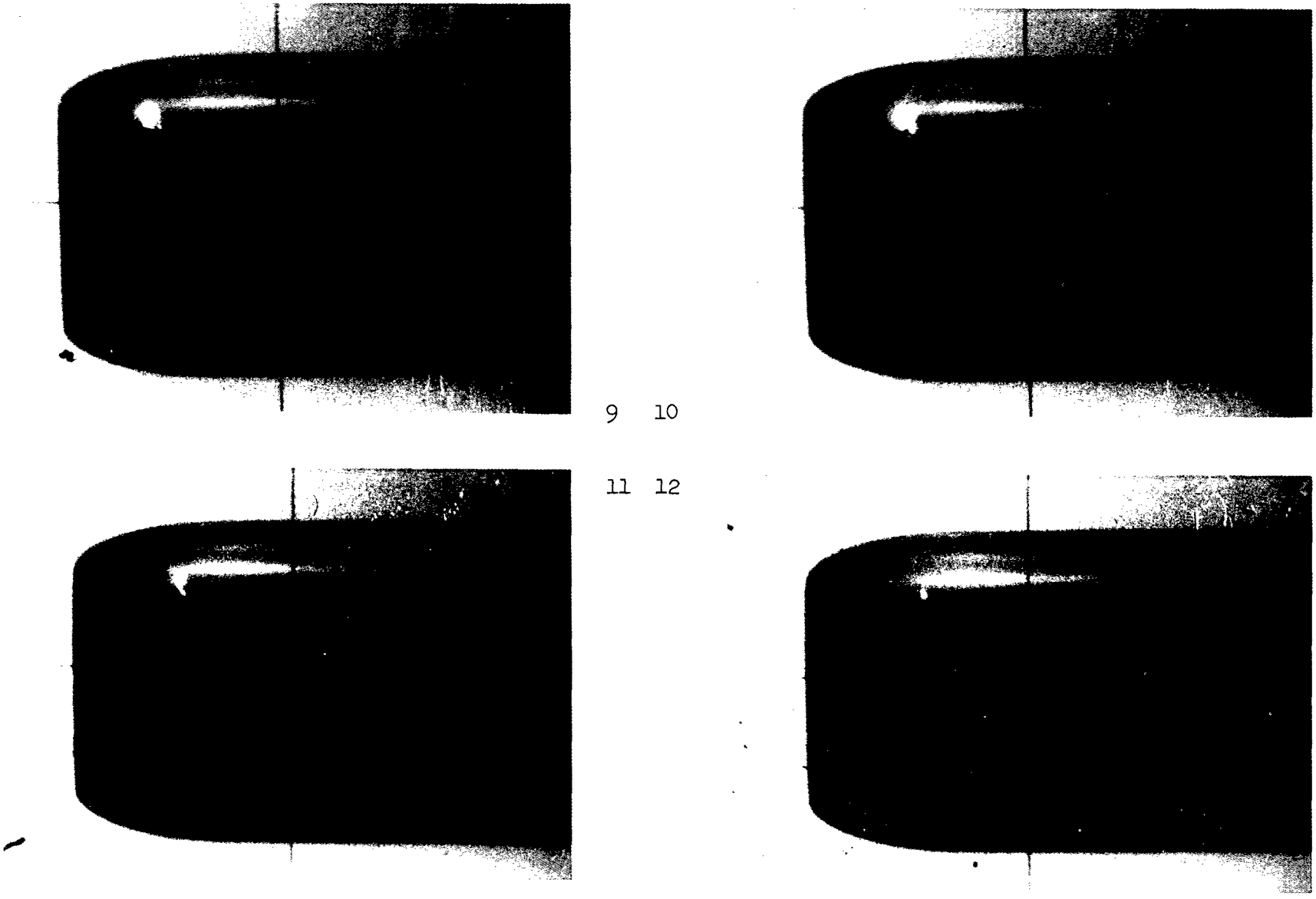

9 10

11 12

Figure 24 (Continued)

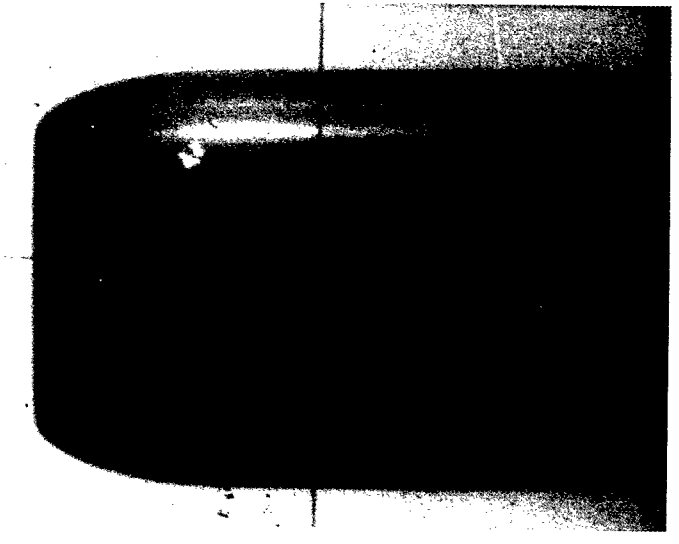

13 14

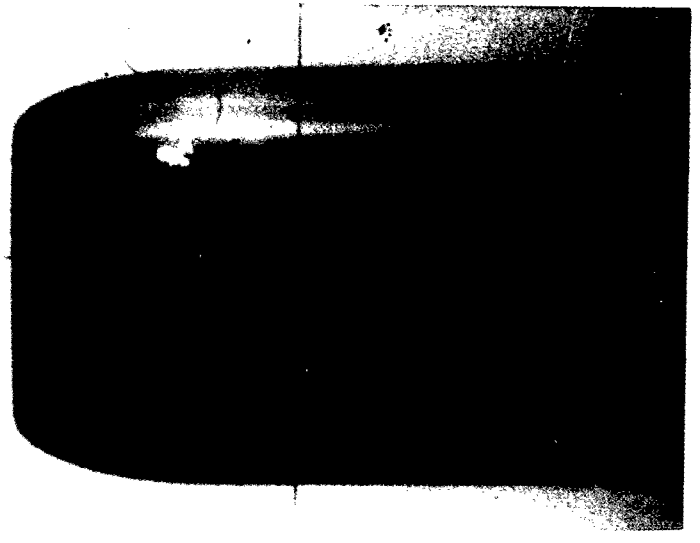

15 16

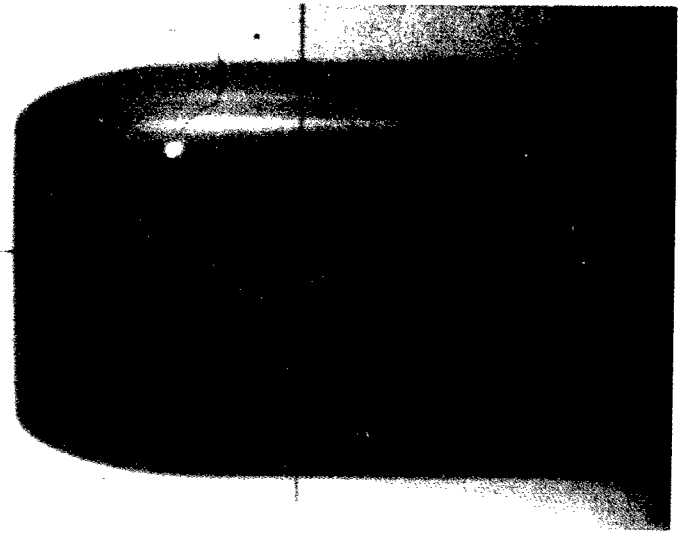

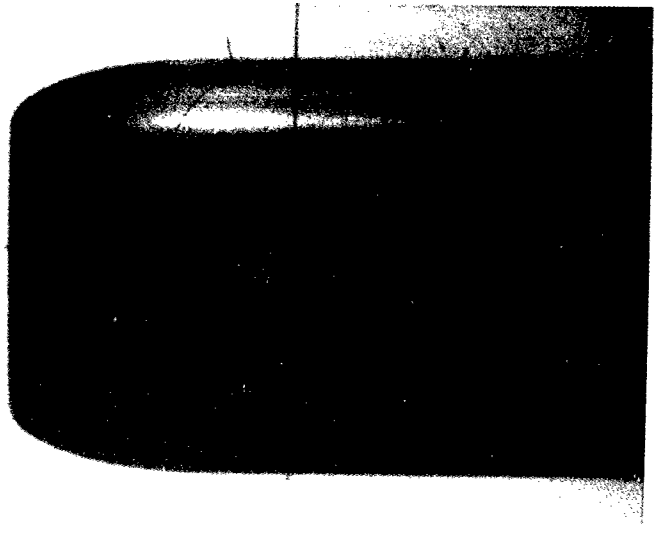

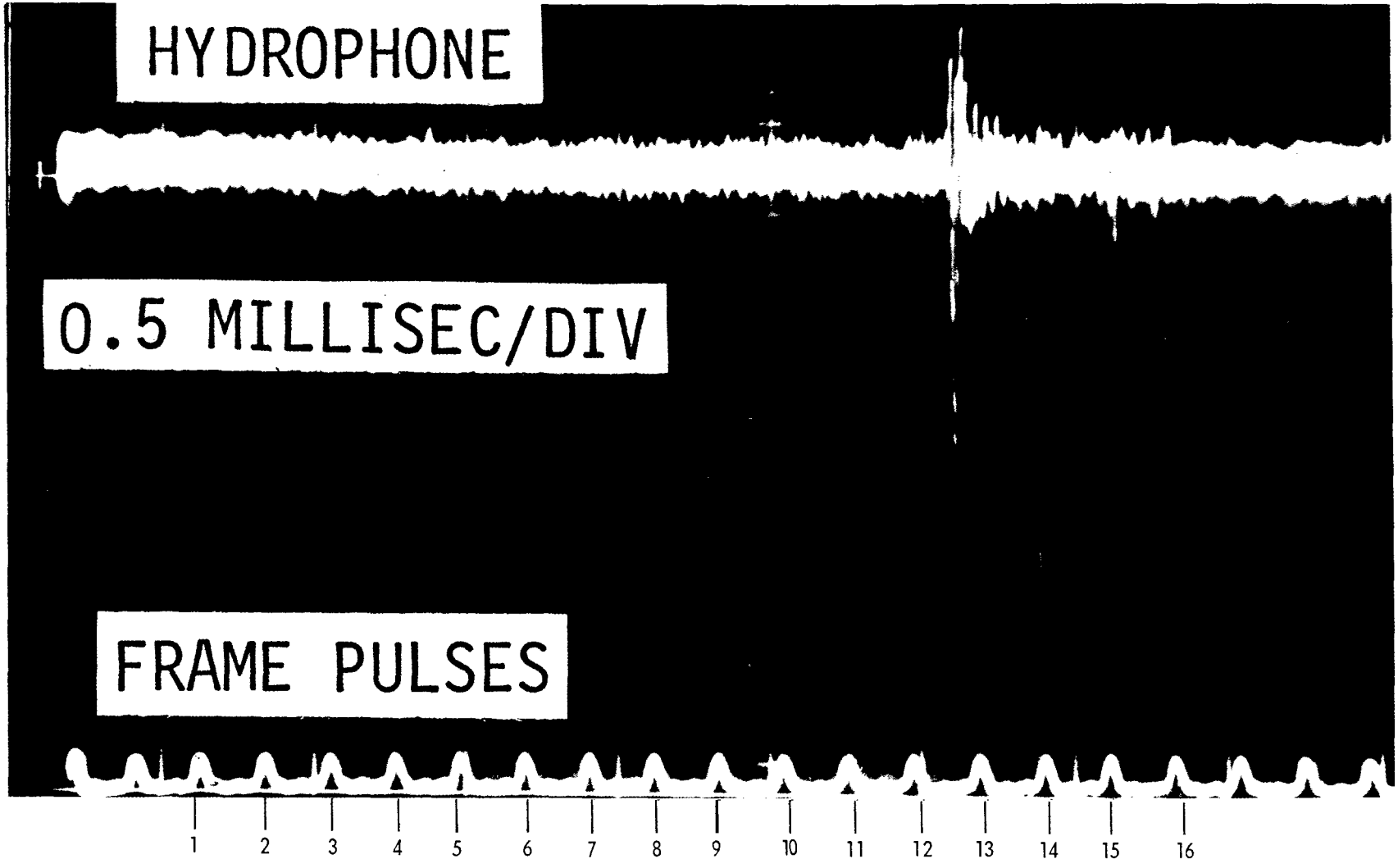

Figure 25 – Hydrophone Signal for Bubble on the Headform

Figure 26 – Cavitation Bubble Originating in the Free Stream

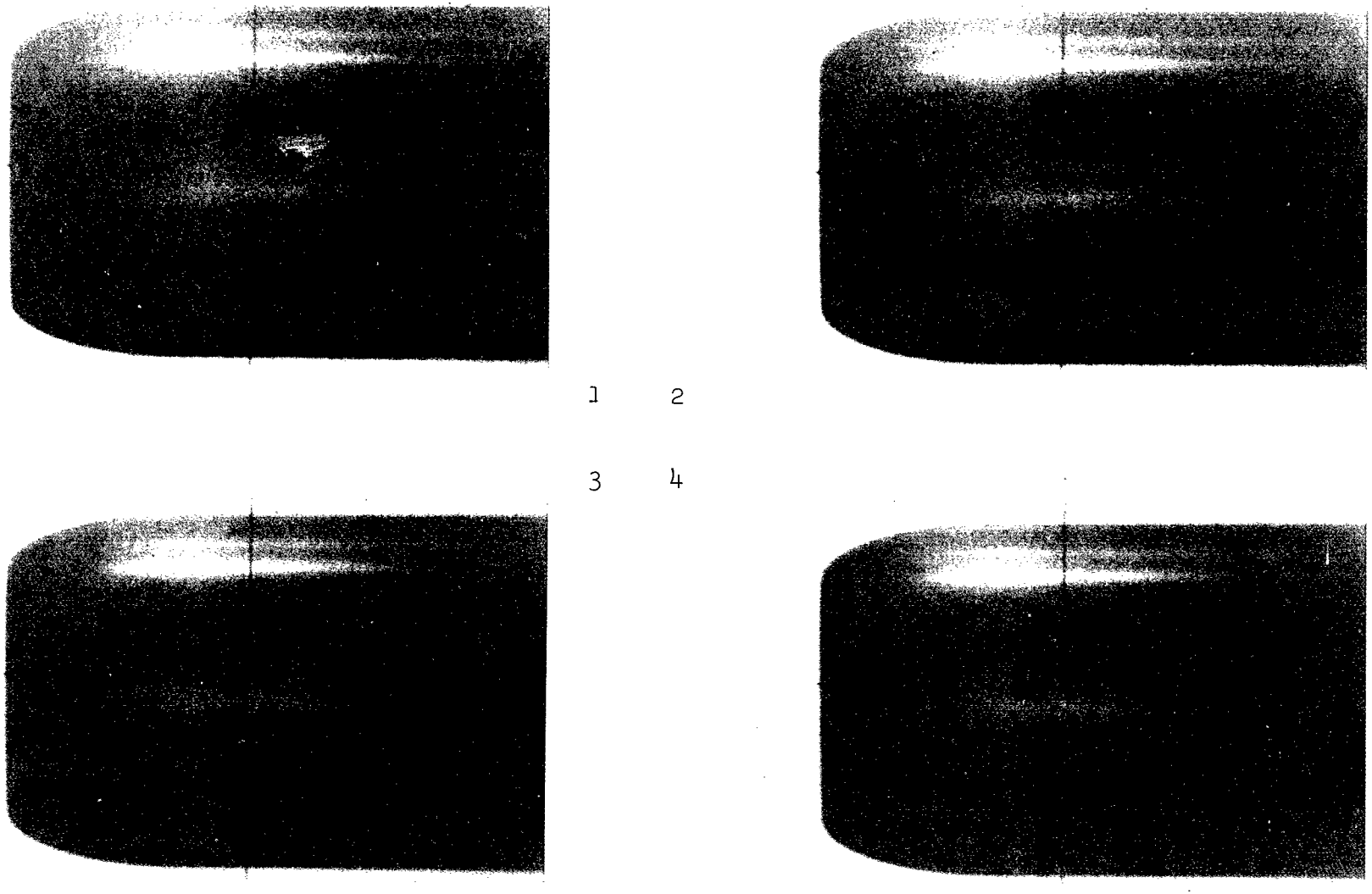

Figure 26 (Continued)

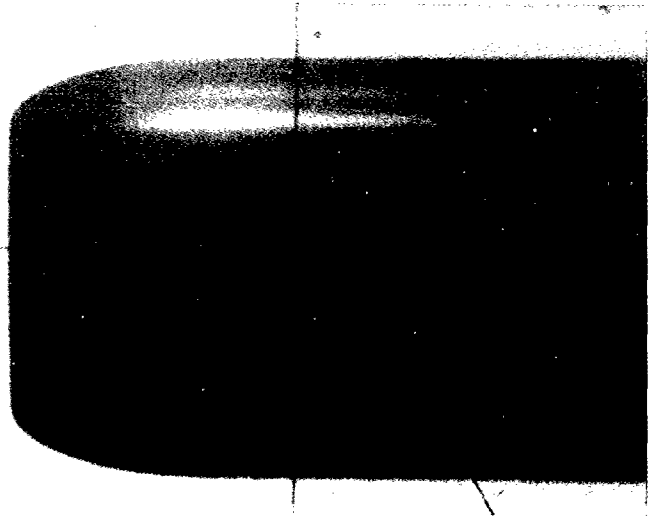

5

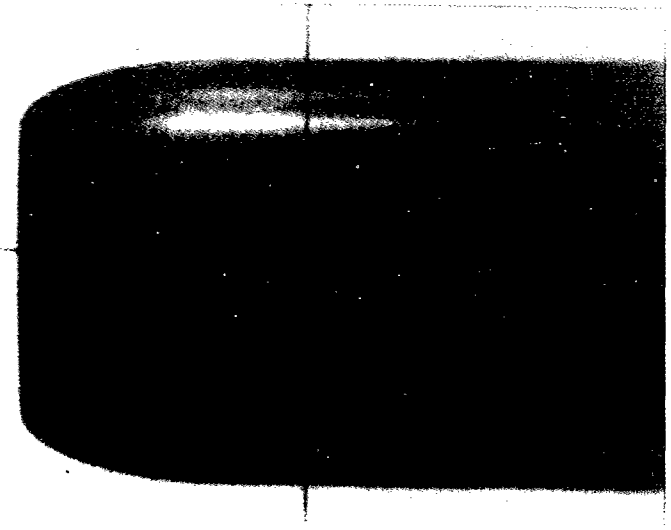

6

7

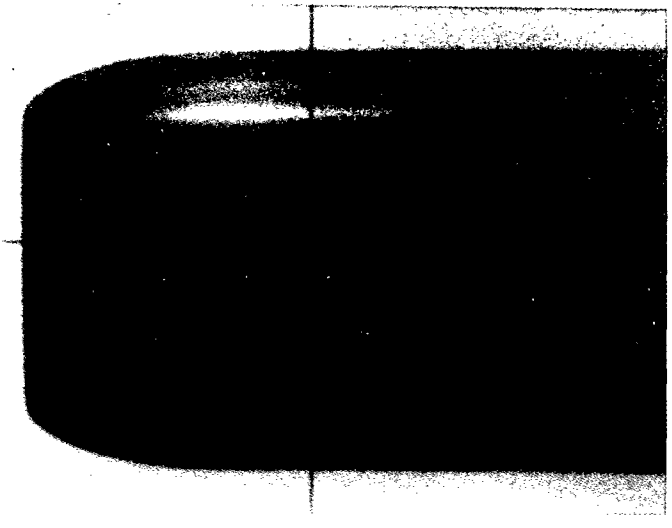

8

Figure 26 (Continued)

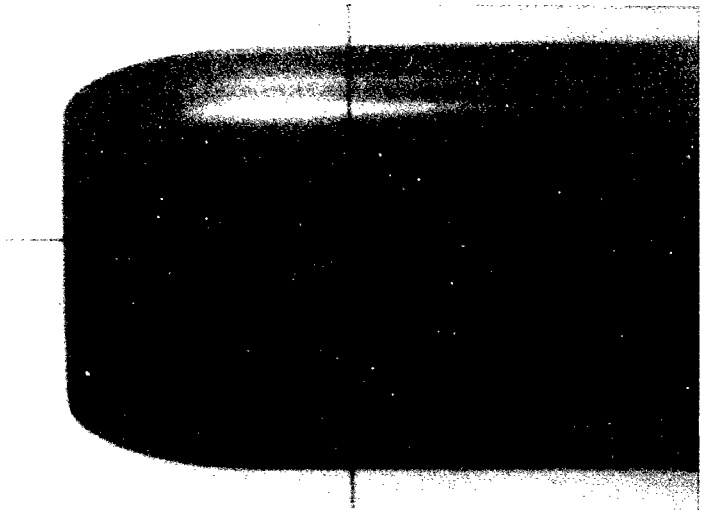

9

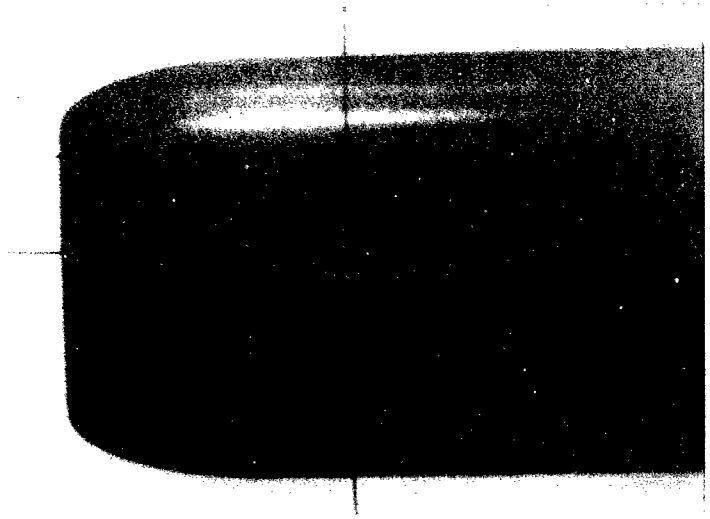

10

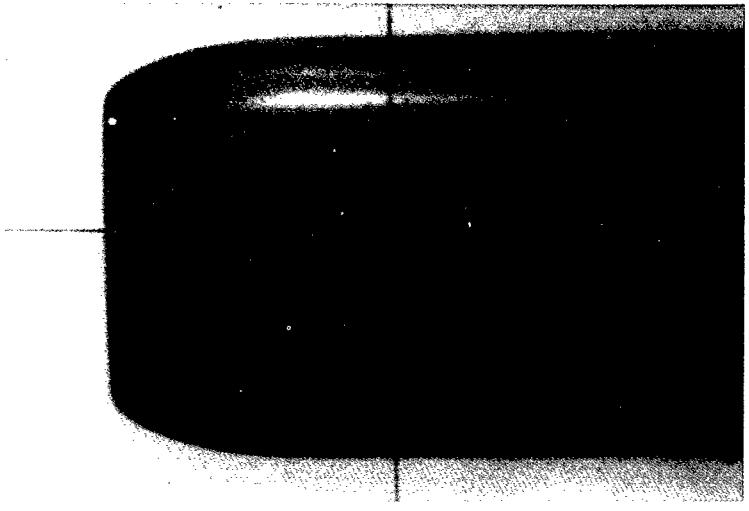

11

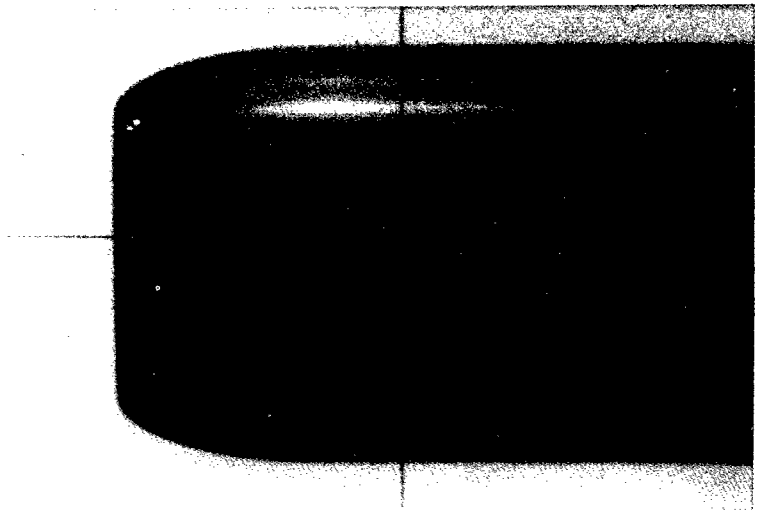

12

Figure 26 (Continued)

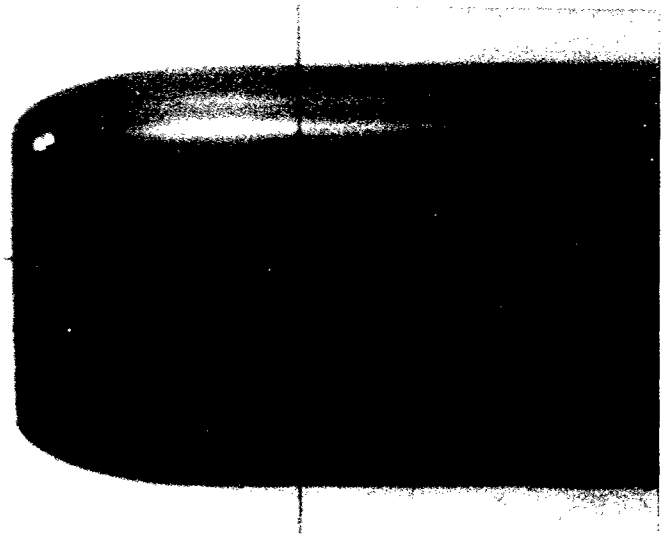

13

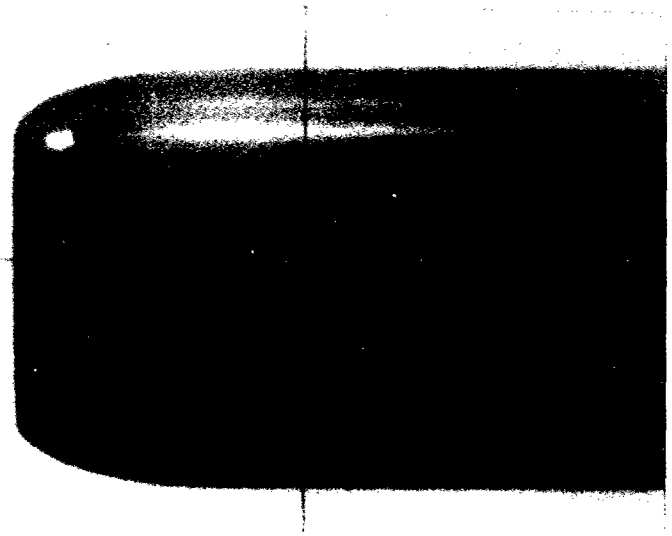

14

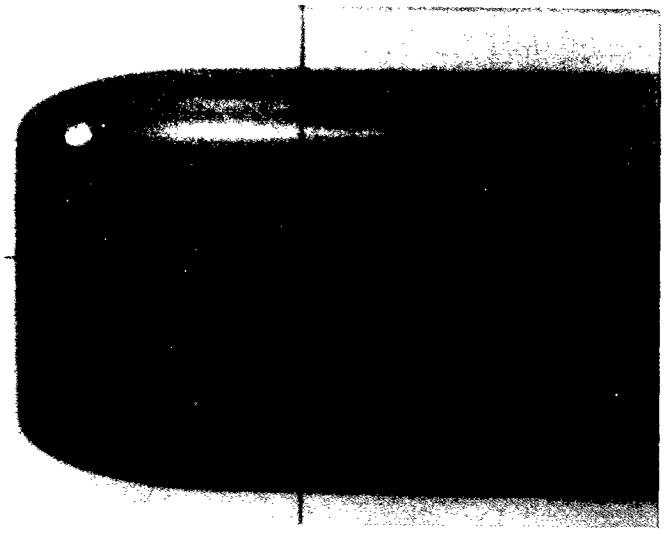

15

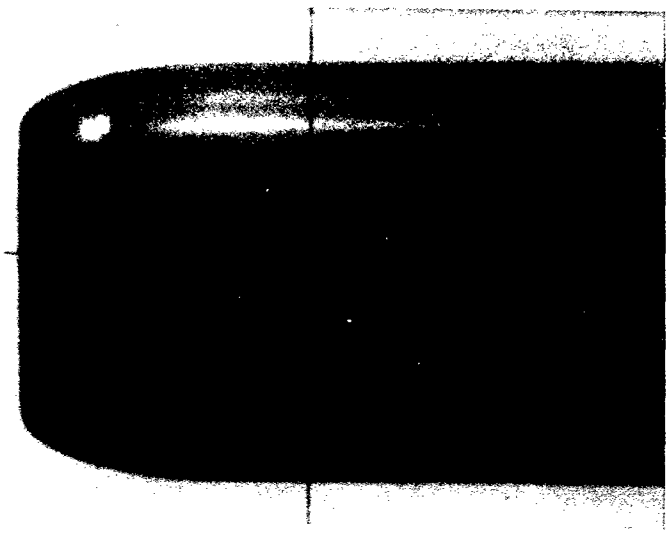

16

Figure 26 (Continued)

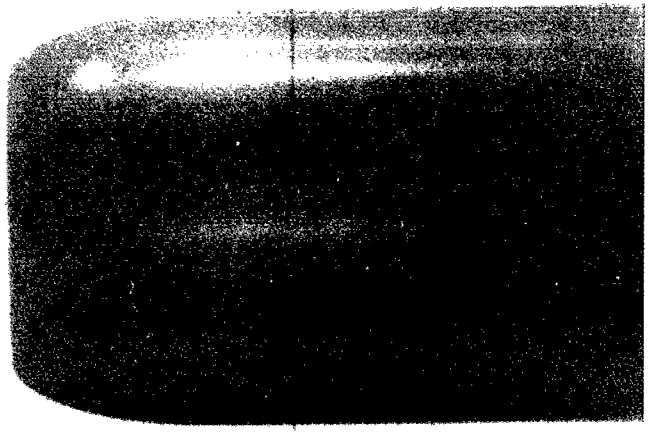

17

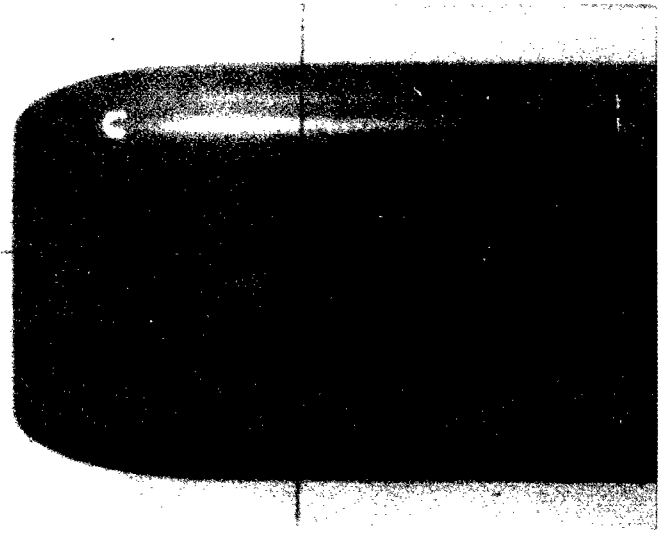

18

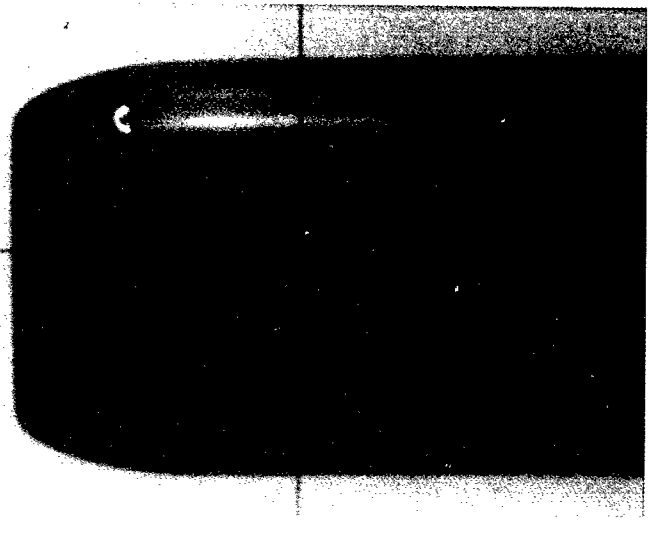

19

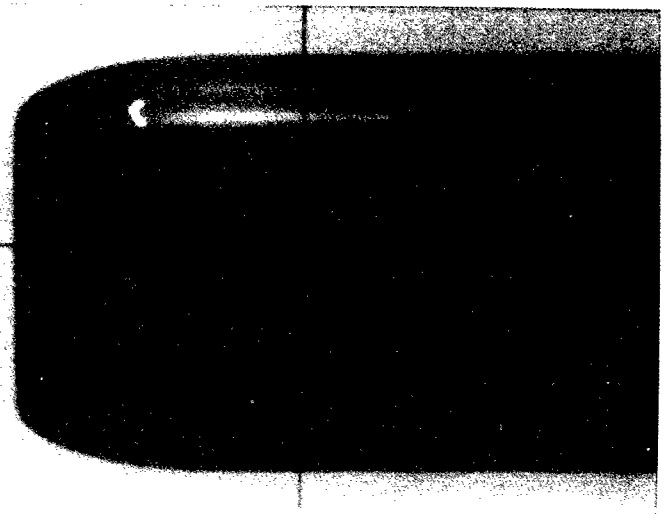

20

Figure 26 (Continued)

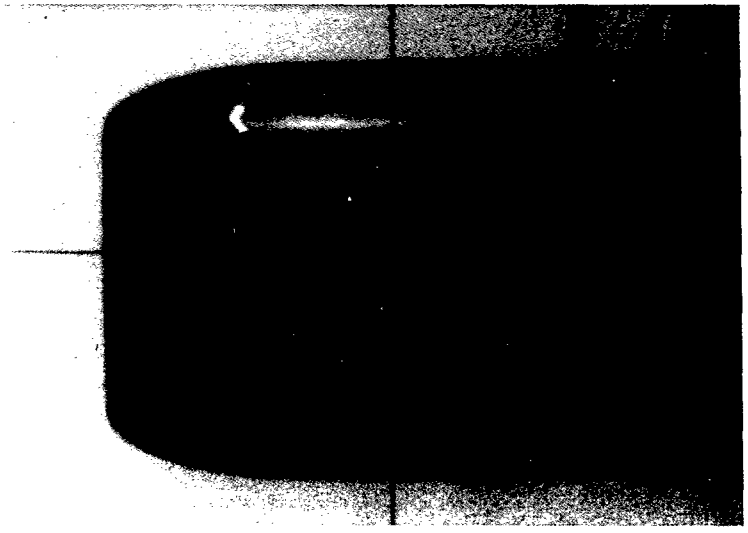

21

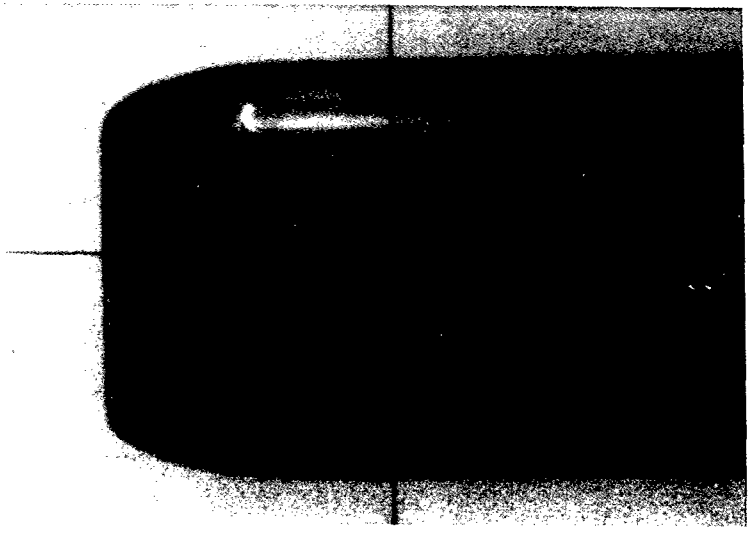

22

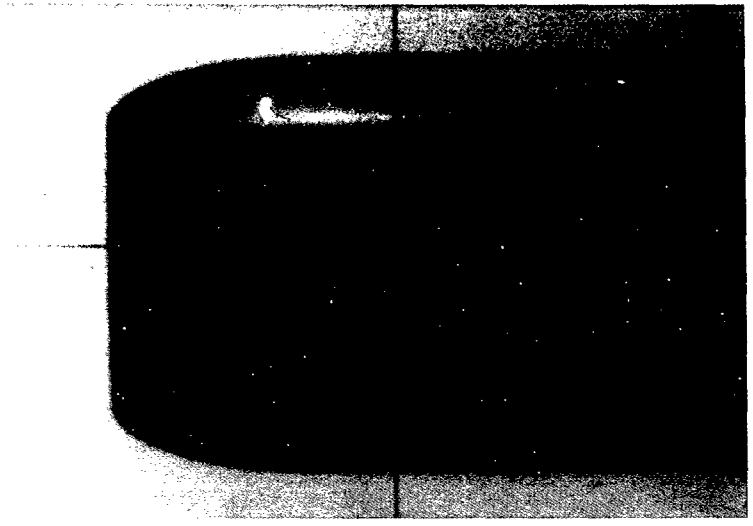

23

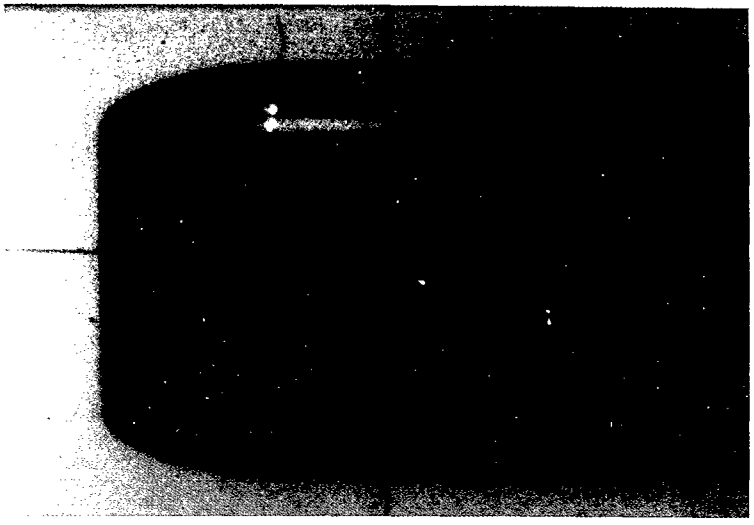

24

Figure 26 (Continued)

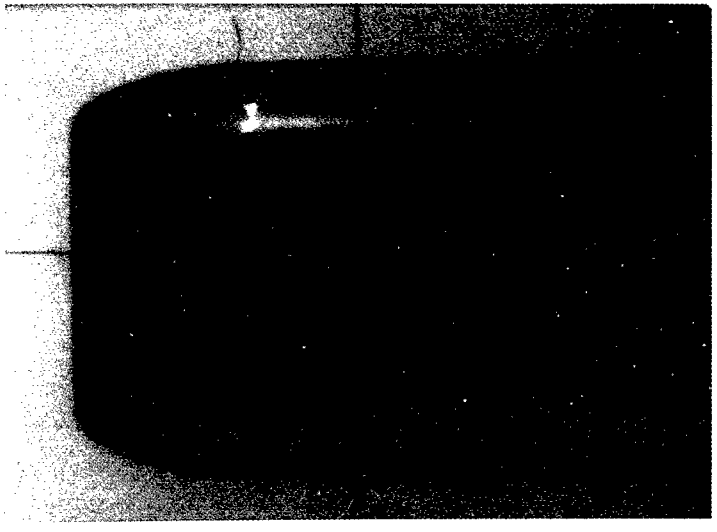

25

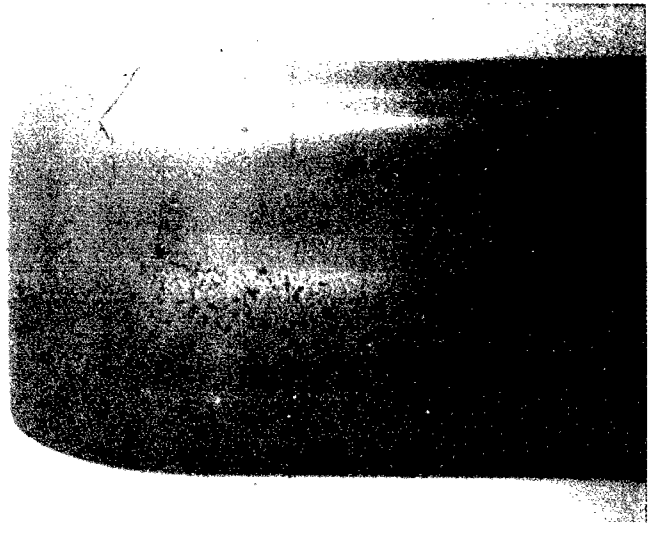

26

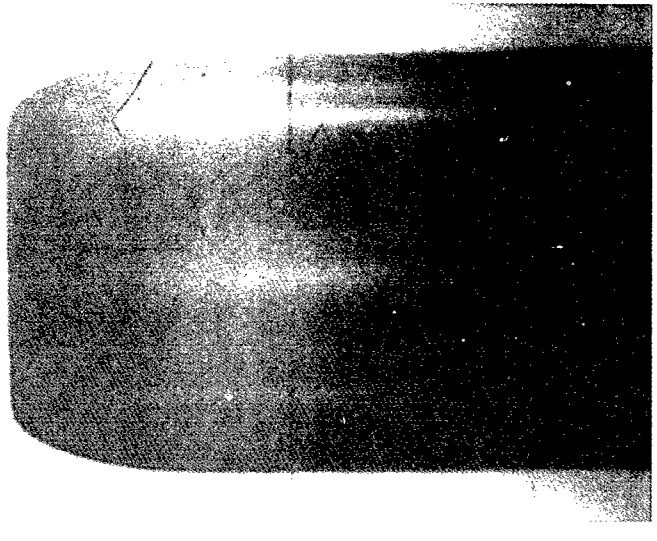

27

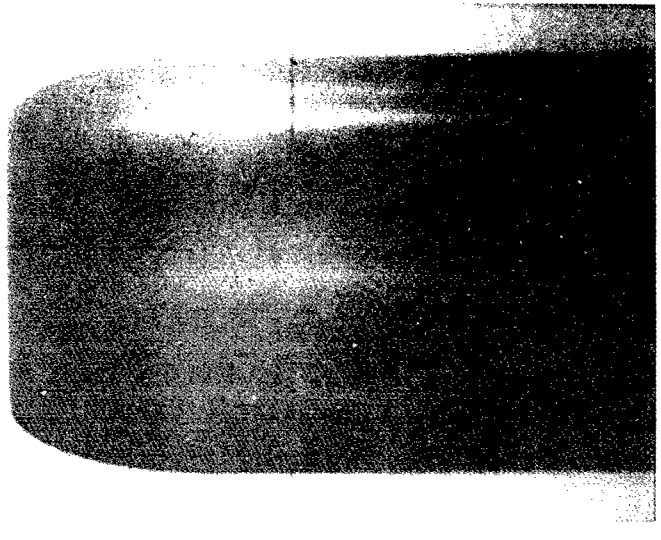

28

Figure 26 (Continued)

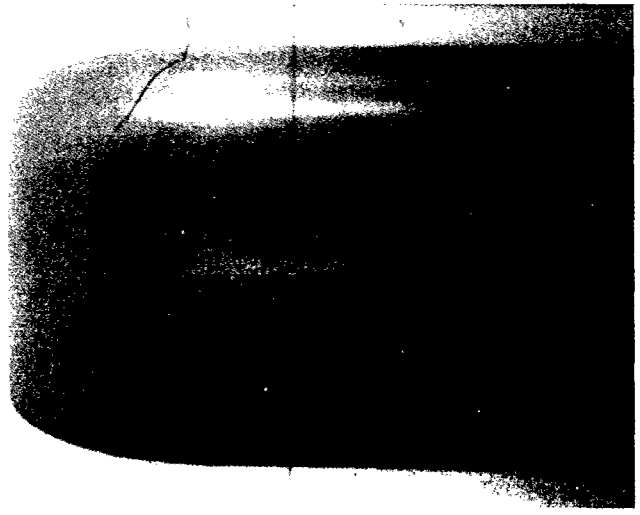

29

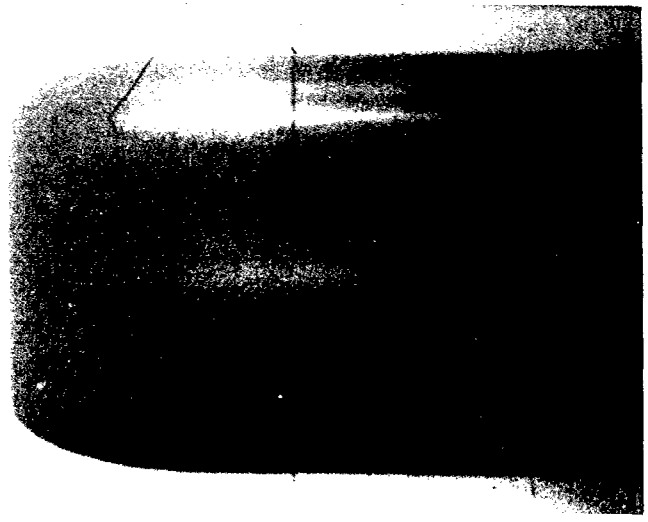

30

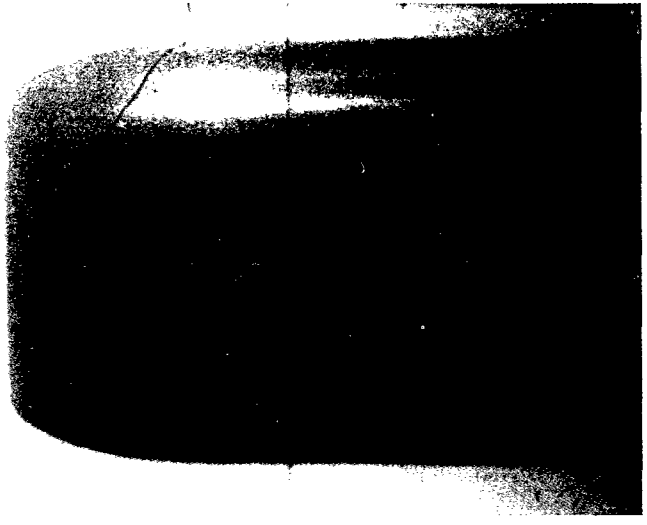

31

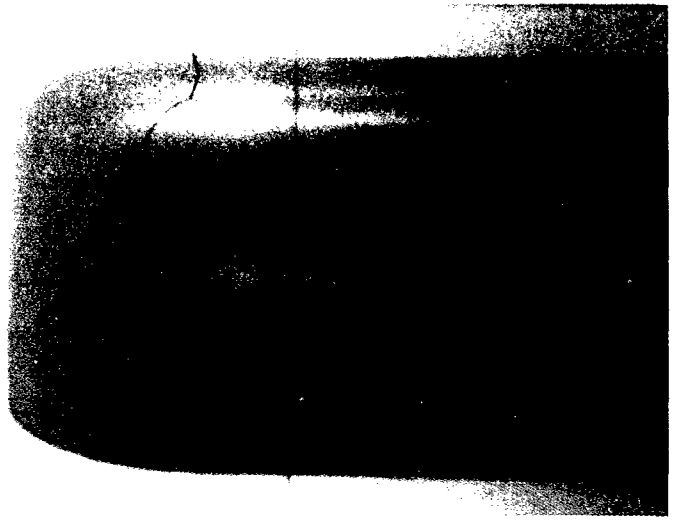

32

Figure 26 (Continued)

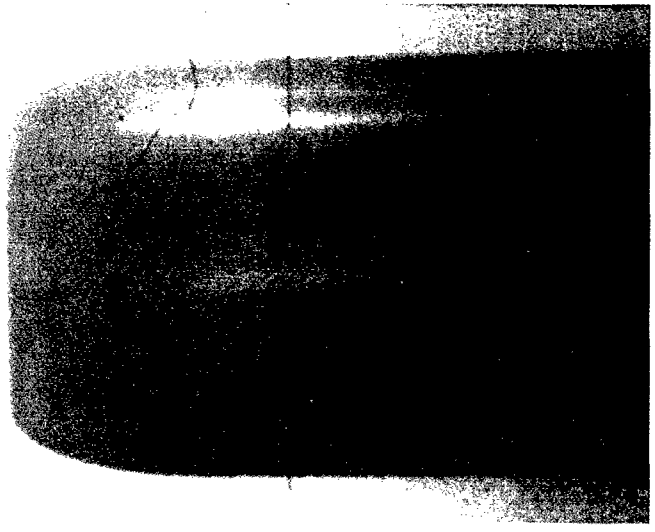

33 34

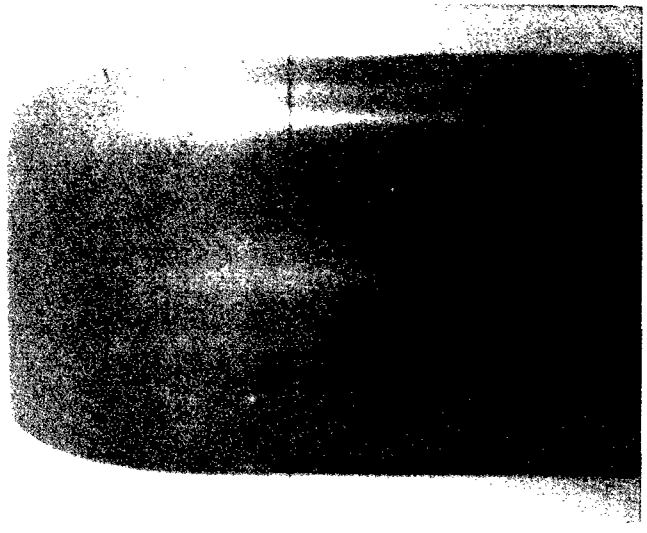

35 36

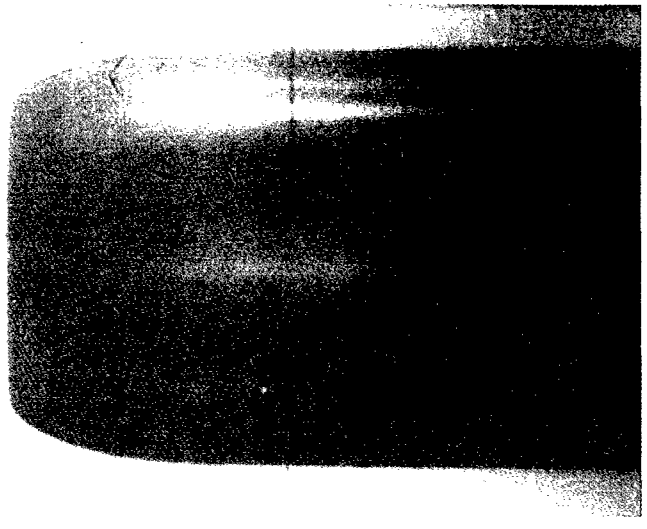

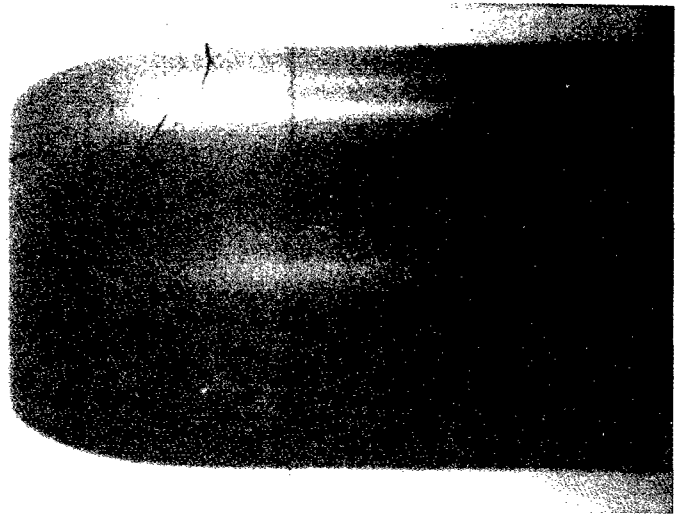

Figure 26 (Continued)

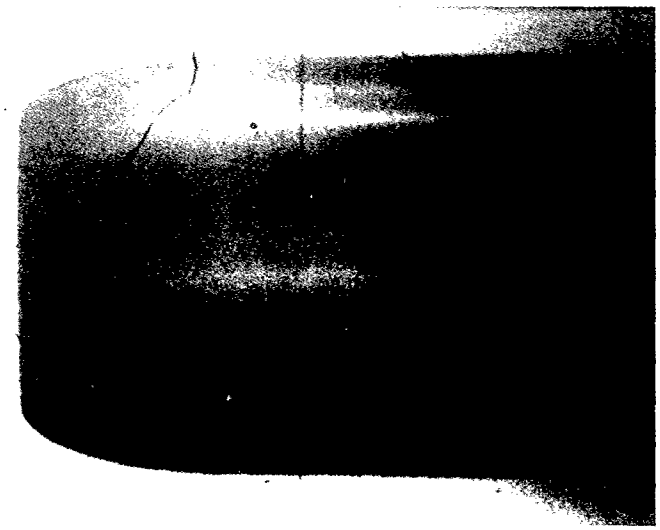

37

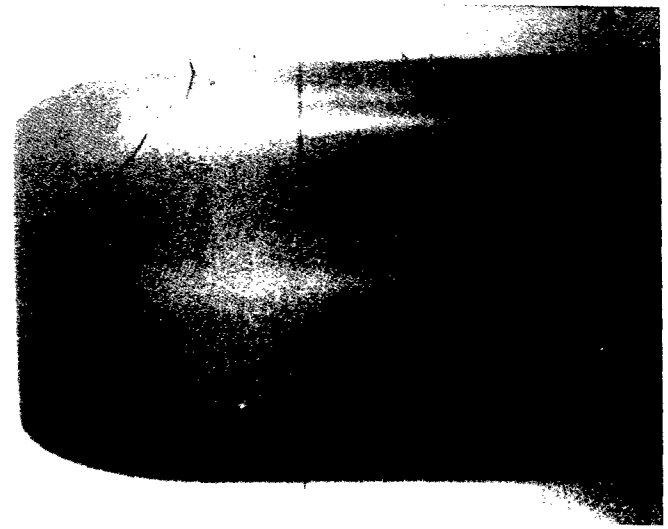

38

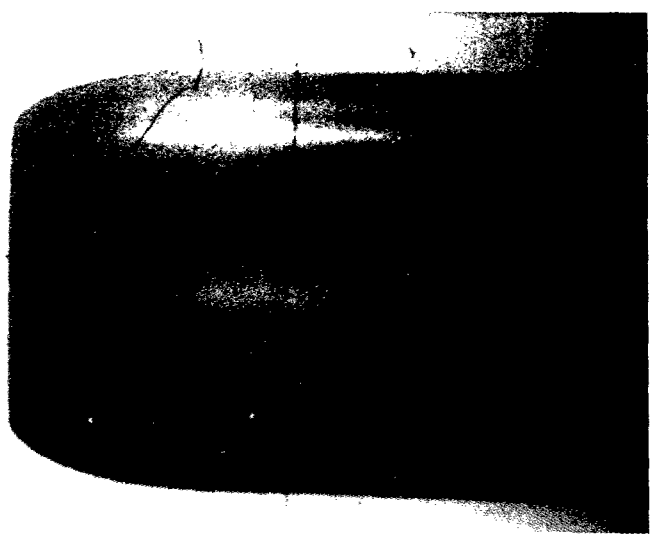

39

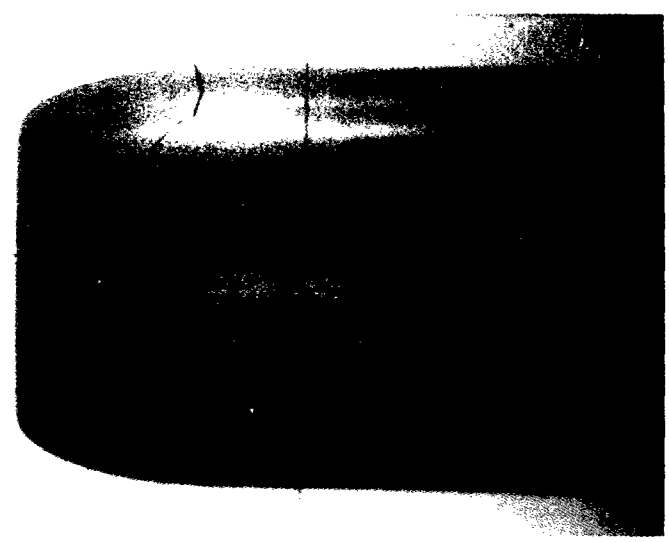

40

Figure 26 (Continued)

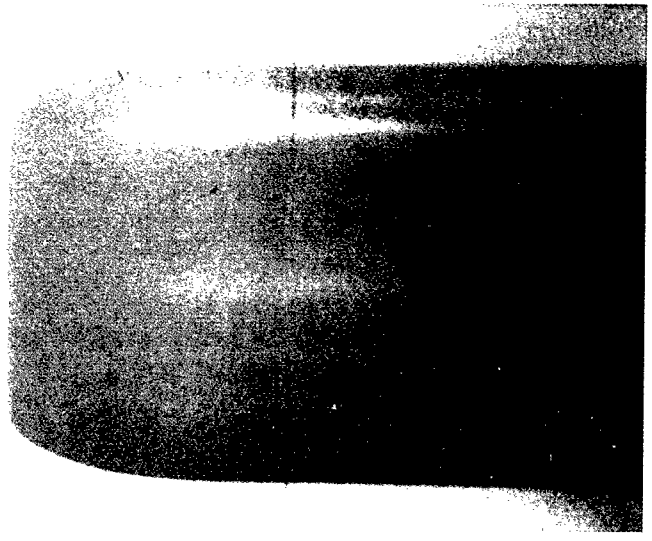

41

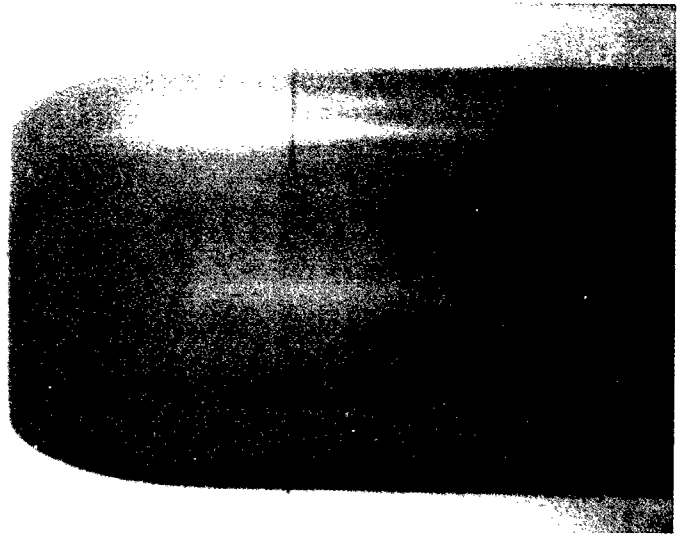

42

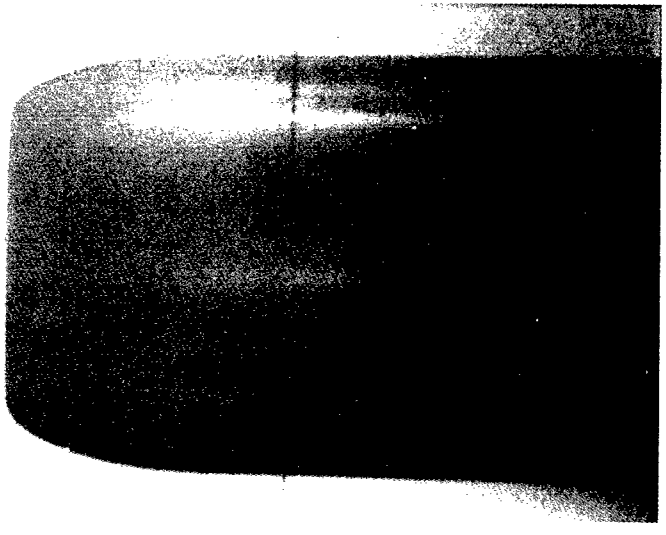

43

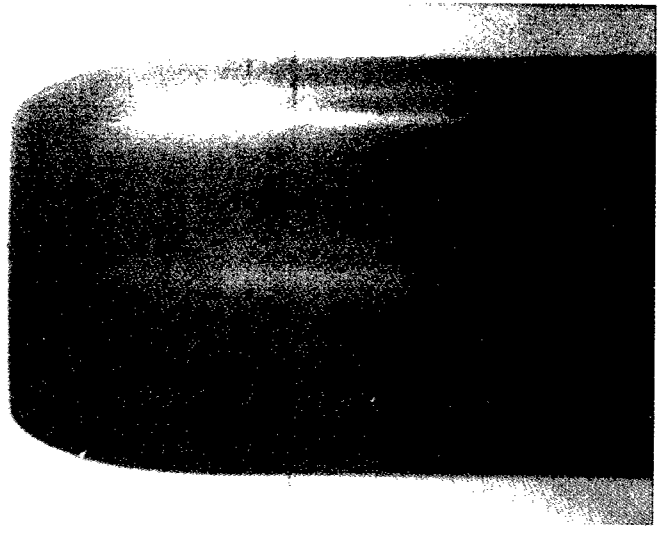

44

45 46

47 48

Figure 26 (Continued)

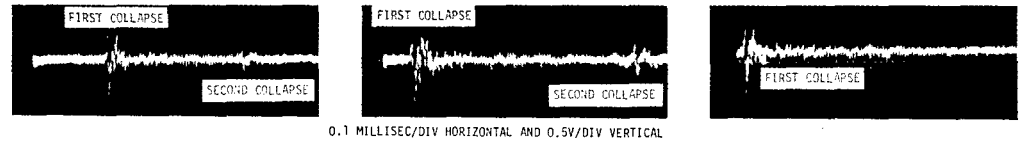

Figure 27 – Typical Pulse Shapes for Bubble Collapse on Plastic Headform

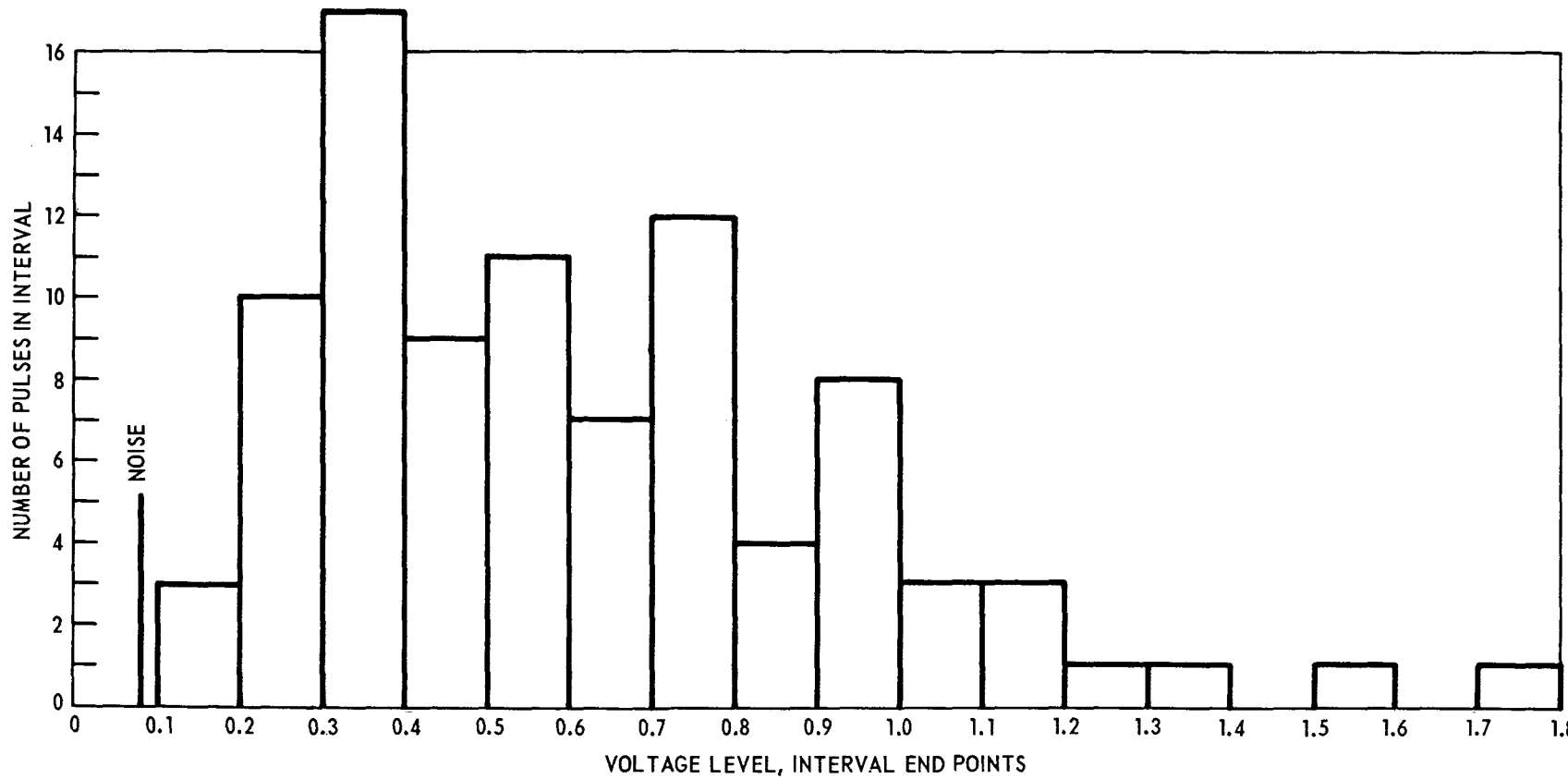

Figure 28 – Amplitude Distribution of Collapse Pulses on Plastic Headform

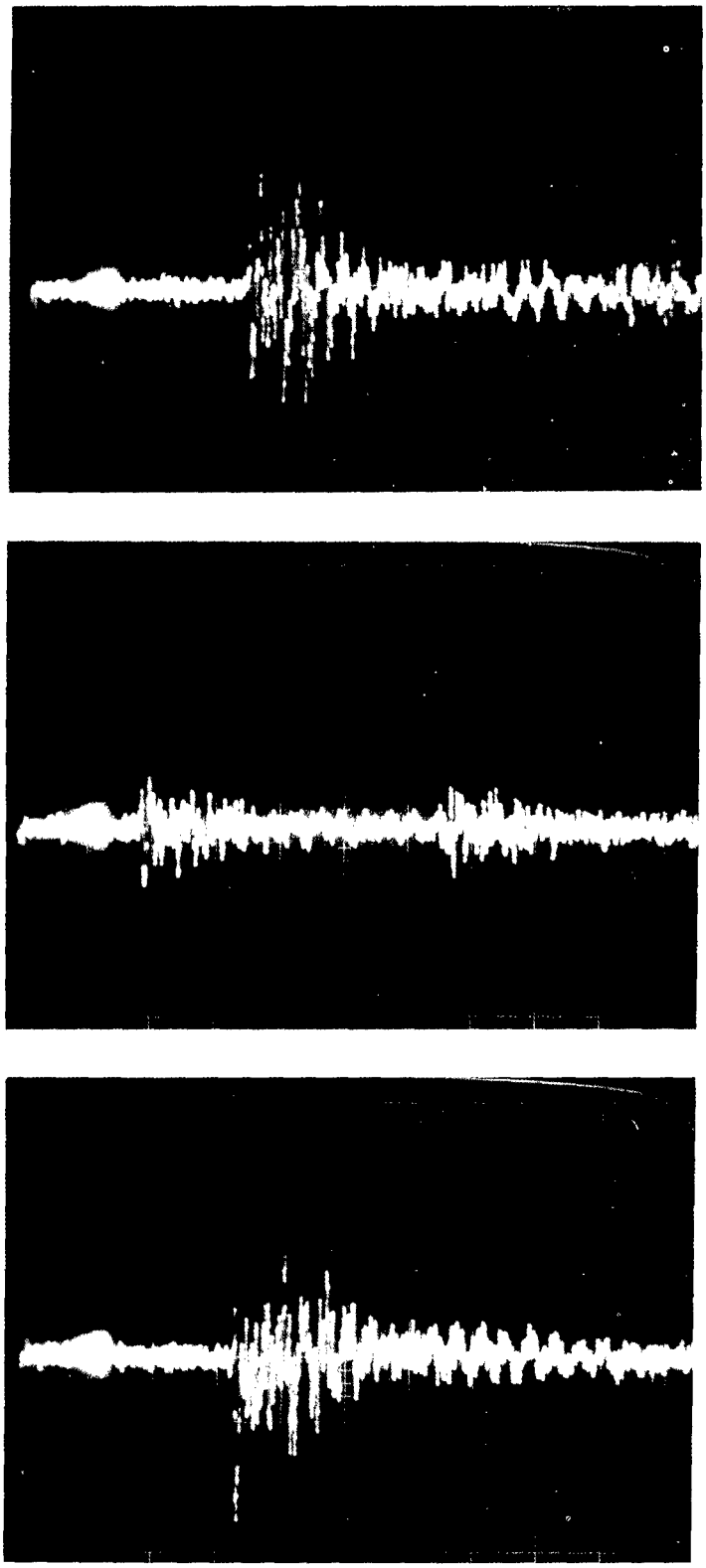

Figure 29 – Typical Pulse Shapes for Bubble Collapse on Brass Headform

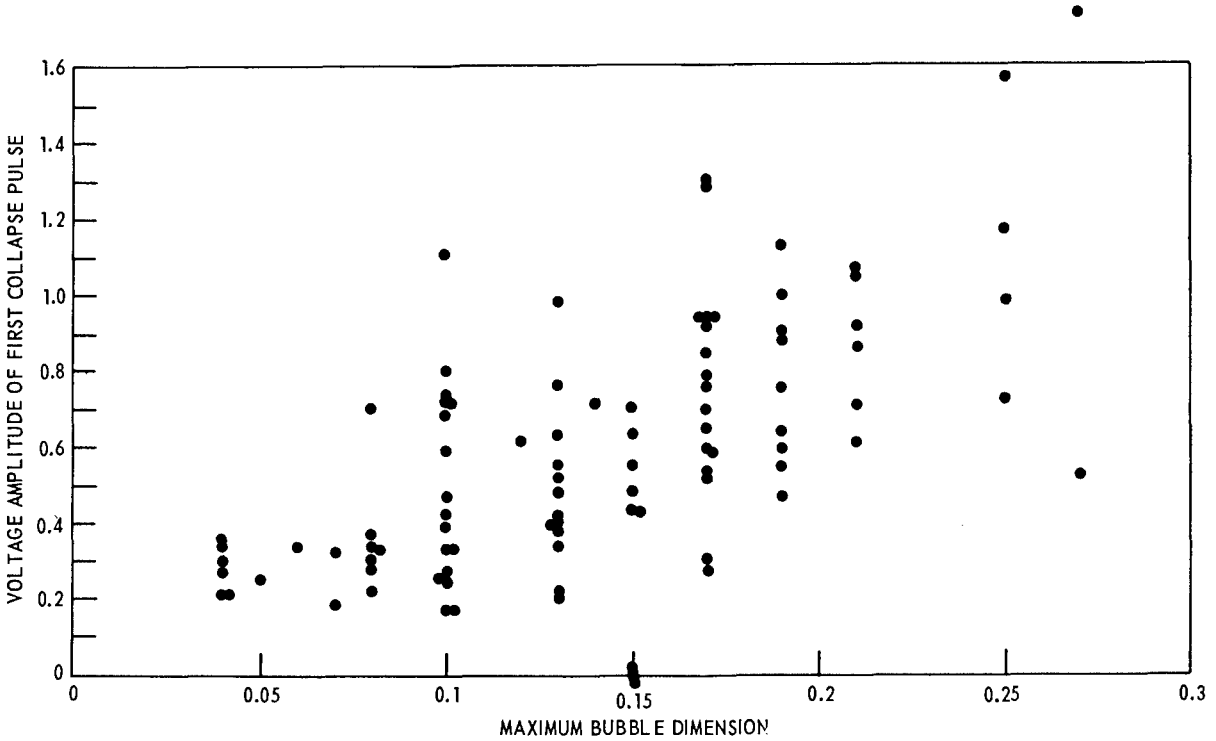

Figure 30 – Maximum Bubble Dimension versus Pulse Amplitude for Cavitation on Plastic Headform

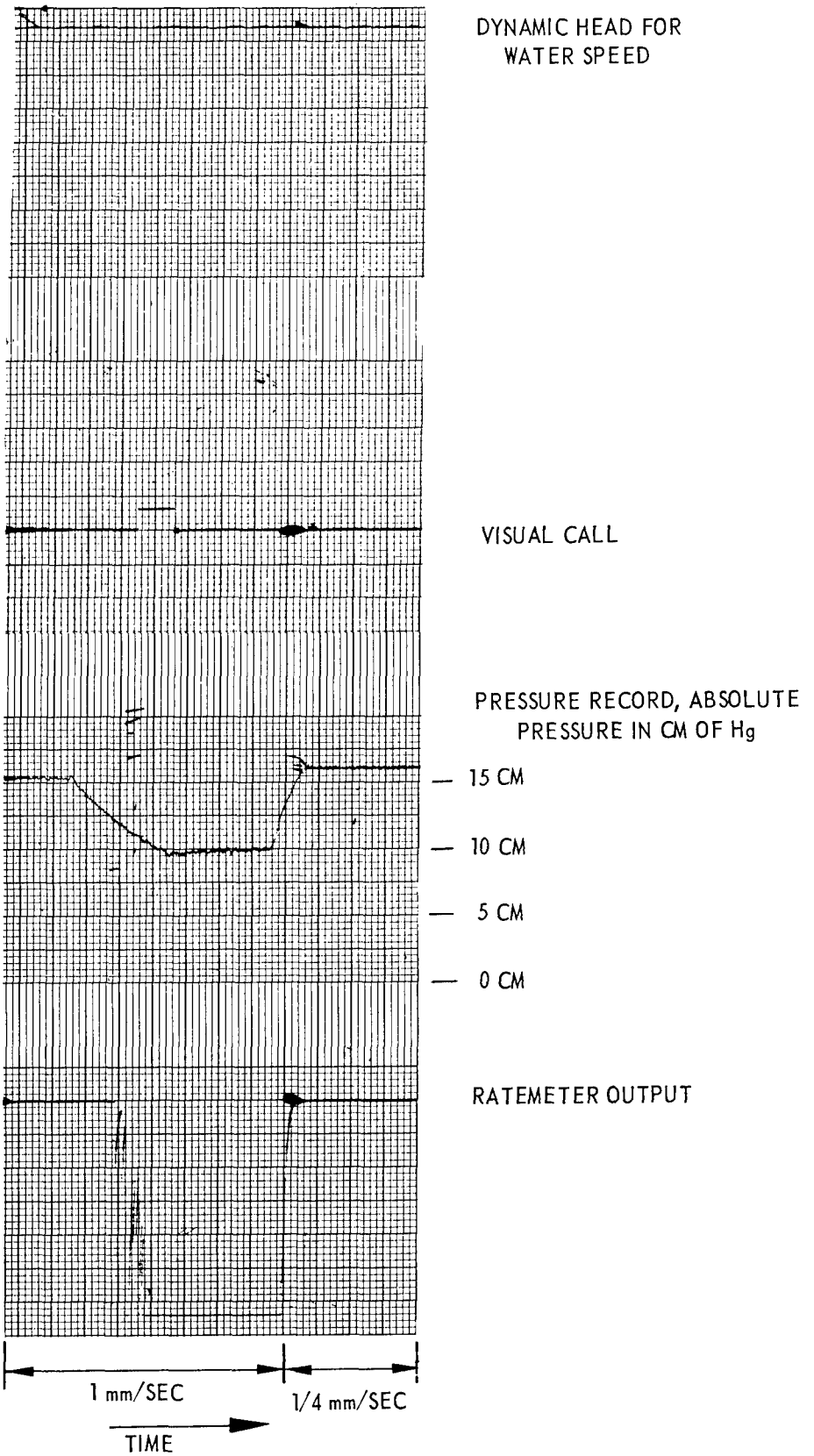

Figure 31 – Sanborn Trace

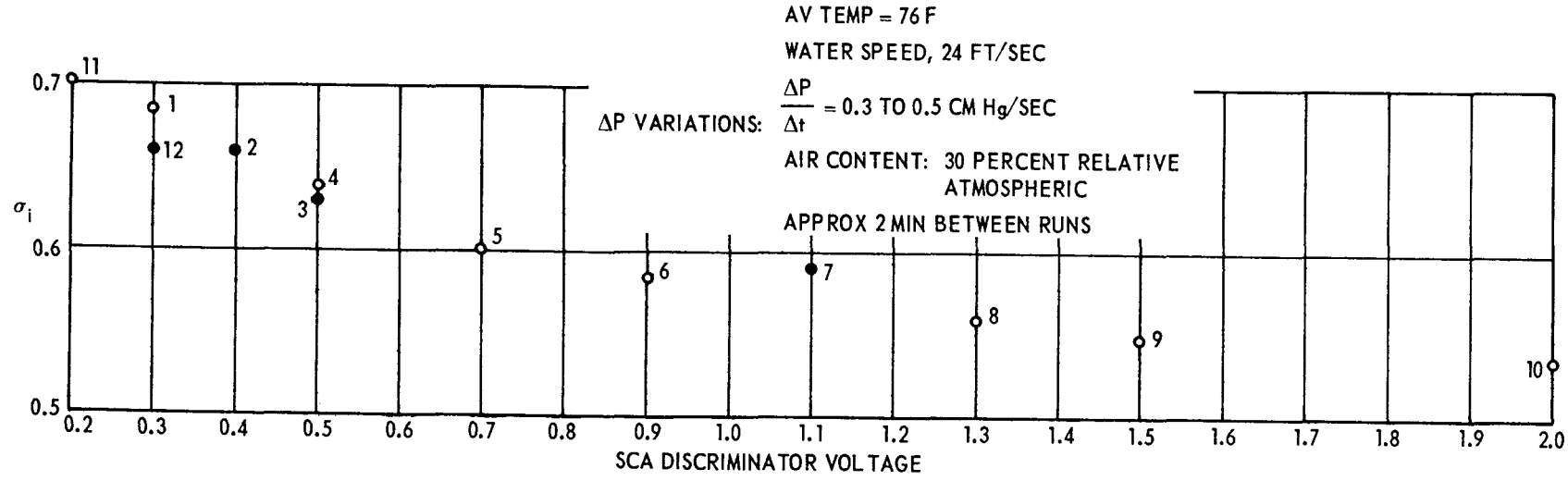

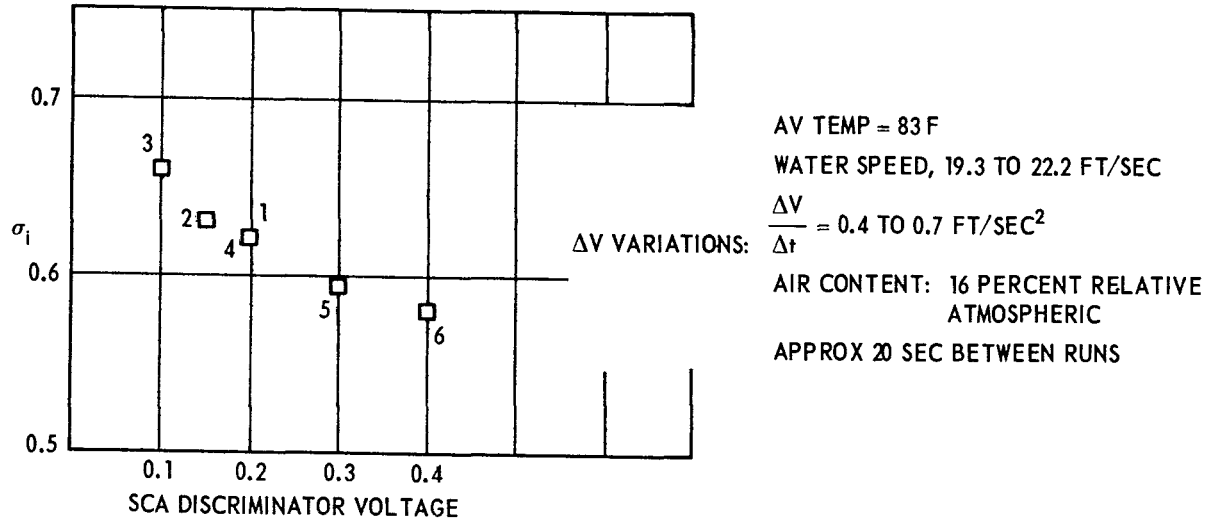

Figure 32 – Cavitation Inception as a Function of Discriminator Setting

TABLE 3 – BUBBLE DATA FROM FILM AND MAGNETIC TAPE WITH PLASTIC HEADFORM

First Seen in Free-Stream	First Seen on Body	First* Collapse	Other Collapse	Last Seen On Film	Maximum Dimension	First Collapse Distance From L. E.	Location +	Free Stream Size and Distance From L.E.	Film Speed	Comments	Maximum Negative Amplitude of Collapse Pulse	Time to Second Collapse	Comments
Frame No.	Frame No.	Frame No.	Frame No.	Frame No.	in.	in.		in.	k Fr/sec		volts	msec	
484	486	489	–	490	0.13	1.17	U	0.03 @ 0.25	1.3	May not have hit body	0.76	0.50	
	812	814		814	0.13	0.54	U		1.7		0.55	0.40	
	846	850		850	0.17	0.71	C		1.7		1.30	0.55	Several Collapse Pulses
	881	887		887	0.17	1.08	U		1.8		1.29	0.80	
	906	909		910	0.15	0.67	U		1.8		0.43	0.80	
	913	915		916	0.17	0.67	C		1.8		0.94	0.65	
	977	980	–	980	0.17	0.60	U		1.9		?		
	979	981	–	981	0.13	0.58	C		1.9		?		
	980	980	–	980	0.04	0.25	C		1.9		?		
	996	998		998	0.06	0.46	U		1.9		0.34	–	
1,063	1,065	1,069		1,073	0.06	0.88	U	0.03 @ 0.13	1.9		–		
	1,075	1,077		1,077	0.17	0.50	C		2.0	Indistinct at first sight	0.52	–	
	1,084	1,086		1,086	0.08	0.52	C		2.0		–		
1,310	1,312(?)	1,317(?)		–	0.03	0.83	U	0.02 @ 0.23	2.1		–		
	1,321	1,323		1,323	0.10	0.40	U		2.1		0.47	–	
1,318	1,321	1,326	1,331	–	0.06	1.00	L	0.02 @ 0.21	2.1		–		
	1,378	1,380		1,380	0.08	0.48	L		2.2		0.37	0.25	
1,388	1,391	1,394	1,404(?)	–	0.05	0.54	C	0.05 @ 0.33	2.2		0.25	–	
	1,499	1,502(?)	1,504	1,510	0.06	0.65	U		2.3		–	–	
	1,512	1,515	?	1,517	0.10	0.75	U		2.3		–	–	
	1,581	1,585		1,586	0.10	0.50	L		2.4		0.27	0.60	
	1,664	1,668		1,669	0.10	0.58	U		2.5		0.80	0.50	
	1,671	1,681		1,682	0.19	0.67	C		2.5	Rebound cloudy	0.90	0.50	
	1,704	1,710		1,712	0.25 × 0.08	0.80	T		2.5		0.72	0.80	Second collapse = 0.70 volts
	1,722	1,726		1,726	0.13	0.67	U		2.5		0.52	–	
	1,739	1,744		1,746	0.17 × 0.06	0.71	T		2.6		0.53	0.70	Second collapse = 0.50 volts
	1,804	1,808		1,810	0.10	0.67	T		2.6		0.33	0.50	Second collapse = 0.37 volts
1,822	1,826	1,833		1,834	0.17 × 0.06	0.92	T	0.03 @ 0.29	2.6	Far side, may be different from free-stream bubble	0.94	0.60	
	1,952	1,955		1,956	0.13	0.54	U		2.7		0.33	0.50	
1,969	1,974	1,980		–	0.08	1.00	U	0.03 @ 0.23	2.7	Bubble shadow on body	–		
	2,166	2,171		2,173	0.14	0.67	T		2.8		0.71	0.60	
	2,178	2,181		2,181	0.10	0.50	U		2.8	Maximum diameter in last frame	0.17	–	
2,176	2,180	2,187		2,188	0.10	0.75	U	Dot	2.8		0.72	0.60	
	2,229	2,233		2,233	0.10	0.52	U		2.9		0.39	–	
	2,318	2,322		2,324	0.17	0.58	C		3.0		0.69	0.50	
	2,365	2,370		2,371	0.19	0.58	C		3.0		0.59	0.50	Middle trace, Ref. 22
	2,471	2,476		2,476	0.13	0.67	L		3.0		0.63	0.50	

*Often difficult to establish, especially at low frame rates. + U Upper, C Center, L Lower

TABLE 3 (Continued)

First Seen in Free-Stream	First Seen on Body	First* Collapse	Other Collapse	Last Seen On Film	Maximum Dimension	First Collapse Distance From L. E.	Location +	Free Stream Size and Distance From L.E.	Film Speed	Comments	Maximum Negative Amplitude of Collapse Pulse	Time to Second Collapse	Comments
Frame No.	Frame No.	Frame No.	Frame No.	Frame No.	in.	in.		in.	k Fr/sec		volts	msec	
2,640	2,645	2,653		–	0.04	1.04	U	0.03 @ 0.25	3.2		–		
2,800	2,805	2,815		–	0.08	1.17	L	0.06 @ 0.25	3.2	Collapse questionable	–		
	3,028	3,035		3,035	0.06	0.75	U		3.4		0.18	–	
	3,035	3,038		3,042	0.08	0.42	U		3.4		0.34	–	
	3,079	3,084		3,085	0.17	0.58	C		3.4		0.59	0.40	
	3,127	3,132		3,133	0.17	0.58	L		3.4		0.62	0.50	
	3,133	3,139		3,140	0.17	0.67	L		3.4		0.78	0.30	
	3,206	3,211		3,211	0.10	0.5	U		3.5		0.42	0.30	
	3,299	3,306		3,308	0.25	0.77	C		3.6		1.17	0.65	
	3,340	3,346		3,349	0.19	0.63	L		3.6		0.88	0.50	
	3,466	3,472		3,472	0.19	0.67	C		3.7		0.63	0.40	
	3,472	3,478		3,481	0.19	0.63	C		3.7		0.75	0.55	
3,509	3,516	3,523		–	0.08	0.83	L		3.7		–		
	3,529	3,536		3,537	0.21	0.67	C		3.7		0.91	0.50	
	3,534	3,541		3,542	0.15	0.71	U		3.7		0.70	0.55	
	3,546	3,551		3,552	0.15	0.63	C		3.7		0.42	0.45	
	3,565	3,572		3,574	0.25	0.71	C		3.7		0.98	0.60	
	3,606	3,611		3,611	0.10	0.54	U		3.7		0.24	–	
	3,608	3,614		3,616	0.21	0.71	C		3.7		0.86	0.65	
3,642(?)	3,645	3,650		3,651	0.10	0.50	U	Blurred	3.7		–	–	
	3,710	3,718	3,722	3,735(?)	0.27	0.71	C		3.8		0.52	0.35	
	3,815	3,819		3,820	0.10	0.50	U		3.8		0.33	–	
3,947	3,947	3,962	3,962	–	0.05	1.04	U	0.03 @ 0.25	3.9		–	–	
	3,985	3,994		3,998	0.25	0.79	C		3.9		1.57	0.80	
4,052	4,055	4,063	–	–	0.08	0.96	U		3.9		–	–	
	4,097	4,105		4,108	0.27	0.79	L		3.9		1.74	0.65	
	4,382	4,387		4,388	0.13	0.46	U		4.1		0.20	–	
	4,541	4,545		4,545	0.04	0.33	U		4.2		0.27	–	
4,592(?)	4,595	4,600		4,612	0.04	0.42	U	Blurred	4.2		–	–	
4,626	4,634	4,640	4,644(?)	–	0.04	0.83	U	0.02 @ 0.17	4.2		–	–	
4,658	4,667	4,673		–	0.10	0.75	C	0.04 @ 0.21	4.2		–	–	
	4,978	4,983		4,983	0.04	0.48	U		4.3		0.21	–	
	5,291	5,298		5,300	0.08	0.46	U		4.4		0.70	0.40	
	5,314	5,320	5,323	5,330	0.13	0.58	U		4.4		0.37	–	
	5,352	5,358		5,359	0.08	0.54	U		4.4		0.33	0.45	
	5,887	5,894	5,897	–	0.13	0.58	U		4.7		0.48	–	
	5,980	5,986		5,987	0.10	0.58	C		4.7		0.25	0.45	
	6,109	6,117		6,119	0.21	0.54	C		4.7		0.70	0.50	
	6,145	6,150		6,151	0.08	0.50	U		4.7		0.30	–	
	6,205	6,215		6,218	0.17 × 0.06	0.71	T		4.7		0.58	0.45	
	6,293	6,303		6,307	0.17	0.67	U		4.7		0.84	0.80	Bottom trace in Reference 22
	6,297	6,304		6,305	0.10	0.63	C		4.7		–		
	6,344	6,351		6,352	0.19	0.57	C		4.8		0.55	–	

*Often difficult to establish, especially at low frame rates. + U Upper, C Center, L Lower

TABLE 3 (Continued)

First Seen in Free-Stream	First Seen on Body	First* Collapse	Other Collapse	Last Seen On Film	Maximum Dimension	First Collapse Distance From L. E.	Location +	Free Stream Size and Distance From L. E.	Film Speed	Comments	Maximum Negative Amplitude of Collapse Pulse	Time to Second Collapse	Comments
Frame No.	Frame No.	Frame No.	Frame No.	Frame No.	in.	in.		in.	k Fr/sec		Volts	msec	
	6,443	6,449		6,452	0.13	0.50	T		4.8	Far side of body	0.40	0.50	
	6,971	6,980		6,987	0.15	0.63	T		4.9	Far side	0.55	0.65	
	7,371	7,376		7,384	0.08	0.46	U		5.0		0.22	0.25, 0.55	Two collapses from signal
	8,188	8,194		8,196	0.04	0.38	U		5.3		0.34	–	
8,744	8,753	8,769		–	0.04	1.08	U	0.03 @ 0.29	5.3		0.21	–	
9,228	9,239	9,250		–	0.08	0.96	U	0.04 @ 0.21	5.4		–	–	
10,322	10,332	10,349	–	–	0.04	1.25	U	0.02 @ 0.21	5.4		–	–	
10,797	10,808	10,820	–	–	0.10	1.17	U	0.08 @ 0.25	5.4	Collapse questionable	–	–	
11,164	11,174	11,188	–	–	0.06	1.08	U	0.04 @ 0.21	5.5		–	–	
11,627	11,634	11,638	–	11,639	0.09	0.46	U	0.03 @ 0.19	5.5		–	–	
	11,636	11,648	–	11,654	0.17 × 0.06	0.75	T		5.5		0.30	0.85	
	11,636	11,653	–	–	0.04	1.04	U		5.5	Collapse questionable	0.30	0.30	
	11,928	11,932	–	11,932	0.08	0.38	U		5.5		0.28	–	
	11,997	12,001	–	12,001	0.04	0.38	U		5.5		0.36	–	
	12,202	12,210	–	12,212	0.13	0.54	U		5.5		0.39	–	
	12,254	12,258	–	12,258	0.10	0.42	U		5.5	May have continued longer	0.68	0.55	
	12,337	12,348	–	12,353	0.10	0.71	U		5.5		1.11	0.60	
	12,367	12,375	–	12,380	0.10 × 0.06	0.54	T		5.5		0.71	0.50	
	12,401	12,409	–	12,411	0.10 × 0.04	0.58	T		5.5		0.59	0.45	
	12,582	12,592	12,596	–	0.19	0.54	C		5.5		0.46	0.60	
	12,607	12,617	12,622	12,625	0.17 × 0.06	0.63	T		5.5		0.94	0.70	
13,297	13,312	13,325	13,333(?)	–	0.13	0.83	U	0.03 @ 0.21	5.4	Bubble flows up to get over body rebounds to about 0.13" again	–	–	Figure 26
	14,187	14,193	–	14,197	0.15	0.50	U		5.3		0.63	–	
	14,879	14,888	–	14,891	0.13	0.67	L		5.1		0.98	–	
	14,889	14,901	–	–	0.04	1.00	U		5.1	May have been free stream bubble, did not strike body	–	–	
	14,891	14,898	–	14,900	0.10	0.58	L		5.1		0.73	–	Top trace in Reference 22
	14,933	14,942	–	14,944	0.19	0.67	L		5.1		1.00	0.60	
14,935	–	14,953	–	–	0.04	1.08	U	Dot	5.1		–	–	
	15,013	15,019	15,021	15,023	0.06	0.46	U		5.0		0.32	–	
15,088	15,099	15,111	15,114	–	0.09	1.04	C	0.04 @ 0.21	5.0		–	–	
15,109	15,119	15,131	–	–	0.10	1.04	C	0.04 @ 0.29	5.0		0.17	–	
	15,158	15,164	–	15,166	0.10	0.50	L		5.0		–	–	

*Often difficult to establish, especially at low frame rates. +U Upper, C Center, L Lower

TABLE 3 (Continued)

First Seen in Free-Stream	First Seen on Body	First* Collapse	Other Collapse	Last Seen On Film	Maximum Dimension	First Collapse Distance From L. E.	Location +	Free Stream Size and Distance From L. E.	Film Speed	Comments	Maximum Negative Amplitude of Collapse Pulse	Time to Second Collapse	Comments
Frame No.	Frame No.	Frame No.	Frame No.	Frame No.	in.	in.		in.	k Fr/sec		Volts	msec	
15,158	15,166	15,183	–	–	0.06	1.25	L	0.04 @ 0.25	5.0		–	–	
	15,235	15,242	–	15,245	0.13	0.54	U		5.0		0.41	0.50	
	15,250	15,259	–	15,260	0.17	0.67	U		5.0		0.65	0.55	
	15,458	15,468	–	15,471	0.19	0.75	U		4.9	Collapse and rebound at fixed point	1.13	0.80	
	15,502	15,507	–	15,508	0.09	0.50	U		4.9		–	–	
	15,504	15,513	–	15,515	0.21	0.69	C		4.9		1.07	0.60	
15,534	15,540	15,545	–	–	0.06	0.46	C	0.03 @ 0.17	4.8	Blurred in free stream	–	–	
	15,581	15,590	–	15,592	0.17	0.67	U		4.8		0.92	0.50	Figures 24 and 25
	15,589	15,597	–	15,598	0.17	0.63	L		4.8		0.76	0.55	
	15,611	15,618	–	15,619	0.13	0.63	U		4.8		0.21	–	
	15,625	15,633	–	15,635	0.15	0.67	U		4.8		0.48	0.55	
	15,738	15,747	–	15,750	0.21	0.75	U		4.8		1.05	0.60	

*Often difficult to establish, especially at low frame rates. + U Upper, C Center, L Lower

REFERENCES

1. Eisenberg, P., "On the Mechanism and Prevention of Cavitation," David Taylor Model Basin Report 712 (Jul 1950).

2. Peterson, F. B., "Cavitation Inception, (Part of Report on Cavitation)," 15th American Towing Tank Conference, Ottawa, Canada (1968).

3. Holl, J. W., "Limited Cavitation," Proceedings of American Society of Mechanical Engineers Symposium on Cavitation State of Knowledge, Evanston, Ill. (Jun 1969).

4. Johnson, V. E., Jr. and P. Eisenberg, "Environmental and Body Conditions Governing the Inception and Development of Natural and Ventilated Cavities," Appendix 1, Report of the Cavitation Committee, 11th International Towing Tank Conference, Toyko, Japan (1966).

5. Eisenberg, P., "Environmental and Body Conditions Governing the Inception and Development of Natural and Ventilated Cavities (an updating of the survey prepared for the 11th ITTC)," Appendix 1, Report of the Cavitation Committee, 12th International Towing Tank Conference, Rome, Italy (1969).

6. Johnson, V. E. and T. Hsieh, "The Influence of the Trajectories of Gas Nuclei on Cavitation Inception," Proceedings of the Sixth Naval Hydromechanics Symposium, AGR-136, Office of Naval Research, Washington, D. C. (1966).

7. Hsieh, T., "The Influence of the Trajectories and Radial Dynamics of Entrained Gas Bubbles on Cavitation Inception," Hydronautics, Inc., Report 707-1 (Oct 1967).

8. Hsieh, T., "Cavitation Inception for a Two-Dimensional Half Body in a Uniform Stream with a Free-Stream and a Solid Bottom," Hydronautics, Inc., Report 707-2 (Mar 1968).

9. Turner, W. R., "Model for the Persistent Microbubble," Abstract Journal of the Acoustical Society of America, Vol. 36 (1964); Vitro Laboratory, Technical Note 01654.01-2 (1963).

10. Schiebe, F. R. and J. M. Killen, "New Instrumentation for the Investigation of Transient Cavitation in Water Tunnels," 15th American Towing Tank Conference, Ottawa, Canada (1968).

11. Brockett, T., "Computational Method for Determination of Bubble Distributions in Liquids," NSRDC Report 2798 (Apr 1969).

12. Van der Walle, F., "On the Growth of Nuclei and the Related Scaling Factors in Cavitation Inception," Proceedings of the Fourth Naval Hydromechanics Symposium, AGR-92, Office of Naval Research, Washington, D. C. (1962).

13. Peterson, F. B., "Cavitation Originating at Liquid-Solid Interfaces," NSRDC Report 2799 (Sep 1968).

14. Reed, R. L., "The Influence of Surface Characteristics and Pressure History on the Inception of Cavitation," Master of Science Thesis, Department of Aerospace Engineering, Pennsylvania State University (Mar 1969).

15. Acosta, A. J. and H. Hamaguchi, "Cavitation Inception on the ITTC Standard Headform, Final Report," California Institute of Technology, Hydro Laboratory Report E-149.1 (Mar 1967).

16. Lindgren, H. and C. A. Johnson, "Cavitation Inception on Headforms, ITTC Comparative Experiments," Appendix V, Report of the Cavitation Committee, 11 th International Towing Tank Conference, Toyko, Japan (1966).

17. Bernd, L. H., "Cavitation, Tensile Strength, and the Surface Films of Gas Nuclei," Proceedings of the Sixth Naval Hydrodynamics Symposium, ARC-136, Office of Naval Research, Washington, D. C. (1966).

18. Rouse, H. and J. S. McNown, "Cavitation and Pressure Distribution Headforms at Zero Angle of Yaw," State University of Iowa Studies in Engineering, Bulletin 32 (1948).

19. Johnsson, C. A., "Cavitation Inception on Headforms, Further Tests," Appendix V, Report of the Cavitation Committee, 12 th International Towing Tank Conference, Rome, Italy (1969).

20. Peterson, F. B., "Water Tunnel-High Speed Basin Cavitation Inception Studies," Contribution to the Cavitation Session, 12 th International Towing Tank Conference, Rome, Italy (1969).

21. Schiebe, F. R., "Cavitation Occurrence Counting–A New Technique in Inception Research," Cavitation Forum Paper, American Society of Mechanical Engineers Annual Meeting (1966).

22. Brockett, T., "Cavitation Occurrence Counting–Comparison of Photographic and Recorded Data," Cavitation Forum Paper, American Society of Mechanical Engineers Conference, Evanston, Ill. (1969).

23. Peterson, F. B., "Cavitation on a Headform Using Occurrence Counting," Cavitation Forum Paper, American Society of Mechanical Engineers Conference, Evanston, Ill. (1969).

24. Smith, A. M. O. and J. Pierce, "Exact Solution of the Neumann Problem. Calculation of Non-Circulatory Plane and Axially Symmetric Flows about or within Arbitrary Boundaries," Douglas Aircraft Company, Inc., Report ES26988 (Apr 1958).

25. Etter, R. J., "Flow Visualization Studies on the ITTC Body of Revolution," Hydronautics, Inc., Report International Towing Tank Conference-2 (Jan 1968).

26. Johnsson, C. A., "Pressure Distribution, Streamlines, and Cavitation Inception Tests on a Modified Ellipsoid Headform," SSPA, PM BK 24-1 (27 Dec 1967).

27. Ripkin, J. F. and J. M. Killen, "Gas Bubbles: Their Occurrence Measurement and Influence in Cavitation Testing," International Association for Hydraulic Research Symposium on Cavitation and Hydraulic Machinery, Edited by F. Numachi, Sendai, Japan (1962).

28. Bindel, S., "Comparison between Model and Ship Cavitation, an Assessment of Available Data," 11th International Towing Tank Conference, Tokyo, Japan (1966).

29. Lehman, A. F., "Some Cavitation Observation Techniques for Water Tunnels and a Description of the Oceanics Tunnel," American Society of Mechanical Engineers Symposium on Cavitation Research Facilities and Techniques, Philadelphia, Pa. (1964).

30. Iyengar, K. S., "Radio Measurement of Cavitation Noise," American Society of Mechanical Engineers Symposium on Cavitation Research Facilities and Techniques, Philadelphia, Pa. (1964).

31. Kendrick, A. L., "Techniques of Cavitation Noise Research," American Society of Mechanical Engineers Symposium on Cavitation Research Facilities and Techniques, Philadelphia, Pa. (1964).

32. Lamb, H., "Hydrodynamics," Dover Publications, Inc., New York (1945).

33. Jones, I. R. and D. H. Edwards, "An Experimental Study of the Forces Generated by the Collapse of Transient Cavities in Water," Journal of Fluid Mechanics, Vol. 7, Part 4 (Apr 1960).

34. Harrison, M., "An Experimental Study of Single Bubble Cavitation Noise," David Taylor Model Basin Report 815 Revised Edition (Nov 1952); Journal of the Acoustical Society of America, Vol. 24 (1952).

35. Millen, R. H., "An Experimental Study of the Collapse of a Spherical Cavity in Water," Journal of the Acoustical Society of America, Vol. 28 (1956).

36. Bohn, L., "Acoustic Pressure Variation and the Spectrum in Oscillatory Cavitation," (In German) Acustia, Vol. 7 (1957).

37. Osborne, M. F. M., "The Shock Produced by a Collapsing Cavity in Water," Transactions American Society of Marine Engineers, Vol. 69 (1947).

INITIAL DISTRIBUTION

Copies	
1	Chief of Res & Dev, Dept of the Army
1	U.S. Army Eng Res & Dev Lab Tech Doc Cen
1	U.S. Army Trans Res & Dev Marine Trans Div
2	CHONR 1 Code 438 1 Code 492
1	ONR Boston
1	ONR Chicago
1	ONR Pasadena
1	NRL
1	USNA
1	NAVPGSCOL
1	NROTC & NAVADMINUNIT, MIT
1	NAVWARCOL
1	NELC
1	NAVUSEACEN
1	NAVWPNSCEN
1	CIVENGRLAB
1	NOL
1	NWL
1	NUSC NPT
12	NAVSHIPSYSCOM 2 SHIPS 2052 1 SHIPS 033 1 SHIPS 037 1 SHIPS 08 1 PMS 300 1 PMS 378 1 PMS 380 1 PMS 383 1 PMS 389 1 PMS 391 1 PMS 392

Copies	
1	NAVORDSYSCOM ORD 05411
1	NAVSHIPYD BREM
1	NAVSHIPYD BSN
1	NAVSHIPYD CHASN
1	NAVSHIPYD LBEACH
1	NAVSHIPYD PHILA
1	NAVSHIPYD PTSMH
9	NAVSEC 1 SEC 6100 2 SEC 6110 1 SEC 6140 2 SEC 6144 2 SEC 6148 1 SEC NORVA 6660
12	DDC
1	USCOGARD Ship Const Comm
1	Library of Congress Science & Technology Div
8	MARAD 1 Ship Division 1 Coord of Research 1 F. Ebel 1 R. Schubert 1 R. Falls 1 E.S. Dillon 1 F. Dashnaw 1 Hammer
1	Merchant Marine Academy CAPT W. Maclean
1	NASA Sci & Tech Info Facility
1	National Science Foundation Engineering Div
1	Univ of Bridgeport Prof Earl Uram Mech Eng Dept

Copies

3 Calif Inst of Technology
  1 A.J. Acosta
  1 M.S. Plesset
  1 T.Y. Wu

2 University of California
  College of Engineering
  Naval Arch Dept
    1 Library
    1 Prof J. V. Wehausen

2 University of California
  Scripps Inst of Oceanography
    1 J. Pollock
    1 M. Silverman

1 Colorado State Univ
  Prof M. Albertson
  Dept of Civ Eng

1 Univ of Connecticut
  Prof V. Scottron
  Hydr Res Lab

2 Cornell Univ
  1 Prof W. R. Sears
  1 Prof J. Burns

1 Harvard Univ
  Prof G. Birkhoff
  Dept of Math

1 Univ of Hawaii
  M. St. Denis
  Dept of Ocean Eng

1 Univ of Illinois
  Coll of Eng
  J. M. Robertson
  Theor & Applied Math

1 Univ of Iowa
  Hunter Rouse

2 Univ of Iowa
  Inst of Hydr Res
    1 L. Landweber
    1 J. Kennedy

2 Johns Hopkins Univ
  1 Dept of Mechanics
  1 Inst of Coop Res

Copies

1 Kansas State Univ
  Eng Experiment Station
  Prof D. A. Nesmith

1 Lehigh Univ
  Fritz Lab Lib

1 Long Island Univ
  Grad Dept of Marine Science
  David Price

8 Massachusetts Inst of Technology
  Dept of Ocean Eng
    1 P. Mandel
    1 J. E. Kerwin
    1 P. Leehey
    1 M. Abkowitz
    1 J. N. Newman
    1 D. Cummings
    1 Library
  Hydrodynamics Lab
    A. T. Ippen

3 Univ of Michigan
  Dept NAME
    1 T. F. Ogilvie
    1 R. B. Couch
    1 H. Nowaki

5 Univ of Minnesota
  St. Anthony Falls Hydr Lab
    1 C. S. Song
    1 J. M. Killeen
    1 F. Schiebe
    1 J. M. Wetzel

2 State Univ of New York
  Maritime College
    1 Eng Dept
    1 Inst of Math Sciences

3 New York Univ
  1 Prof W. Pierson, Jr.
  Courant Inst of Math Sci
    1 Prof A. S. Peters
    1 Prof J. J. Stoker

1 Univ of Notre Dame
  Dept of Mech Eng

1 Penn State Univ
  Ordnance Res Lab

Copies

1 Rensselaer Polytechnic Inst
Dept of Math

1 St. John's Univ
Prof Jerome Lurye
Dept of Math

2 Southwest Res Inst
1 H. Abramson
1 Applied Mechanics Review

1 Stanford Res Inst
Lib

1 Stanford Univ
Prof H. Ashley
Dept of Aero and Astro

4 Stevens Inst of Technology
Davidson Lab
1 J. P. Breslin
1 S. Tsakonas
1 J. Mercier

1 Utah State Univ
College of Eng
Roland W. Jeppson

1 Univ of Washington
Applied Physics Lab

1 Woods Hole Oceanographic Inst
Ocean Eng Dept

2 Webb Institute
1 E. V. Lewis
1 L. W. Ward

1 Worcester Polytechnic Inst
Alden Res Lab

1 SNAME

1 Aerojet-General
W. C. Beckwith

1 AVCO Corp
Lycoming Div

1 Baker Mfg

1 Bethlehem Steel New York
H. De Luce

1 Bethlehem Steel Sparrows Point
Central Tech Div
A. Haff, Tech Mgr

Copies

1 Boeing Aircraft
AMS Div

1 Bolt Beranek and Newman
N. Brown

1 Cambridge Acoustical Assoc.
M. C. Junger

1 Cornell Aero Lab
Applied Mech Dept

1 Esso International
R. J. Taylor, Manager
R&D Tanker Dept

1 General Dynamics Corp
Electric Boat Div
V. Boatwright, Jr.

1 Grumman Aircraft Eng
W. Carl

4 Hydronautics, Inc
1 P. Eisenberg
1 M. Tulin
1 J. Dunne
1 J. O. Scherer

1 Institute for Defense Analysis
A. J. Tachmindji

1 Itek Corp
Vidya Div

1 Litton Systems, Inc

1 Lockheed Aircraft Corp.
Lockheed Missiles & Space Co.
R. Waid

1 Marquardt Corp
General Applied Sciences Lab
F. Lane

2 McDonnell Douglas Corp
Douglas Aircraft Co.
1 John Hess
1 A.M.O. Smith

1 National Steel & Shipbuilding

1 Newport News Shipbuilding
Lib

Copies

1 Oceanics, Inc
Paul Kaplin

1 Puget Sound Bridge & Drydock

1 George G. Sharp, Inc

1 Sperry-Gyroscope Corp
Sperry Sys Mgmt Div
D. Shapiro, MS G2

1 Sun Shipbuilding
F. Pavlik

1 Tetra Tech, Inc
Chapkis

1 United Aircraft Corp
Hamilton Standard Div

CENTER DISTRIBUTION

Copies	Code	
1	15	Dr. W. E. Cummins
1	1502	G. R. Stuntz, Jr.
1	1504	V. Monacella
1	1506	Dr. M. K. Ochi
1	152	R. Wertmer
1	154	Dr. W. Morgan
11	1544	R. Cumming
2	1552	J. Mc Carthy
1	156	J. Hadler
1	94	

UNCLASSIFIED

Security Classification

DOCUMENT CONTROL DATA - R & D

(Security classification of title, body of abstract and indexing annotation must be entered when the overall report is classified)

1. ORIGINATING ACTIVITY *(Corporate author)*

Naval Ship Research and Development Center
Bethesda, Md. 20034

2a. REPORT SECURITY CLASSIFICATION

UNCLASSIFIED

2b. GROUP

3. REPORT TITLE

SOME ENVIRONMENTAL EFFECTS ON HEADFORM CAVITATION INCEPTION

4. DESCRIPTIVE NOTES *(Type of report and inclusive dates)*

5. AUTHOR(S) *(First name, middle initial, last name)*

Terry Brockett

6. REPORT DATE	7a. TOTAL NO. OF PAGES	7b. NO. OF REFS
October 1972	91	37

8a. CONTRACT OR GRANT NO.	9a. ORIGINATOR'S REPORT NUMBER(S)
b. PROJECT NO.	3974
c.	9b. OTHER REPORT NO(S) *(Any other numbers that may be assigned this report)*
d.	

10. DISTRIBUTION STATEMENT

APPROVED FOR PUBLIC RELEASE: DISTRIBUTION UNLIMITED

11. SUPPLEMENTARY NOTES	12. SPONSORING MILITARY ACTIVITY
	NSRDC

13. ABSTRACT

Cavitation-inception tests were performed on two headforms for which changes were made in the environment. Quantities which were varied, included type and amount of dissolved gas, chemical additives, time rate of change to cause inception, and temperature changes. Experimental procedure and relative air content had an appreciable effect on cavitation inception while the other environmental changes had little effect. Both headforms had the same designed minimum pressure coefficient; however, for one it was located 0.03 diam from the nose, and for the other, 0.73 diam. Although inception was characterized by traveling bubbles on both headforms, significant differences occurred in the bubble dynamics. Inception was determined both visually and by counting the number of cavitation occurrences.

14. KEY WORDS	LINK A		LINK B		LINK C	
	ROLE	WT	ROLE	WT	ROLE	WT
Headform Cavitation Inception						
Cavitation Inception Bubble						
Modified Dynamics Ellipsoid Headform						
Computer-Lathe-Shaped Headform						
Plastic Headform–Cavitation Inception						
Brass Headform–Cavitation Inception						
Pointed Headform–Cavitation Inception						